Study of Changes in Lung Transfer Impedance due to Ventilation Using Focused Impedance Measurement (FIM) Technique

Humayra Ferdous

Department of Physics

Faculty of Mathematics and Natural Sciences

University of Oslo, Norway

Series of dissertations submitted to the
Faculty of Mathematics and Natural Sciences, University of Oslo
No. 1560

ISSN 1501-7710

Cover: Hanne Baadsgaard Utigard.
Printed in Norway: AIT Oslo AS.

Produced in co-operation with Akademika Publishing.
The thesis is produced by Akademika Publishing merely in connection with the thesis defence. Kindly direct all inquiries regarding the thesis to the copyright holder or the unit which grants the doctorate.

Contents

Acknowledgements

The theoretical and computational part of the present work was performed at the Department of Physics, University of Oslo, Norway, where I have been admitted as a PhD candidate since 2011. However, the practical part of this work took place at the Department of Biomedical Physics and Technology, University of Dhaka, Bangladesh between 2012 and 2013.

I would like to express my heartiest gratitude to my supervisor Professor Ørjan G. Martinsen, whose optimistic approach towards every problem kept the momentum going throughout the work. His technical efficiency, analytic judgment and cordialness boosted me at each step of the work. His ready to help and responsive attitude also paced the work with maximum extent.

I sincerely thank my co-supervisor Håvard Kalvøy also for his technical contribution to the present work.

In this special occasion, I would like to say thank you to my co-authors and research fellows Fred-Johan Pettersen, Christian Tronstad, and Jan Olav Høgetveit for their endless support in this present work, especially for simulation with computer software programme, statistical analysis and logistic assistance to the present work.

The journey in Norway would have been more difficult for me unless I obtained the full support and assistance from the Oslo Bioimpedance Group. Starting from 2010, the Oslo Bioimpedance Group of University of Oslo (UiO), Norway has been patronizing my thoughts, ideas and concepts in a very positive attitude which ultimately achieved a shape through this present work. Therefore, I would like to say a very special thanks to the entire group.

Besides, I sincerely would like to thank Professor Dr. Khondkar Siddique-e-Rabbani and his entire team of the Department of Biomedical Physics and Technology, University of Dhaka, Bangladesh for their enormous support in this work. The volunteers, who took part in the present work, deserve heartfelt thanks for their truthful contribution to the clinical study of the present work.

Acknowledgements are due to the staffs of Department of Physics and International Education Office of University of Oslo (UiO) too, for their administrative support to this study. I express my sincere gratitude to the Norwegian State Education Loan Fund (Lanekassen) for their financial assistance to the present work.

I would like to thank Malik Mohammad Fozlul Huq, Md, Atikul Islam, Farida Adib Khanum, Anjuman A Islam, Waliullah Fuad, Wasif Al-Imran, my parents-n-laws: Mohammad Abdul Hannan and Faizunnahar Begum, brother-n-laws: Mostafa Mohsin, M S Raunak, sister-n-law Sajeda Sharmin and all of my friends, my teachers who have braced love on me tremendously and inspired me unconditionally over the years.

In this very important occasion, I would like to remember late Professor Khodiza Adib Khanum, who passed away in 2009, for her guidance and adoration during my childhood. Her motivation for research work led me to take up the current study in the field of Biomedical Physics.

Finally, I am immensely grateful to my husband Mustafa Mamun for his continuous inspiration and motivation during the entire period of the present work. In reality, no word can narrate his contribution to this work. All can be said is, without his constant love, sacrifice, support, care and patience, this thesis would have been impossible for me to complete.

1. Introduction

Chapter Contents

Starting from the middle of the last century, bioelectricity as well as bioimpedance gained much attention of the researchers, scientists and academicians. Especially for healthcare purpose, bioimpedance has shown its potentiality through different research.

In 1911 Rudolf Hoeber, a German physicist discovered frequency dependence of conductivity of blood and postulated the existence of cell membranes. Ten years later Philippson measured tissue impedance as a function of frequency and found that capacitance varied approximately as the inverse square root of the frequency. However, Gildemeister's contribution of constant phase character of tissue in late 1920s also enhanced the knowledge of electrical properties of living tissues.

Kenneth S. Cole, who worked in Deby's laboratory for a long period, calculated the impedance of a suspension of spheres (1928a). Here the sphere was coated with a layer having capacitive properties. Experimentally he presented the measuring cell and tube oscillator used and the results obtained with a suspension of cells (1928b). In 1934 he repeated his presentation with quasi-four-element equivalent circuit. In another original paper in 1940, Kenneth S Cole introduced the famous Cole equation. It was for the first time that a mathematical impedance dispersion corresponding to the circular arc was found empirically. One year later the famous Cole-Cole equation was presented, which instigated long debate about its interpretation. Though it is was not completely for biological tissues, rather Kenneth S Cole and Robert H. Cole put emphasis on permittivity and the equation focused on dielectrics. The paper also presented the equivalent circuit for the Cole-Cole equation. In 1963 Hodgkin and Huxley won the Nobel Prize as they revealed some of the principle features of nerve transmission.

In 1950, Herman Paul Schwan, one of the founder of the biomedical engineering discipline, first revealed the frequency dependence of muscle tissue capacitance and established it as a relaxation phenomenon. He was the first to put light on dispersion and described α-dispersion in muscle tissue (Schwan 1954). His two mostly cited papers (Schwan 1957 and 1963) discussed elaborately on electrical properties of tissue and various processes to determine biological impedances. He categorised different dispersions such α, β, γ in his 1957 paper. In addition Schwan pioneered (Schwan *et al* 1962*)* other features for example low frequency precision measurement, four electrode techniques and gigahertz measurements. Besides, he explored the field of electrophoresis, electrorotation and non-linear phenomena of interfacial polarization (Schwan's law of linearity, McAdams and Jossinet, 1994).

However, as the knowledge on bioelectricity and bioimpedance gradually developed, lung transfer impedance has become an area of interest for the researchers and scientists of this field. Here the major reason is to employ bioimpedance as medical diagnosis as well as practical application for the humankind. Some techniques such as Electrical Impedance Tomography (EIT) and Tetra Polar Impedance Measurement (TPIM) etc have been employed to measure lung transfer impedance (details can be found in section 1.3). Focused Impedance Measurement (FIM) technique is another approach to measure transfer impedance for different tissues and organs including lungs, though proper standardization is required to turn FIM technique into a commercial tool

1.1 Focused Impedance Measurement (FIM) Technique

Focused Impedance Measurement (FIM) is a technique where two pairs (orthogonal to each other) of electrodes are used to inject current to the conductor and another two or four of electrodes are used to measure the potential drop across the desired zone.

Rabbani *et al* 1998, 1999 & 2010 showed how two sets of independent current carrying (CC) electrodes develop a central zone when one or two pair of electrodes is employed to measure the potential drop. In Figure 1.1.1 (Rabbani *et al* 1998 & 1999), it can be seen that A & B and C & D are the two sets of CC electrodes, perpendicular to each other whereas p, q, r *&* s are potential measurement electrodes. They are establishing the common zone of interest in Figure 1.1.1 Here, p and q work for the CC pair A & B while r and s perform the same for CC pair C, D.

Conventional Tetra Polar Electrode Measurement (TPIM) through ApqB gives the effective impedance of the zone bounded by equipotentials aa′ and bb′ (shown shaded) with sensitivity falling away from the center at any given depth. Similarly, measurement through electrodes CrsD gives the effective impedance between the equipotentials cc′ and dd′ (shown shaded) with sensitivity varying in a similar way.

If these two perpendicular measurements are summed up, the impedance of the central common zone obtains an enhanced weight, thus offering focusing effect. The combination can be performed by algebraic addition of admittance or of impedance when an enhanced sensitivity for the central zone can be expected (Rabbani *et al* 1998 & 1999, 2010).

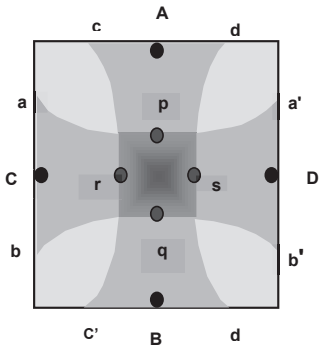

Figure 1.1.1: 8-electrode Focused Impedance Measurement (FIM) technique

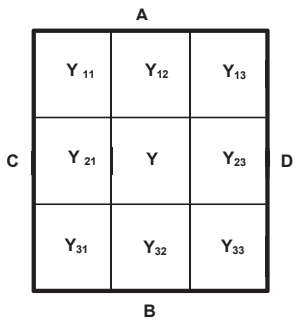

Figure 1.1.2: Simplified Admittance model of the zone of interest for FIM.

An estimate of the zone focusing was provided using a simple admittance model as shown in Figure 1.1.2 (Rabbani *et al* 1998, 1999 & 2010) for an equally spaced electrode system where the curved equipotentials have been replaced by straight lines.

The square zone bounded by the current electrodes and divided into 9 squares as shown in Figure 1.1.2 is assumed to be the total sensitive zone. Each of the small 9 zones is labeled with an admittance value (Y_{11}, Y_{12}, …etc.). It is assumed that the admittance of a zone is the same if measured along any direction. When current is driven through AB and potential is measured across pq, the measured admittance is thus the combination of ($kY_{21}+Y_{22}+kY_{23}$), where k is a constant factor, usually less than 1, which takes care of the sensitivity differences between the central zone and the outer ones.

Similarly for the perpendicular measurement through electrodes CrsD, the admittance is ($kY_{12}+Y_{22}+kY_{32}$).

An algebraic addition of the two measurements gives the total measured admittance (Y_T) as

$$Y_T = 2Y_{22} + k(Y_{21} + Y_{23} + Y_{12} + Y_{32}) \tag{1.1.1}$$

$$\frac{\delta Y_T}{\delta Y_{22}} = 2 \tag{1.1.2}$$

$$\frac{\delta Y_T}{\delta Y_{ij}} = k \tag{1.1.3}$$

where i and j stand for the other subscripts in the above equation.

These two derivatives present a simple picture of the sensitivity differences of the outer zones from the central one. Since k<1, the central zone has more than twice the sensitivity of the outer ones. Thus in this description the central zone may be said to be 'focused'.

For impedance, the algebraic addition of the two perpendicular impedance measurements would be, using the same subscripts as before,

$$Z_T = \frac{Z_{21}Z_{23}Z_{23}}{Z_{21}Z_{23}+KZ_{21}Z_{22}+KZ_{22}Z_{23}} + \frac{Z_{12}Z_{22}Z_{32}}{Z_{12}Z_{32}+KZ_{12}Z_{22}+KZ_{22}Z_{32}} \tag{1.1.4}$$

Nevertheless the sensitivity in the central zone is not easy to obtain. However, it can be said that the impedance of the central zone *(Z_{22})* would have more contribution compared to the outer zones.

Practically, the equipotentials would change shape and location if there are objects of various conductivities in the active region. Nonetheless, assuming that the conductivities do not differ much from a case of uniform conductivity throughout, this model would provide a simple approach.

In the study of measuring gastric emptying, FIM with its 3D sensitivity was found effective (Rabbani *et al* 1999). The FIM techniques have shown great potential for a wide range of other applications such as cancer diagnosis (Amin *et al* 2014), bladder emptying and lung ventilation (Rabbani *et al* 2011).

Measurement of abdominal fat thickness is another area of application of FIM (Surovy *et al* 2012, Haowlader *et al* 2010). A linear relationship to change in expired volume of air was found in a previous study when implemented to a focused zone of the lung in a subject (Kadir *et al* 2009) which led to further studies on FIM on lung impedance.

1.2 Electrical Bioimpedance and its Numerical Analysis

Bioimpedance is an electrical property of biological tissue by which it shows the ability to impede or hinder the electric current flow through the tissue. Since it is a passive electrical property, it can only be measured exogenically as a response to a known electric excitation unlike an action potential from nerve which is endogenic by nature. However electric excitation can emerge if current is applied or if a volume of tissue is coupled in a galvanic way using electrodes.

The resulting impedance of a certain volume can be obtained if a current is applied and the potential drop is measured over that volume like in the Focused Impedance Measurement described in section 1.1. The opposite of impedance is admittance, it is measured when potential is applied and current passing through a certain volume is measured.

Immittance is another term which is also used to describe the conducting status of the tissue and to combine both impedance and admittance.

Biological tissues are considered as electrical conductors as they are composed of both the free and bound charges, and due to the free charges they have the ability to conduct electrical current. On the contrary, dielectric contribution comes from the bound charges.

The rate of the movement of ions within the tissue is dependent on water content, ion concentration and cellular structures (Grimnes and Martinsen, 2008).

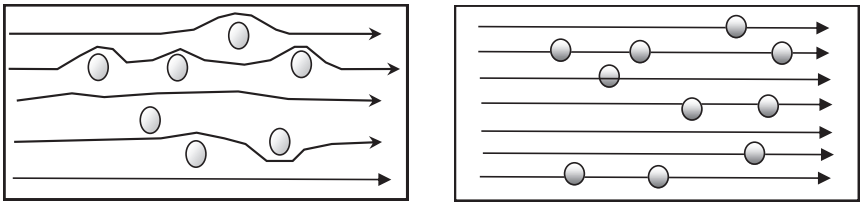

(a) (b)

Figure 1.2.1: Current flow through the cell at (a) low frequency (b) high frequency

Different tissues (e.g. muscle, bone etc.) have different intrinsic conductivities. This electrical conductivity is a characteristics property of different tissues. Therefore measurement and images of electrical conductivity can often resolve structure and even be indicative of pathology (Crile *et al* 1922).

The impedance of heterogeneous biological tissue involves two components, the resistance and reactance. The conductive characteristics of body fluids provide the resistive component; whereas the cell membranes behave as imperfect capacitors, add frequency dependence.

In the biological tissue, the membranes behave as a dielectric or an insulator separating two conducting media (Grimnes and Martinsen, 2008); the extra-cellular fluid and the intra-cellular fluid. These fluids act the role of armatures of the biological capacitor. Since the membranes are not good insulators, they make up leakage capacitors. Current at low frequencies does not penetrate cell membranes because of the high reactance of the membrane capacitance, but will pass through cell membrane at higher frequencies because the reactance will be relatively lower (Figure 1.2.1).

As tissues of the living body are made of non-homogeneous material, their physiological properties should be considered carefully. Different tissues, body fluids such as blood, saliva etc. and organ layers have miscellaneous cell structures. In general tissues, electrolytes and body have small cellular density. Dielectric behavior may arise from confined polarizable molecules and the movement of ions along membranes in the tissue. It will also contribute to the characteristic time constants and such variation may have effect on the measured impedance and in what manner it varies with the measurement frequencies.

Bode Plot

In 1957, HP Schwan illustrated different mechanisms for the dielectric dispersion of biological tissue. He developed three groups for relaxation mechanism such as α, β and γ dispersions (Figure 1.2.2). In bode plots (for detail on dispersion and electric properties of cell and tissue, see Grimnes & Martinsen, 2008); it can be found that there is a clear drop in modulus between two plateaus and a corresponding rise in the phase shift. In Figure 1.2.3, dispersions can be seen as circular elements.

In Figure 1.2.2 the modulus and phase angle are plotted as a function of frequency (impedance spectra). Logarithmic scale is widely used when the measured modulus spans more than a decade of ohms. The logarithmic scale in Y-axis is also a better choice for curve fitting Fricke's law (Fricke 1932) or constant phase element (CPE, eq 1.2.1, 1.2.2), which is introduced in the Cole model (eq. 1.2.3). They both show exponential relationship with frequency. Such quantity can be evaluated by fitting a straight line in a logarithmic plot (Schwan 1992, Khambete *et al* 1995, Raicu *et al* 1998, and Bordi *et al* 2001). For admittance model, the phase angle varies from 0 to 90 degree whereas for impedance, it goes to the opposite scale. Because of negative phase angle, inverse Y-scale is given priority for impedance model.

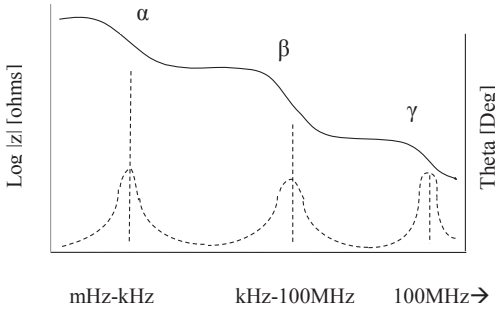

Figure 1.2.2: α, β and γ dispersions

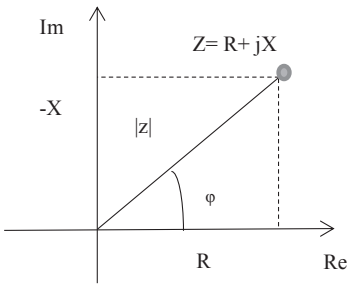

Figure 1.2.3: Wessel Diagram

Wessel Diagram

Figure 1.2.3 is known as Wessel diagram, it is often used to illustrate bioimpedance. Here complex numbers are plotted with the real part (Re) on X-axis whereas the imaginary part (Im or j) takes place on Y axis.

Cole Model

Figure 1.2.4 shows a possible equivalent circuit for the mathematical model developed by Kenneth S Cole from curve fitting to a large number of measurements (Cole 1940).

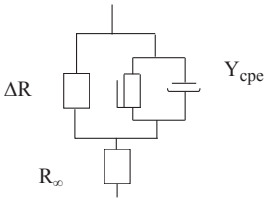

Figure 1.2.4: Cole Model

This model is vastly taken up as a general model for one dispersion system. More complex systems, can be developed by adding Cole-elements in Figure 1.2.4.

Frequency spectra of biological tissue often have frequency independent phase angle and it is a challenge to model it with a finite number of ideal resistors and capacitors, therefore the model is developed with a so-called Constant Phase Element (CPE). The CPE is defined by setting up φ_{CPE} to a constant value. Here, real and imaginary parts of the CPE are considered to be dependent on the frequency in such a way that the phase angle remains frequency independent. Grimnes and Martinsen (2008) showed that the CPE can be presented as an impedance (Z_{CPE}) or an admittance (Y_{CPE}) such as,

$$Z_{CPE} = R'(j\omega\tau)^{-\alpha} \tag{1.2.1}$$

$$Y_{CPE} = G'(j\omega\tau)^{\alpha} \tag{1.2.2}$$

Here, R´ and G´ are the resistance (Ω) and conductance (S) respectively, ω is the angular frequency (2πf), τ is the characteristic time constant and α is an exponent with relation to the phase angle.

The equivalent circuit in Figure 1.2 4 can be understood from the Cole equation which is,

$$Z = R_{\infty} + \frac{\Delta R}{1+(j\omega\tau)^{\alpha}}$$

$$\Delta R = R_0 + R_{\infty} \tag{1.2.3}$$

where the impedance Z of the system is given by Y_{CPE} (eq. 1.2.2) and the resistance at zero (R_0) and infinite (R_∞) frequency.

Sensitivity Calculation

The sensitivity in a given point in the sample (voxel) can be calculated using following equation.

$$S = \mathbf{J'_{cc}} \cdot \mathbf{J'_{reci}} \qquad [1/m^4] \tag{1.2.4}$$

Here, $\mathbf{J'_{cc}}$ is the unity current density vector (the ratio between local current density vector & the total excitation current) in the voxel that is formed by external currents from the current carrying electrodes.

$\mathbf{J'_{reci}}$ is the theoretical reciprocal unity current density vector, which is obtained from the current density vector when electrode pairs in the voxel are exchanged i.e., voltage pick up electrodes are employed to send the excitation signal and current carrying electrodes pick up voltage in the volume.

The spatial sensitivity for a particular measurement arrangement in a single voxel can be obtained from eq. 1.2.5. The contribution from one voxel in the total measured impedance is called Volume Impedance Density (VID).

It is defined as follows: Volume Impedance Density (VID) = $\rho S dv$ (1.2.5)

Where, S is the local sensitivity, ρ is resistivity and dv is the infinitesimal volume of the voxel.

In a monopolar or bipolar arrangement the reciprocal current is identical to the excitation current. Thus, $\mathbf{J'_{reci}}$ equals $\mathbf{J'_{cc}}$. So sensitivity for a given point is achieved by the squaring the local unity current density ($S=|\mathbf{J'}|^2$). The total impedance (Z) of any particular arrangement can be found by taking the integral over all voxels as given in eqn (1.2.6).

$$Z = \iiint \rho |\mathbf{J'}|^2 dv \qquad [\Omega] \tag{1.2.6}$$

In some cases analytical calculations for spatial sensitivity are often used if the shape of a particular set-up is less complex and if it fits to standard models.

However, in practical life, various difficulties arise when steps are taken to measure local resistivity and dimensions of any particular set. Therefore good approximations of the sensitivity field through analytical calculation can assist in this regard. So to measure lung

transfer impedance with FIM it is important to gather information on lung anatomy as well as how the respiratory system functions in the human body, which is described in section 1.3.

1.3 Lung Impedance Measurement and Existing Techniques

There are two lungs in the chest of the human body, one on right side and another on the left side (Figure 1.3.1). Each lung is comprised of sections called lobes. The lung is soft and protected by the ribcage. The purposes of the lungs are to fetch oxygen into the body and to eradicate carbon dioxide from it.

In humans each lung is encased in a thin membranous sac called the pleura, and each is attached with the trachea (windpipe) by its main bronchus (large air passageway) and with the heart by the pulmonary arteries.

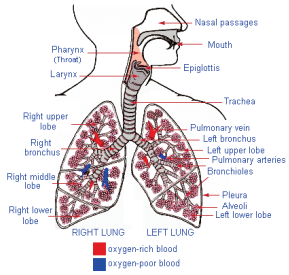

Figure 1.3.1[1]: Lung in human body

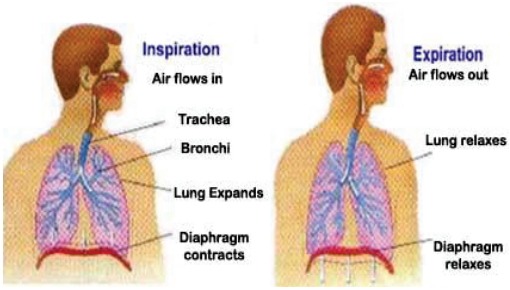

(a) (b)

Figure 1.3.2[2]: Ventilation process of human body

After entering the nose or mouth (http://en.wikipedia.org/wiki/Lung), air travels down through the trachea. Behind the trachea, the oesophagus is located. The trachea is distributed into two breathing tubes; the bronchi. The left bronchus is directed to the left lung and the right bronchus leads to the right lung.

[1]Image taken from http://www.methuen.k12.ma.us/mnmelan/respiratory_system_study_guide.htm

[2]Images taken from http://www.thoracic.org/clinical/copd-guidelines/for-patients/anatomy-and-function-of-the-normal-lung.php

The main bronchus branches out several times inside the lung forming an upside down tree which finally leads to the alveoli, where oxygen and carbon dioxide are interchanged between the respiratory spaces and the blood capillaries.

The complete process of respiration is regulated by the diaphragm, a large muscle below the lungs. It lies under the lungs and separates lungs from the organs below, such as the stomach, intestines, liver, etc.

As the diaphragm moves down, the ribs flare outward, the lungs enlarges and air is drawn in. This process is known as inhalation or inspiration (Figure 1.3.2 (a)). when the diaphragm relaxes, air leaves the lungs and they come back to their original position. This is known as exhalation or expiration (Figure 1.3.2 (b)). The diaphragm, muscles between the ribs and one of the muscles in the neck called the scalene muscle participate in almost every breath we take. The process by which the air enters the lungs is called ventilation.

Transfer impedance of lungs increases during the process of inspiration as air goes inside and decreases during expiration as air is released (Nopp *et al* 1993). Therefore, from the change in impedance due to ventilation, it would probably be possible to investigate lung condition if proper standardization is achieved beforehand.

Additionally, for a diseased lung, where part of the lungs is filled with water or some other fluid, air will not enter into these zones of lungs; so impedance changes between inspiration and expiration will be different compared to that of normal lungs which offer an arena to examine with one of the impedance measurement technique.

As mentioned in the beginning there are several tools to measure lung impedance change for pathological purpose such as Electric Impedance Tomography (EIT) (Barber and Brown 1984), Tetra Polar Impedance Measurement (TPIM), Magnetic Resonance Imaging (MRI), Positron Emission Tomography (PET) (Ter-Pogossian, 1975; Phelps, 1975). X-ray (Rontgen 1895) etc is also used to produce lung imaging for disease diagnosis.

Electrical Impedance Tomography (EIT) is extensively developed in Sheffield, UK (Barber and Brown 1984). In EIT current is injected (about 1 mA) into one electrode pair and the voltage between other electrodes are recorded (Rosell *et al* 1988b). Current injection is successively shifted so that all electrode pairs are used. This technique has also been referred to as conductivity imaging, impedance CT and Applied Potential Tomography (APT). Electrical Impedance Tomography (EIT) provides images of tissue impedance distribution.

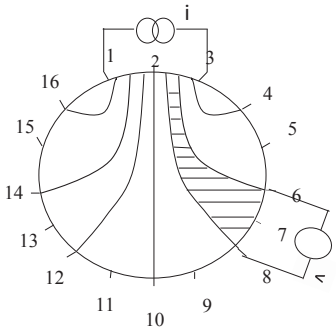

Figure 1.3.3: Applying current and measuring potential difference between interleaved in a homogenous medium

When a current is applied to two points on the peripheral surface of a cylindrical biological material through a cross sectional plane, a potential distribution is established within that plane (Figure 1.3.3). If this is sampled by making measurements of peripheral potentials at various points, such measurements can be backprojected along the curved isopotentials to create an image. Repeating the procedure for different locations of the stimulating electrodes leads to a form of computed tomography.

In comparison with the other imaging modalities, the distinguishing features of EIT are: the possibilities of very rapid data collection, modest computing requirements, relatively low cost, and no known significant hazards. Against these, limitations can be summed up as poor spatial resolution and technical difficulties arising from the over–simplified assumptions concerning the distribution of the isopotentials. When the number of drive electrodes is increased, the practical problems of data collection rise.

As the resolution of EIT is not satisfactory, usage of EIT for vast clinical application is a challenge to overcome till today. EIT is employed for gastric function (Mangnall *et al* 1987, Smallwood *et al* 1994), pulmonary ventilation (Harris *et al* 1987), perfusion, brain haemorrhage (Murphy *et al* 1987), hyperthermia (Griffiths *et al* 1987), epilepsy and cortical spreading depression (Holder 1992), swallowing disorder and breast cancer (Jossinet, 1996).

As mentioned earlier, to measure the change of lung transfer impedance due to ventilation and using this phenomenon for lung disease detection and lung monitoring has been one of the major area of interest for the scientists of this field over the years. Khambete *et al* (1999) narrated experimental and theoretical studies to determine an optimum placement of four electrodes for impedance pneumography. The studies showed that the

sensitivity of an electrode pair is dependent on the distance between the drive and receive electrode pair. In addition it is dependent on the anatomical location of the lungs with respect to placement of the electrode. However, focusing a region of lungs with the existing techniques such as EIT and TPIM has remained a challenge to overcome.

However, as seen in section 1.4, the relatively new Focused Impedance Measurement technique has shown potentials in this regard. From the previous studies it was found that more research is necessary in order to develop FIM as lung disease detection tool.

1.4 Previous Studies on Lung Impedance Using FIM and its Prospects

In the Focused Impedance Measurement (FIM) process, electrodes are applied on the surface of the human body. For lung ventilation study electrodes are placed on a certain area of the thorax and voltage change between inspiration and expiration were measured (Kadir *et al* 2009 , Rabbani & Kadir *et al* 2011). The output voltage, measured after amplification, is proportional to the amplitude of the potential developed between the voltage measuring electrodes. This measurement is also proportional to the impedance of the region within the voltage measuring electrodes (Rabbani and Kadir *et al* 2011). In the referred studies, subjects were directed to take deep breath and then expired air at a time in steps and held the breath for a short while each time. During the breath holding period the FIM data was recorded from electrodes placed over the right anterior thorax.

Rabbani and Kadir *et al* 2011

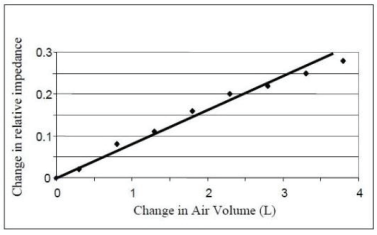

Fig. 1.4.1: Relationship between changes in relative Impedance vs change in air volume

The volume of air expired was also measured simultaneously using a standard type spirometer. Fig. 1.4.1 (Rabbani and Kadir *et al* 2011) shows a typical data from one of the subjects and the very good correlation between the relative FIM values and the volume of air expired

showing the utility of FIM in measuring lung ventilation in localised regions, and from any direction.

In another assessment study (Kadir *et al* 2010) for healthy individuals, localized ventilation maps in terms of transfer impedance were obtained from two normal male subjects using 6-electrode FIM with some modifications. The measurement was carried out in a matrix formation around the thorax, both at anterior plane and posterior plane of the human body with limited number of samples.

Here focused impedance values for inspiration and expiration were measured and the percentage difference with respect to the latter was employed for investigation purpose. Besides some of the measured values had artefacts due to movements of the heart and the diaphragm in the relevant anatomical positions which suggested to be considered in future with due care for any further interpretation for lung impedance change.

A study carried by Kadir *et al* 2010 gave a brief idea on how to analyse lung impedance as well as to develop thorax mapping in terms of impedance using a FIM in depth approach. In the study it was also intended to see if FIM could be used to detect and quantify changes in localised lung ventilation as it is important for potential use of FIM in detection and diagnosis of localized lung ventilation disorders. The idea of the study was change in impedance due to ventilation in a particular segment of lung will be different when measured with FIM, if that part of the lung is filled with water, blood of injury, or any other substance. Thus to be able to compare, calibration of change in impedance due to ventilation of healthy lungs is required in great extent.

Moreover, if it is possible to detect the change of lung impedance using non-invasive FIM technique, it would benefit many who suffer pulmonary problems but due to financial status cannot bear the healthcare costs.

Study shows that in developing countries like Bangladesh and others, lung disease is a major problem. Among them Pneumonia is the leading cause of infant and childhood deaths globally (Bryce *et al* 2005) and 90 % of all deaths occur in developing countries (Mulholland *et al* 2003; Black *et al* 2003), including Bangladesh (Ahmed *et al* 2000; Baqui *et al* 2001). In Bangladesh Demographic Health Survey 2004 conducted by National Institute of Population Research and Training, Dhaka/Calverton 2005 showed that in Bangladesh serious infections,

including lower respiratory tract illness, are responsible for up to 52 % of the mortality among children aged below 5 years.

Population-based studies also have reported a high incidence of pneumonia among children aged below 5 years who live in rural areas (0.23 episodes per child-year) and urban areas (0.56 episodes per child-year) in Bangladesh (Brooks *et al* 2005; Zaman *et al* 1997). So it would be highly beneficial to have a disease detection tool which can provide first-hand information to the physicians for early cure especially for the new-born babies who face pneumonia and cannot ask for medical help because of their tender age. On the contrary, the existing techniques such as X-rays, PET, and MRI etc. (mentioned in section 1.3) require human resources with very special skills along with higher installation cost. X-ray has radioactive hazards too.

Therefore it can be said that Focused Impedance Measurement (FIM), which is developed in the Biomedical Physics laboratory in the University of Dhaka (Rabbani *et al* 1998; Rabbani *et a1* 999) can show a great potential with its less complex characteristics, non- invasive criterion and minimum level of education in FIM handling, if proper research is executed.

Nonetheless to achieve the mentioned goals, it is important to have sensitivity mapping of the volume conductors such as lungs with proper electrode configuration which basically offers more area for further research.

1.5 Electrode Configuration and Sensitivity Plotting of FIM for Lung Impedance Studies

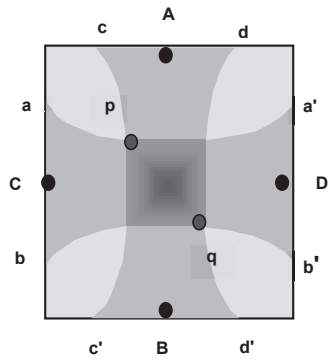

Figure 1.4.1: 6-electrode Focused Impedance Measurement (FIM) technique

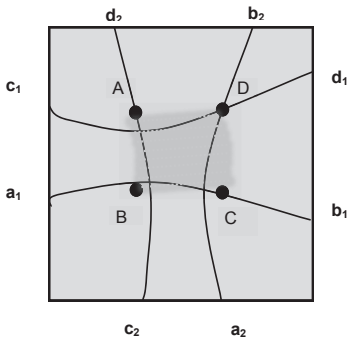

Figure 1.4.2: 4-electrode Focused Impedance Measurement (FIM) technique

Several electrode configurations can be developed using Focused Impedance Measurement (FIM) technique. Figure 1.1.1 illustrates 8-electrode FIM configuration whereas 6-electrode electrode configuration with FIM has been outlined in Figure 1.4.1 (Rabbani *et al* 1998; Rabbani *et al* 1999).

In 6-electrode configuration current carrying (CC) electrode pairs are A, B and C, D (same as FIM-8, Figure 1.1.1), but voltage pick up (PU) electrodes are placed in the diagonal position of the focused zone only to reduce the number of electrodes to avoid hazard and complexity (Figure 1.4.1, Rabbani *et al* 1999).

Karal *et al* 2008, has shown that 4-electrode FIM can be developed (Figure 1.4.2) making FIM even less complex in terms of electrode number. In 4-electrode-FIM current is injected through electrodes A and B and voltage are picked by electrodes C and D. Then again current is passed through B and C, which is perpendicular to A and B, and the voltage is measured by D and A. The zone with gradient effect in Figure 1.4.2 shows the zone of interest which is being focused with FIM whereas lines a_1b_1, a_2b_2 & c_1d_1, c_2d_2 show the equipotential lines for FIM with four electrodes. With different electrode configurations, it is important to know the sensitivities which vary due to the separation of current carrying (CC) and voltage pick up (PU) electrode.

Iquebal *et al* 2010 has shown the depth sensitivity of the 6 electrode FIM using a fixed-geometry-phantom-saline model. In the referred studies, depth sensitivities of spherical conductors, insulators and of pieces of potato (targeted objects) of different diameters were measured for fixed CC and PU electrodes. The sensitivity dropped drastically with depth steadily levelling off to background for insulating and living tissue (piece of potato), and objects could be identified down to a depth of about twice their diameters. The sensitivity at a certain depth increases showed almost linear relationship with volume for objects with the same conductivity in the referred studies.

Karal *et al* 2008 showed a study of the sensitivity with three cylindrical objects of different conductivities using 4-electrode FIM technique. It was performed using a 2D phantom made up of saline with a focused square zone at the centre where neighbouring square zones showed sensitivities of about 22% of that at the centre for the insulator, it shrunk to 13% for the conductor and about 10% for potato (living tissue). The outward zones had insignificant sensitivities.

Degrees of perturbation of equipotential lines (Figure 1.4.2) were indicated to be the cause of the above differences in focusing. In short it can be said that less perturbation would give optimum

focusing in 4-electrode FIM. In this study, few negative sensitive zones were found in the sensitivity map with an organic conductor. Negative sensitive zones appeared more when measured with the remaining two objects of different conductivities. Therefore, Karal *et al* 2008 concluded that the difference between the conductivity of the saline and the object might be the cause for this observed difference but to make concrete conclusion further study were suggested.

Brown *et al*, 2000 and Islam *et al* 2010 have also referred the difficulties of investigating the sensitivity field distribution using Matlab simulations based on Geselowitz' lead field theory (Geselowitz 1971) in detail for different configuration of FIM.

These analyses were performed for points in a mesh with 1 mm distance in the *x*, *y*, and *z*-directions. The models were made of 343 000 and 8000 000 points, respectively. These models can be used to determine the sensitivity in each point.

However, to obtain a finer model further studies are required. For instance the Matlab-based model only gave sensitivities but to have current density vectors and potential available for all points in a model, further simulation study was necessary for better understanding. Another interest was to achieve a graphical display of the sensitivities and to calculate transfer impedance from the simulation. Moreover the Matlab-based model was limited to a semi-infinite homogenous medium.

Nevertheless to develop a model with FIM which would be applicable to any geometrical shape is a challenge to overcome. Besides, from the eqn (1.2.4), it can be seen that negative sensitivity in a given point in the sample (voxel) arise when $\mathbf{J'_{reci}}$ and $\mathbf{J'_{cc}}$ have opposite direction with each other. So to determine the negative zones in sample with inhomogeneity applying FIM technique is an area of interest as well. It is also important to compare different electrode configurations of FIM and to find out the impact of the electrode configuration on the measurement result as the sensitivity field distribution of FIM becomes significant when the transfer impedance of biological tissue or any sample of non-homogenous nature is measured.

In short it can be said that if a new tool is developed for selecting the optimal electrode configuration for a given FIM problem (lung impedance study for present work), it could benefit the above mentioned problem. This basically paved the path for simulation study with FIM using Finite Element Model (FEM) based software programme, Comsol Multiphysics, in the present work.

1.6 Present work of Lung Impedance Study Using FIM

In 2009, a pilot study was executed by the author using 6-electrode FIM configuration with a spring loaded hand-held electrode probe in order to develop a thorax map of the human body due to ventilation in terms of change (%) in lung transfer impedance.

A paper template with 6 X 4 matrices, shown in Figure 1.6.1, was employed to serve the purpose. Since the study was taken as part of time-bound master's thesis project, it was not possible to carry out the study on a large number of samples at that point of time.

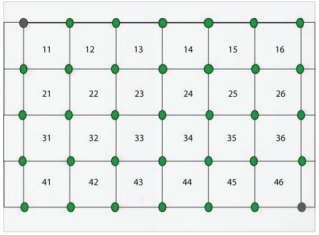

Figure 1.6.1 Paper template to develop body mapping matrix

However, during the development of the study, it was evident that substantial information can be extracted from the lung impedance study using FIM, if further research is carried out.

For instance, comparing the change in impedance (%) with respect to expiration at both anterior plane and posterior plane it was found that measurements of the former vary more than that of the latter. Though to establish this as a concrete conclusion, more in depth research was required.

However, since many features of FIM regarding simulation and negative sensitive zones were still to be explored at that point of time, it was a challenge to analysis the data obtained from the pilot study in detail. Furthermore, as lung is an organ which is exposed to air successively, so how the smoking habit of the subjects influences lung impedance change (%) due to ventilation when measured using FIM was also considered something to be looked upon with great interest. To develop the relation between physiological properties of the subjects such as body Mass index (BMI), age of the subjects and lung impedance change (%) due to ventilation was also required for practical implementation of FIM. But limited knowledge of statistics restricted the study further.

Considering all the limitations, it was a demand of the situation to run another project in large scale in terms of sample subject and time, where priority would be given to curb the obstacles faced during analysing the data of the pilot project as well to acquire more information on lung impedance study using FIM including its simulation and lung impedance related statistics for further interpretation of the results.

2. Aim & Objectives of the Study

The ultimate aim of the present work is to develop a low cost, simple and non-invasive tool to detect lung disease among the children in developing countries such as Bangladesh, India etc. In this regard the Focused Impedance Measurement (FIM) technique has shown potentials in previous research works, as mentioned in section 1.4.

However, to use FIM technique for lung disease detection commercially and on the grass root level, more investigation are required with an in depth approach. In order to achieve such a final goal a comparative study and several pilot studies were executed in the present work using the FIM technique.

The sub-goals of each paper can also be found in the reprints of the Paper I-IV. In short the sub-goals can be listed as:

1. **To compare change in impedance (%) at anterior plane and posterior plane of the body using FIM**

   From the Paper I and Paper II, it can be found that change of impedance of lungs due to ventilation were measured using 6-electrode and 8-electrode FIM at both anterior and posterior plane among a very limited number of subjects.

   As the anatomical structure of human body is different at anterior plane and posterior plane (more muscle tissue at back) and lungs are spread over on the upper portion of the body, a comparative study of the impedance change of lungs between anterior

plane and posterior plane became an area of interest and inspired us to take up studies with large number of samples.

2. **To determine the cardiac contribution in the change in lung impedance (%) of lungs due to ventilation**

   During the result analysis of pilot study described in Paper II, it was found that the anterior plane of thorax has higher value of change in impedance (%) due to ventilation. As the heart of the human body is located mostly in the anterior plane of thorax, it could contribute to the result. So an effort was made to determine the cardiac contribution to the change in impedance of lungs due to ventilation when measured using 6-electrode FIM.

3. **To eliminate the complications that arose during the process of developing body mapping matrix on the subjects when a spring loaded hand-held electrode probe is used**

   During the second pilot study (Paper II), a paper template having a 6 X 4 matrix was used to develop sensitivity mapping of the entire thorax in terms of lung impedance change (%) due to ventilation (Figure 1.6.1). It was believed that such mapping would be beneficial for standardization of lung impedance change (%) among healthy subjects.

   But through the practical experiment, it was found that the subjects felt exhausted as it is a lengthy process. Moreover after analysing the result we can conclude that such small element of matrix would not be able to bring fruitful result. So in the next pilot study (submitted Paper IV) thorax plane had been divided into eight segments for data collection (Table 3.3.2.1 and Table 2.4 in submitted paper IV).

   In addition a spring-loaded electrode probe (Figure 3.1.3, Figure 3 of Paper II) was used to measure the impedance change (%) due to ventilation. During the experiment it was experienced that such a rigid electrode probe faced problems when it is placed on the human thorax due the curviness of human structure. Therefor the next challenge became to design an electrode probe which will be flexible and fit on the human thorax. The next pilot study (Submitted Paper IV) was carried out with a newly designed pillow-like hand-held probe (Figure 3.3.1, Figure 2.2.2 of Submitted IV).

4. **To compare different types of FIM configurations such as 4, 6, 8-electrode FIMs using Comsol Multiphysics numerical software**

   There are different types of FIM configurations such as 4-electrode FIM, 6-electrode FIM, and 8-electrode FIM. It was also necessary to compare different FIM configurations so that the limitations and advantages of each type of FIM can be obtained. To serve the purpose a Finite Element Model (FEM) based on Comsol Multiphysics (MPH) was employed (Paper III).

5. **To develop a model which calculates current density and potentials at all points, when applied FIM technique**

   FIM can focus the sensitivity to a region roughly shaped as a half-sphere (Rabbani *et al* 1999). But it is still difficult to know to what degree different sub-volumes in the conductor contribute to the measured result, i.e. the sensitivity field distribution. Besides the cases where we want to measure the impedance in a particular volume with a uniform sensitivity in our target volume and as little influence from others volumes as possible, the challenge becomes more complex. FEM-based MPH enabled us to calculate current density and potentials at all points in a model when different types of FIM are applied on a volume conductor (Paper III).

6. **To graphically display sensitivities and to calculate transfer impedance using volume impedance density and sensitivity equations using FEM-based MPH**

   Islam *et al* 2010 in his sensitivity analysis study obtained only sensitivity at each point of the model using the Matlab software programme. But with the models developed in FEM-based MPH it was possible to add expressions for sensitivity (equation 3.5) and volume impedance density (equation (equation 3.6)) which enabled us to graphically display sensitivities and to enable us to calculate transfer impedance (Paper III).

7. **To find out whether smokers have different respiration-derived impedance change compared to non-smokers**

   As physiology of the inner lung surface changes due to smoking (Scott 2004), it was assumed that change of transfer impedance of lungs due to ventilation would also be affected for smoking. In order to achieve such goal in the next pilot study between smokers and non-smokers a linear statistical model was developed where smoking

habit of the subjects was kept as a factor to the impedance change (%) of lung (Submitted Paper IV).

8. **Which electrode position is best suited for measuring changes in respiration-derived impedance due to smoker status?**

   In the third pilot study, the thorax was divided in to eight positions for data collection, as mentioned before (Table 3.3.2.1 and Table 2.4 of Submitted Paper IV). Here, one of the interests was which of the thorax position among the eight is best suited for measuring change of lung transfer (%) impedance when measured using 8-electrode FIM technique among smokers and non-smokers, and using 5 kHz and 50 kHz.

9. **To test if different ages of the subjects have different effects on impedance changes due to ventilation for the same frequencies**

   In the pilot study carried in submitted Paper IV the ages of the subjects were considered as a factor in the statistical model to investigate if it has any influence on change on impedance (%) due to ventilation when measured using 8-electrode FIM at 5 kHz and 50 kHz.

3. Materials and Methods

Chapter Contents

This section of the thesis is comprised with the description on the methods and materials that were employed for the experimental studies. However, as described in Section 1, the studies can be divided into three segments.

Each of the segments benefited the research work to move forward to the next step with a broader approach. Short descriptions on each segment are given below whereas published and submitted papers on each topic with the details can be found in the next section of this thesis.

3.1 Analysing Data for Thorax Mapping Using FIM----A Pilot Study

This work was run in the Department of Biomedical Physics and Technology of University of Dhaka, Bangladesh. The main aim of this work was to investigate lung impedance change due

to ventilation in order to develop a complete mapping of the thorax in terms of impedance using the Focused Impedance Measurement (FIM) technique with 6-electrodes.

The block diagram of the instrument is shown in Figure 3.3.1. A sinusoidal signal, 10 kHz, is divided into two isolated current drives (AA´ and BB´) through voltage to current converters and isolating transformers.

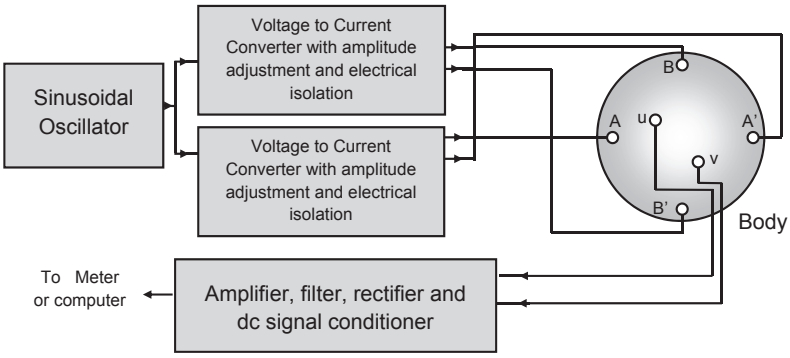

Figure 3.1.1: A block diagram of the 6-electrode FIM

In this process a spring loaded hand held electrode-probe (Figure 3.1.3) was used to measure the change of lung impedance (%) with the electrode configuration given in Figure 3.1.2.

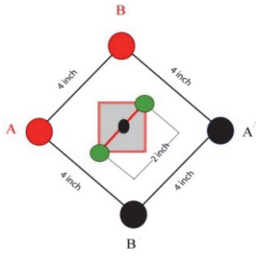

Figure 3.1.2: The Schematic diagram of 'Diamond' type electrode configuration for the 6-electrodes FIM system, the shaded square region bounded by red colour represents the focused zone.

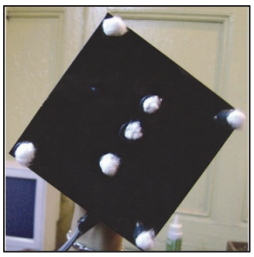

Figure 3.1.3: The handheld electrode probe. Wet cotton wool is inserted into recesses touching the metallic electrode inside. The stems of the electrodes are spring loaded to ensure good contact at curved body surfaces.

A paper template was used to develop a matrix (Figure 3.1.4) on both anterior plane and

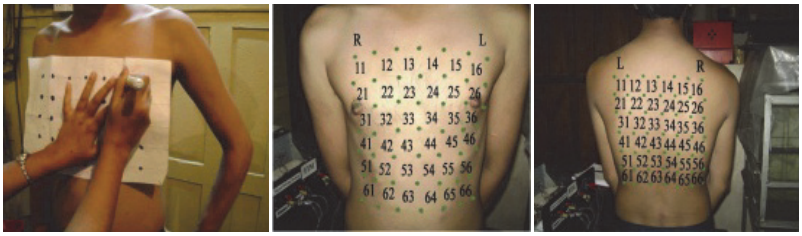

Figure 3.1.4: Technique for marking out identification of points on thorax for the desired matrix for measurement. The cell numbers shown were superimposed later on the photographs.

posterior plane of the subjects. Moreover, Figure 3.1.5 shows how the hand-held electrode probe was placed on the body mapping matrix to measure transfer impedance change due to ventilation.

Figure 3.1.5: Measurement of localised ventilation using the hand- held probe with spring loaded electrodes.

Four volunteers aged between 18-26 years, who reportedly had no lung complains before, participated in this pilot project. They were instructed to breathe in with their full capacity and asked to hold their breath to record the transfer impedance due to inspiration at 10 kHz while injecting 1 mA (rms). The same process was followed to measure transfer impedance for breathe out. Vital capacity, height, weight, and chest perimeters of the subjects were also recorded to develop a correlation with transfer impedance change. The relative change in impedance (%) with respect to expiration (when the lung is empty) was calculated to gather the general indication of the link between transfer impedance and other the recorded covariates.

3.2 A Simulation Study for Different Configuration of FIM with Comsol Multiphysics

From the study in section 3.1 and description in 1.5, it was evident that a simulation task was needed to understand the sensitivities of FIM with its entire configurations such as 4, 6, or 8 electrodes. Moreover, the sensitivity field distribution turns out to be a significant dimension in all living tissue which is non-homogenous in character. To serve the purpose Finite Element Method (FEM) based computer software COMSOL Multiphysics was used in this section of the present work (Pettersen F-J *et al* 2014). As mentioned earlier, FIM is a special set-up for impedance measurement where two or four electrodes are current carrying (CC), and two or four electrodes are used for voltage pick-up (PU). Some configurations have two steps where the electrode usage is changed. In these cases, the configuration requires simple post-processing.

3.2.1 Model Description

All models in the simulation work were 50 cm wide × 50 cm long × 25 cm high. The height was set to half the width since previous work (Brown *et al* 2000, Islam *et al* 2010) had shown that sensitivity decreases when moving away from the electrode plane. The electrodes were placed on top of the models. Electrode radii were 2, 4, 6 and 8 cm for each of the simulation set. The electrode height was equal to electrode radius. A half-sphere was made under the electrode. The half-sphere had the same electrical properties as the bulk material, and was used to make the mesh finer in these regions and to specify a region for volume integration. The radius of this half-sphere was varied from the same radius as the electrode and up to 10 mm in 2 mm steps. The inner electrodes for all models form a square with 4 cm sides. For FIM6, FIM8a, and FIM8b, the CC electrodes form a square with 12 cm sides (Figure 3.2.1). A sphere of 1.33 cm, with the same electrical properties as the bulk material, was placed just underneath the surface and it touched the top surface of the model.

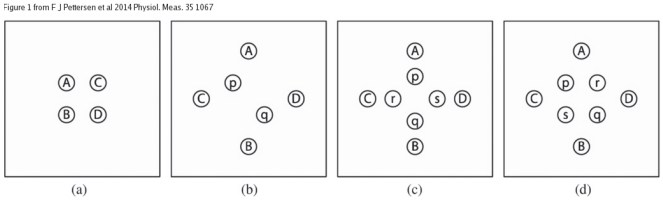

Figure 3.2.1: Top view of FIM electrode configurations. (Dimensions are not to scale) (a) FIM4 (b) FIM6, (c) FIM8a, (d) FIM8b.

To simulate the impact of an inhomogeneous material under an electrode, two ellipsoids were placed under one CC-electrode in the FIM8a-model. One ellipsoid was placed in the region with positive sensitivity and the other in the region with negative sensitivity. The regions of positive and negative sensitivity were found in the previous simulations. The ellipsoid had radius identical to the radius of the electrode in x-direction, and y-direction, and radius identical to half the electrode radius in the z-direction, which is shown in Figure 3.2.2.

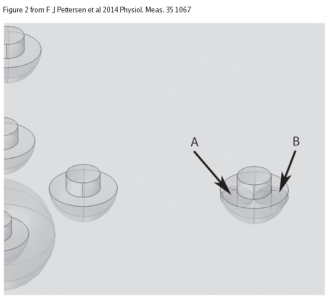

Figure: 3.2.2: Placement of ellipsoids beneath one electrode. The one marked A is in the region of negative sensitivity, while the one marked B is in the region of positive sensitivity.

The meshes were generated with settings that gave approximately 75 000 tetrahedral elements.

Material	Conductivity (sigma) (S/m)	Description
Bulk	1	The bulk of the model
Electrode	100	Electrode material
Low conductivity	0.01	Inhomogeneity below electrode
High conductivity	100	Inhomogeneity below electrode

Table 3.2.1: Material properties

For all set-ups, it can be said that several measurements were taken of the same quantity. In a standard setting, each measurement would have given the same value, and a summation of two measurement results would have given the double of the real value, therefore, to achieve the actual value, we calculated the mean of the two values. To be specific, what was done was to calculate the sensitivities for the different measurements and then average was calculated with MPH. This method is different to the work by Islam *et al* where results were added

together (Islam *et al* 2010). Adding the results benefited us for comparison. However, it did not let us use the result when calculating expected transfer impedance as we also do. The validity of our method has been verified by comparing FIM-simulations to phantom measurements (Abir *et al* 2013). Since all set-ups gave different results, normalization might also be an option, but the idea was abandoned as only the estimation of final impedance was the priority.

3.2.2 Simulation Set-up

Simulations were done in COMSOL MPH version 4.3. A set of partially differential equations was required to define how the FEM-tool would do its calculations. As an appropriate pre-defined equation set was not defined, the generic equations (3.1) through (3.4) were used. It must be noted that for the case of COMSOL MPH, an arrangement of pre-defined equation sets that model several physical systems such as heat flow, electric currents, magnetic fields, acoustics, fluid flow etc. can be found. For our models, a predefined set called *Electric Currents* physics interface (COMSOL 2013) which contains the equations (3.1) through (3.4), were employed.

The interior of the materials were handled by

$$\nabla \cdot \mathbf{J} = Q_j \tag{3.1}$$

$$\mathbf{J} = (\sigma + \mathrm{j}\omega\varepsilon_0\varepsilon_r)\mathbf{E} + \mathbf{J_e} \tag{3.2}$$

$$\mathbf{E} = -\nabla V \tag{3.3}$$

and the external boundaries by

$$\boldsymbol{n} \cdot \mathbf{J} = 0 \tag{3.4}$$

The simulations are done for DC only, which means that ω = 0 in equation (3.2).

The symbols in equations (3.1) through (3.4) mean:

$\nabla \cdot$ is the divergence of a vector field.

J is electric current density.

E is electric field intensity.

Q_j is electric charge.

σ is electric conductance.

j is the imaginary unit.

ω is frequency in radians per second.

ε_0 and ε_r are vacuum permittivity and relative permittivity, respectively.

$\mathbf{J}_e$ is external current density.

∇V is the gradient of the potential.

For a complete explanation please see the MPH reference manual (COMSOL 2013). For further information on FEM for electromagnetic problems, there are excellent text books available (Humphries 1997).

3.2.3. Extracted Numbers

Several numbers are extracted from the model simulations.

3.2.3.1 Fractions

The negative fraction (NF) described how much volumes with negative sensitivity contribute to the measured transfer impedance. This was a number between 0 and 1, and should ideally be 0. The next number was called sphere fraction (SF) and it gave an idea on how much the sphere just below the model surface contributes to the measured impedance. SF was a number between 0 and 1 for a configuration with NF = 0 and should ideally be 1 if we wanted to focus our measurement on the sphere. Non-zero NF meant the number might be higher than 1.

To calculate NF and SF, volume impedance density (z) was defined for each point in the model. This was sensitivity multiplied by the resistivity as shown in (3.6) whereas Sensitivity is given in equation (3.5). The integral of Z for all the points in the volume gave the transfer impedance. If integration was done over a smaller volume, V_{SUB}, then it delivered the contribution from V_{SUB} to the total transfer impedance. MPH allowed us to select such smaller volumes based on geometry or any available numerical property of a given point. This functionality allows us to investigate regions of special interest

$$S = \rho \frac{\overrightarrow{J_{CC}} \cdot \overrightarrow{J_{PU}}}{I_{CC} I_{PU}} \left[\frac{1}{m^4}\right] \tag{3.5}$$

$$Z = \rho s \left[\frac{\Omega}{m^3}\right] \tag{3.6}$$

Where,

ρ is the resistivity of the material.

S is sensitivity.

$\overrightarrow{J_{CC}}$ is the current density originating from simulation where current is sent into the model through the CC electrodes.

$\overrightarrow{J_{PU}}$ is the current density originating from simulation where current is sent into the model through the PU electrodes, i.e. the reciprocal current.

I_{CC} is the measurement current used in the model.

I_{PU} is the reciprocal measurement current used in the model.

Both I_{CC} and I_{PU} are set to 1 A to simplify calculations. Then the NF is calculated using

$$NF = \frac{|\iiint \mathrm{Z}_{NEG}\mathrm{d}V|}{\iiint \mathrm{Z}\mathrm{d}V} \tag{3.7}$$

Where

$$Z_{NEG} = \begin{cases} if\ \mathrm{Z} \leq 0 \colon \mathrm{Z} \\ if\ \mathrm{Z} > 0 \colon 0 \end{cases} \tag{3.8}$$

and SF is calculated

$$SF = \frac{\iiint_{SPHERE} \mathrm{Z}\mathrm{d}V}{\iiint \mathrm{Z}\mathrm{d}V} \tag{3.9}$$

3.2.3.2 Depth of Negative Sensitivity

To quantify how deep the region where *S* is negative is, the parameter negative sensitivity depth is defined as

$$NSD = \frac{Depth\ of\ negative\ S}{Distance\ between\ inner\ electrodes} \tag{3.10}$$

It was found by probing an isosurface plot of $S = 0$.

3.2.3.3 Sensitivity Ratios

Two ratios of sensitivities are defined in table 3.2.3.3. SR_{MAX} defines how large the sensitivity ratios are. A very high number indicates regions with high sensitivity that could potentially cause problems. The SR_{SPHERE} says how high the sensitivity is in the sphere where we want sensitivity to be high is. A high number means that the focus on the sphere is high.

Variable definition	Description
$SR_{MAX} = \frac{\max(\lvert S \rvert)}{S_{AVERAGE}}$	Ratio between maximum $\lvert S \rvert$ for the whole model and average S for the whole model. Electrodes are not included.
$SR_{SPHERE} = \frac{S_{AVERAGE-SPHERE}}{S_{AVERAGE}}$	Ratio between average S for the sphere and average S for the whole model. Electrodes are not included.

Table 3.2.3.3 Sensitivity variables

3.2.3.4. Contribution from Electrode Regions

The fine simulation mesh in the electrode regions allowed us to have a closer look at the contribution to final impedance form these regions. Four electrode related contributions are defined in table 3.2.3.4

Variable definition	Description
$Z_{EL-ABCD} = \iiint_{ELECTRODES\ ABCD} Z \mathrm{d}V$	Contribution from electrodes A, B, C and D to final measured impedance
$Z_{HSP-ABCD} = \iiint_{HALFSPHERES\ ABCD} Z \mathrm{d}V$	Contribution from half-sphere below electrodes A, B, C and D to final measured impedance
$Z_{EL-pq[rs]} = \iiint_{ELECTRODES\ ABCD} Z \mathrm{d}V$	Contribution from electrodes p, q, r and s to final measured impedance
$Z_{HSP-pq[rs]} = \iiint_{HALFSPHERES\ ABCD} Z \mathrm{d}V$	Contribution from half-sphere below electrodes p, q, r and s to final measured impedance

Table 3.2.3.4: Impedance contribution definitions

3.2.3.5 Inhomogeneity

An extra set of simulations was done to the FIM8 a-model to investigate the effect of inhomogeneity in the region below the electrodes. A base simulation was done with no inhomogeneity, and a number of combinations of low and high conductivities in the two regions were simulated. The percentage change in total averaged transfer impedance was found.

3.3 Study of Change in Lung Transfer Impedance due to Ventilation Using FIM technique

3.3.1 Instrument and Electrode Configuration

In this section, a BioScan 920-II, made by Maltron, UK was employed to measure the lung impedance change due to ventilation (submitted Paper IV). The measurements were taken in order to develop a relationship between change in impedance with other physiological factors of the subjects such age, smoking status and body mass indices (BMI).

In addition, how smoking status of the subjects influences the change in impedance (%) when measured using FIM technique was also an area of interest in this study. The used instrument had two channels and each channel has four leads. The leads were connected to a handheld probe (discussed later). The measurements on each subject were carried out at two frequencies i.e. 5 kHz and 50 kHz. In this case transfer impedance of lungs due to ventilation was measured using two pairs of electrodes, which are orthogonal to each other. These quantities were summed up and divided by two to get the average transfer impedance for inspiration and expiration. The change in impedance (%) was calculated as follows:

If lung transfer impedance due to inspiration =Z_{in}

and lung transfer impedance due to expiration =Z_{out}

Then, change in impedance (%) due to ventilation with respect to inspiration,

$$\mathrm{M} = \frac{Z_{in} - Z_{out}}{Z_{in}} \times 100 \tag{3.11}$$

and change in impedance (%) due to ventilation with respect to expiration,

$$\mathbf{N} = \frac{Z_{in} - Z_{out}}{Z_{out}} \times 100 \tag{3.12}$$

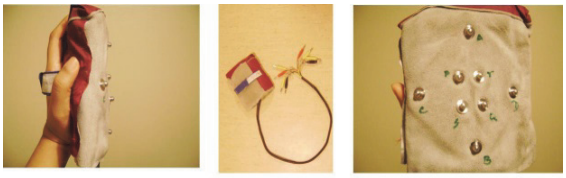

(a) (b) (c)

Figure 3.3.1(a), (b) & (c): Different angles of the hand-held probe used in the measurement of lung impedance due to ventilation

A customized handheld probe (Figure 3.3.1) was used to measure change in lung impedance (%) due to ventilation. This is an improved and modified version of the spring loaded electrode probe that was used in previous studies [Kadir *et al* 2010], [Ferdous *et al* 2013] with FIM. At one end, there are eight leads whereas the other end has specially designed electrodes. The pillow-like probe, made by leather, had foam inside it to keep it soft, smooth, and user-friendly. The foam also gave the opportunity to bend the probe slightly when it was placed on the human body.

3. 3. 2 Subject Selection & Measurement

Thorax Plane	Thorax Position	Abbreviation
Anterior Plane	Front Right Top	FRT
	Front Right Bottom	FRB
	Front Left Top	FLT
	Front Left Bottom	FLB
Posterior Plane	Back Right Top	BRT
	Back Right Bottom	BRB
	Back Left Top	BLT
	Back Left Bottom	BLB

Table 3.3.2.1: Thorax positions

Here twenty male subjects were chosen whose ages were between 23 and 30 years. They were divided into two groups; one was constituted by the subjects who were aged between 23 years and 26 years while another group is comprised of 27-30 years old subjects. These subjects were also categorised into two more groups based on their smoking habit, thus one group possessed smokers and another non-smokers. They were also labelled with different colours for convenience.

In addition, the thorax of each subject was divided into eight positions given in Table 3.3.2.1 Figure 3.3.2.1(a), (b), (c), (d) shows the thorax positions for FRT, FLB, BRT, and BLB of a subject respectively. Figure 3.3.2.2 (a), (b), (c), (d) shows how the hand-held electrode probe was placed on each of the thorax position for the measurement of lung impedance change (%) due to ventilation using FIM technique. Similar ways were followed to measure the other positions (FRB, FLT, BRB, and BLT) of the thorax.

In previous studies in Paper I & Paper II with FIM6, a paper template was used to develop a 6 x 4 or 6 x 5 body mapping matrix on the thorax (Figure 1. 6 and Figure 3.1.4) on the basis of anatomical shape of the thorax. It was found that to develop such thorax consumes long period of time (2.5-3hours for each subject for both plane at single frequency) which makes the entire system non-user-friendly and lengthy. Therefore in the submitted Paper IV, the thorax of each subject was divided into eight segments such as four in the front and four in the back (Table 3.3.2.1).

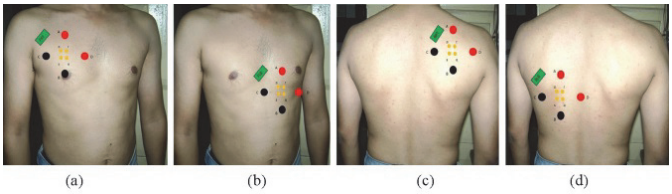

Figure 3.3.2.1: Thorax Position (a) FRT (b) FLB (c) BRT (d) BLB on a subject with superimposed electrode configuration of FIM 8-electrode B

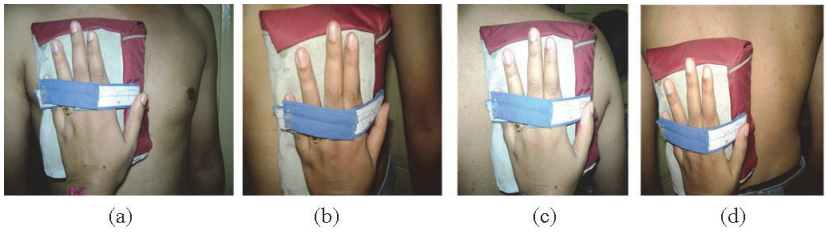

Figure 3.3.2.2: Measurement of lung transfer impedance due to ventilation on (a) FRT (b) FLB (c) BRT (d) BLB with the hand-held electrode probe on a subject

Each of the subjects were instructed to take a deep breath and hold it for a while, then the handheld electrode probe was placed in the anterior plane first at FRT positions described in section 3.3.2 [Figure 3.3.2.1-a and Figure 3.3.2.2-a] and photographs were taken on transfer impedance shown in the Maltron 920-II 's display screen. Then the subject was asked to

breathe out with full capacity keeping the hand-held probe on the same place (FRT in this case) as it was during inspiration and a similar procedure was followed to record the transfer impedance for exhalation. In this way the handheld electrode was placed at the other positions such as FRB, FLT, FLB, BRT, BRB, BLT, BLB and measurements were taken for lung impedance change due to ventilation at 5 kHz and 50 kHz. The measurements during inspiration and expiration were taken at 5 kHz first, followed by 50 kHz later for each subject at each position, i.e., in total eight positions for each subject.

The Maltron equipment generated a sinusoidal constant current of 0.5 mA (rms) amplitude. As per the International Electrotechnical Commission, the safe current boundary for medical equipment is 100μA (rms)/kHz, so that 0.5 mA at 5 kHz is within this safe range (IEC1977). A larger safe margin is obtained at 50 kHz.

Finally a dataset with 640 measurements (20 subject times 8 electrode positions for both inspiration and expiration using 5 kHz and 50 kHz) was recorded. They were grouped according to the factors Smoker Status, Age Group and Electrode position. The body mass index (BMI) was acquired for each subject in order to enable adjustment for this parameter in the statistical analysis. Table 3.3.2.2 gives a structural overview of the data and variables.

Variable name	Description	Type of variable	Values
Electrode position	Electrode	Nominal	[FRB, FLT, FLB, BRT, BRB, BLT, BLB]
%Zin(Electrode position)	Percentage wise change in impedance relative to inspiration, according to electrode position	Dependent variables	Continuous, $\%Zin = \frac{Z_{in} - Z_{out}}{Z_{in}} \times 100$
%Zout(Electrode position)	Percentage wise change in impedance relative to inspiration, according to electrode position	Dependent variables	Continuous, $\%Zout = \frac{Z_{in} - Z_{out}}{Z_{out}} \times 100$
Smoking status	Classification of subjects based on whether they smoked regularly or not	Fixed factor	[Smoker, non-smoker]
Age Group	Classification of subjects based on two age-groups.	Fixed factor	[23-26y ,27-30y]
Frequency	Impedance measurement frequency	Fixed factor	[5kHz, 50kHz]
BMI	Adjustment for body-mass index	Covariate	Continuous

Table: 3.3.2.2: Structural overview of the data and variables

3.3.3 Statistical analysis

The purpose of the statistical analysis was to observe the effect that the factors Smoking Status, Age Group and Frequency had on %Zin and %Zout for all the electrode positions when measured using FIM technique. A multivariate analysis of covariates (MANCOVA) was used to achieve this. These statistical operations were done in the computer software programme SPSS v18 using the General Linear Model function.

In the beginning, all interaction terms were included to the model and discarded if found to be non-significant. For significant interaction terms, separate analyses were executed. BMI was considered as a covariate to the model, and the MANCOVA was run with and without BMI correction for comparison.

A p-value below an alpha = 0.05 was considered to reject the null-hypothesis of the smoker status or age group factors not having an effect on the measured impedance change.

However, alpha came down to 0.025 due to multiple testing from the impedance change with respect to both inspiration and expiration.

In addition, for interaction terms and simple effects analysis, Bonferroni correction was considered. Thus it was adjusted by the number of simple effects within each factor. In order to compare different electrode positions with respect to detecting differences in impedance change due to Smoking Status and Age Groups, the p-values for the smoker status factor within each electrode position were compared against each other.

4. List of Original Papers

I. Ventilation mapping of chest using Focused Impedance Method (FIM)
M Abdul Kadir, **Humayra Ferdous**, Tanvir Noor Baig, K Siddique-e-Rabbani.
Journal of Physics Conference Series 05/2010; 224(1):012031.
doi:10.1088/1742-6596/224/1/012031

Contribution from Humayra Ferdous: She took part in the development of the objectives for the study. She provided assistance to install experimental set up and data collection from the subject using 6-electrode FIM system. She also participated in the writing of the article.

II. Thorax mapping for localized lung impedance change using focused impedance measurement (FIM): A pilot study
Humayra Ferdous, Tanvir Noor Baig, K. Siddique-e Rabbani.
Journal of Electrical Bioimpedance 12/2013; Volume 4, 2013(December):pp. 57–61.
doi:10.5617/jeb.778

Contribution from Humayra Ferdous: During the experiment, Humayra Ferdous collected data employing the FIM technique, developed the body mapping matrix on the subjects, developed the content of the article, executed the calculation and analyzed the results. She also prepared the graphical works for the paper.

III. Comparison of four different FIM configurations-a simulation study

F J Pettersen, **Humayra Ferdous**, H Kalvøy, Ø G Martinsen, J O Høgetveit.

Physiological Measurement 05/2014; 35(6):1067-1082. doi:10.1088/0967-3334/35/6/1067

Contribution from Humayra Ferdous: Humayra Ferdous was central in formulating the basic problems and questions to be addressed in this study. She assisted in the simulations and participated in the discussion of the result. During the development of the article she took part in framing the structure and outline. She contributed in providing the background information on FIM for the article with references. She also assisted in revising the article after the remarks came from the reviewers.

Special Note: Please read CD instead of AC in section 2.1.2. of this paper. Efforts are underways to correct the typing mistake.

IV. Measuring Ventilation Based Changes in Lung Transfer Impedance Using Focused Impedance Measurement (FIM) Technique

Humayra Ferdous, Christian Tronstad, Håvard Kalvøy, Khandker Siddique-e Rabbani, Ørjan G. Martinsen

Submitted to Physiol Meas. August 2014

Contribution from Humayra Ferdous: Humayra Ferdous developed the hypothesis, organized and carried out the experiment. She collected the data from the subjects using the FIM technique and calculated the change in impedance due to ventilation. As a first author she designed the outline of the article, analysed the result and wrote the article.

5. Discussion

Chapter Contents

As the present study had been split into three phases (described in the Methods and Materials sections), the Discussion segment is also divided in such a way for convenience. At the end of this section an overall assessment of the pilot studies (Paper I, II, Submitted Paper IV) and the simulation study (Paper III) has been presented to describe how present work will be beneficial for lung disease detection. However, readers are humbly requested to consider that the discussions on Paper IV are subject to change as the paper has been submitted for publication.

5.1 Analysing Data for Thorax Mapping Using FIM----A Pilot Study

This pilot study based on the Focused Impedance Measurement (FIM) technique with few subjects (a total of four) was analysed (Paper II) only to give a general idea on how the transfer impedance of the lungs change due to ventilation when it is measured using FIM. Because of low sample number, the opportunity to develop a solid conclusion was very narrow. Though some features were found that lead us to put emphasis on more investigation in the area of lung impedance (Paper III & Paper IV). Therefore the observations achieved in this pilot study helped in structuring further studies in the same area. Some on the key features and other conclusions drawn from Paper II are highlighted below.

5.1.1 Higher Change in Impedance (%) at Anterior Plane

From the pilot study (Paper II), it was seen that the maximum change in impedance (%) due to ventilation occurred at the anterior plane of the subject. This conclusion is made after analysing the data in this regard for all the subjects. The anterior plane of the subjects also possessed the second maximum change in impedance (%).

It must be mentioned that the electrode array was always kept in position on the body between the measurements recorded at inspiration and expiration so that any measurement error caused by repositioning of the electrodes can be avoided.

However, it was noticed that the edge of the thorax (the right most and the left most column at each plane) had larger values in comparison with the other columns, though the change in impedance (%) in the frontal plane still remained prominent than that of the back plane. A reason for higher values of impedance percentages in the anterior plane might be the location of heart or result from the greater depth of the lung tissue in the posterior plane. Variations in vital capacity for each subject were possibly also a cause in this regard. Subjects unable to follow the instruction of full expiration and full inspiration may have influenced the result too.

5.1.2 Cardiac Contribution on Change in Impedance (%)

It was found in Paper II that the average ratio between total impedance percentage change of the anterior plane and posterior plane is 2.1 i.e., on average the total impedance percentage changes at the frontal plane is twice as much as that of the back plane for each subject, which left an important dimension to look into in future studies. The probable reason for such higher values of impedance percentage change at the anterior plane might be the location of the heart.

The matrix column 2, 3, 4, 5 (Figure 3.1.4) at the frontal plane resembles the cardiac region of the human body and from the obtained changes in impedance (%) due to ventilation, it can be seen that the impedance percentage change in these focused zones varied significantly, especially when the anterior plane was under consideration. Thus the ratio also briefly tells on how the heart and solid ribs contribute to the impedance change of the lungs due to ventilation, though studies with larger number of subjects are required to establish this result.

Besides, it was found from the pilot study that the impedance percentage change of the right side of the frontal plane of the human body is ~1.6 times that of the left side of the same plane. The same value came down to ~1 when the comparison of the right and left side of the back plane is considered. The possible reasons for such a difference might be the same as mentioned earlier, i.e., contribution of the heart at the frontal plane and existence of muscles at the back plane.

5.1.3 Dependence on Anatomical Structure and other Physiological Properties

Principally, the analysis in the pilot study (Paper II) was carried out to get an overview of localized impedance change across the thorax of the human body due to breathing employing 6-electrode FIM. The ultimate target of such a study was to introduce the non-invasive FIM technique in detecting lung disease.

It is based on the understanding that the change in impedance of diseased lungs during ventilation would be significantly different compared to that of a healthy one since air content will vary by the presence of water, blood, fluid, other substance or any other injury. Nevertheless, this idea will only be useful when the calibration is executed with a large number of normal lungs and a standard set of values are offered to compare with the diseased lungs of different categories.

Furthermore, the changes in impedance at different regions at each plane (both front and back) are also dependent on anatomical structure of the lung as well as the body structure of the subjects, which led us to use a 6×6 matrix or 6×5 matrix. The change in impedance at the lower side (the bottom most row in each matrix) of the lungs of each plane varies abruptly in some cases. The likely reason could be the diaphragm of the lungs, which expands and shrinks due to ventilation in this region and contributes to the change in impedance (%). So lung impedance studies using FIM for different shapes of the thorax as well as different age groups are needed for an in-depth understanding (Paper IV).

It is also essential to understand how lung condition influenced on the change in impedance due to ventilation when using the FIM technique. As the smoking habit of the subjects and similar habits of the subjects influence lung condition, it is also essential to develop a model which would predict how the change in impedance interacts with such habits of the subject (submitted Paper IV).

5.1.4 User Friendly Electrode Probe for Measurement

In paper II, a spring loaded handheld electrode-probe was used to measure the lung impedance on the subjects. But due to the curved shape of the body and due to rigidity it was sometimes difficult to make contact with the body using the spring loaded electrode probe. So to develop a user friendly probe was a demand to extract more information from lung impedance measurements. To meet the demand a pillow like electrode probe was developed in order to place the electrodes on thorax in such a way so that the effect of cylindrical shape reduces.

5.1.5 Negative Sensitivities and Electrode Configuration

Because of thoracic movement during respiration, it is possible to obtain negative sensitivities when lung impedance changes are measured. So in the pilot study, there were matrix positions where negative values were also found. N D Khambete *et al* in 2000 carried out a study by establishing a volume conductor model of the thoracic cavity and simulated movement artefacts by shifting the electrodes to a different location. A six-electrode configuration was used in this study and the measurements were suitably combined to reduce the movement artefacts. But negative values were not considered during the result analysis although these negative sensitivity zones paved the path to carry out more studies with FIM. Furthermore it prompted us to think about an accurate electrode configuration of FIM (like 4-electrode FIM, 8-electrode FIM) for extended object like lungs of human body. However, negative sensitivity zones provide important information on physiological and anatomical features of lungs and this ultimately led us to take up the simulation study (Section 5.2 & Paper III) on FIM.

5.2 A Simulation Study for Different Configuration of FIM with Comsol Multiphysics

5.2.1 Sensitivity plots

There are noteworthy differences among the FIM electrode configurations. The sensitivity fields of FIM4, FIM8a, and FIM8b (Paper III) are symmetrical around the *x*- and *y*-axis, while FIM6 (used in Paper II) is clearly not symmetrical. The simulations with inhomogeneities (table 6 of Paper III) showed us that the impact is small, which can be explained by seeing the electrode and the inhomogeneity as a different shaped electrode. Figure 8 in Paper III gave an idea on how the sensitivity is changed if there are inhomogeneities. The plots also illustrate that in general the sensitivity is low when conductivity is low.

Besides, we can compare different shapes of negative sensitivity regions for different configurations of FIM from the figure 4-7 in the Paper III. These plots, developed by the Finite Element Model (FEM) based Comsol Multiphysics (MPH) software programme would be beneficial in order to select suitable FIM configuration for any particular purpose without real life experiment as it is mentioned in Section 2.

5.2.2 Numbers

The results in table 4 of Paper III described that large differences would occur for different electrode configurations of FIM. If only one electrode radius is considered, 4 mm, NF (Negative Fraction) varies from 0.208 for FIM4 to 0.532 for FIM6. So the risk of errors caused by objects placed in a region with negative sensitivity is higher for FIM6 (used in Paper II) than for the other configurations. The SF (Sphere Fraction) in Paper III tells us that the contribution to the sphere is highest for the FIM4 configuration, though the SF still remains in the range of 0.100–0.262.

The electrode size influences all numbers, but the sensitivity ratio numbers (SR_{MAX} and SR_{SPHERE}) are most affected. The smaller the electrodes are, the higher the sensitivity ratios are leaving us to think that large electrodes might be better if not other factors dictates use of small electrodes. The SF and NF were relatively little affected by electrode size for all models except FIM4. FIM4 has best values for SF and NF, but if constant electrode size is to be considered, then FIM4 might get less priority.

The results in table 5 of Paper III narrated us that the contributions from the electrodes and the regions just below the electrodes are small even if the local sensitivities are very high. Even for high inhomogeneities in these regions (Table 6 of Paper III). The inhomogeneites were modelled as ellipsoids with conductivity that was either 100 times higher or lower than the conductivity of the surrounding material placed under the electrode as shown in Figure 2 of

Paper III. It can be said that where the resistivity of a region is increased, the current density will naturally decrease as long as the current has an alternative way to flow (as it has here), and thus reduce sensitivity according to equation (5) of Paper III. When looking at equation (6) of Paper III, we see that the regions contribution to measured impedance is not only given by sensitivity, but also by resistivity, and that is changing in the opposite direction, and thus trying to cancel out the effects of sensitivity change. More detail can be found in the Discussion section of Paper III in this regard.

5.3 Study of Change in Lung Transfer Impedance due to Ventilation Using FIM technique

5.3.1 Change in Impedance (%) due to Ventilation at Anterior and Posterior Plane

From the Figures 3.1.1 and 3.1.2 of Paper IV, it was found that if we compare the anterior plane and posterior plane at 5 kHz and 50 kHz, the anterior plane produces the maximum amount of change in impedance (%) due to ventilation among a large number of subjects in this study. It supported the previous studies of Papers I and II. Contribution of the heart and bone structure of the ribcage could cause for higher impedance change (%) at the anterior plane, as mentioned in Paper II. However, the electrode probe was placed on the same place of a few subjects, for instance FRT, and transfer impedance of lungs was recorded using FIM technique to ensure reproducibility of the study. It must be noted too that the electrode array was always kept in position on the body between the measurements recorded at inspiration and expiration so that any measurement error caused by repositioning of the electrodes can be avoided.

5.3.2 Negative Sensitive Zones of Thorax among the Subjects at 5 kHz and 50 kHz

Between the two frequencies used in Submitted Paper IV, a higher numbers of negatively sensitive zones due to ventilation of the thorax lie at 50 kHz (Figure 3.1.3 of Paper IV). However, most subjects gave negative sensitivities at 5 kHz in the thorax location FRB (Front Right Bottom). Negative sensitive zone is found when unity current density vector set up by the excitation signal from the current carrying electrodes and the reciprocal unity current

density vector have opposite direction in an area of interest. Since FRB is a location where the bone structure of the ribcage is located (also mentioned in 5.3.1), this might influence the change in impedance (%).

In addition, as diaphragm of the lungs and other organs such as heart, arteries, vain move due to breathing process, they might influence on the change of impedance due to ventilation and cause negative values of impedance change (%) in the studies.

During the experiment the volunteers were asked to stand still and requested not to move their other body parts. It was possible to follow the instruction as adult volunteers were chosen for study but for the babies specially the new born babies this would be a challenge to overcome for further studies.

5.3.3 The Effect of Smoking Status, Age Group and Frequency

It is seen from Table 3.3. of the submitted Paper IV that the Back Left Top (BLT) became an influential position of the thorax for measuring differences in ventilation-derived impedance due to smoking and age. Whenever the factor Age Group and Smoking Status were taken account for developing a model, it showed significant p-value. But among the 20 subjects only a few had their maximum change in impedance in terms of inspiration and expiration at the posterior position BLT when measured at 5 kHz and 50 kHz (Figure 3.1.1 of submitted Paper IV) using the 8-electrode FIM technique.

From Figure 3.3 of the submitted Paper IV, we can conclude that there is a disparity between smokers and non-smokers in changes in impedance (%) with respect to inspiration and expiration at 5 kHz (though some outliers are also present) when measured with the FIM technique. It demands a study where data will be collected from a larger number of samples.

At 50 kHz, in the change in impedance (%) with respect to inspiration and expiration, this difference between the smokers and the non-smoker was not present in the Submitted paper IV.

During the study of lung impedance with tetra polar impedance measurement system (TPIM), it was obtained that at 5 kHz, beta-dispersion can be observed and at 50 kHz the measured tissues show their distinctive characteristic behaviour [Martinsen *et al* 2014], at 5 kHz membranes have poor conductivity while at 50 kHz current lines can pass through the cell membranes.

However for the smokers it can be expected that tars and other chemicals will deposit on sac walls and cell linings of the alveoli of their lungs. That results physiological changes in the lung inner surface [Scott 2004]. Due to physiological change of the lungs, smokers could have higher change in impedance at 5 kHz. Deposition of tar at extra cellular level in the inner lungs of the smokers will also reduce the effective capacitance and the dispersion frequency will be different.

Therefore the values at 5 and 50 kHz should show less discrepancy for smokers compared to that for non-smokers. On the other hand smokers should have less change than that of the non-smokers at the frequency where both conduct current in good manner (such as 50 kHz). This can be found in Figure 3.1.1 (a) and Figure 3.3 of submitted paper IV.

The influence of Age Group on impedance change (%) due to ventilation can be found from the Table 3.2.2 of submitted Paper II with and without BMI correction. This factor showed an influence on the outcome when change of impedance (%) is considered with respect to expiration when measured at 5 kHz and 50 kHz.

It is also true for inspiration, though based on the p-values, we found that it is not the same as Age Group influenced change in impedance with respect to expiration at 5 kHz.

However, it must be noted that as we implemented the conservative Bonferroni correction to the hypothesis test, only the influence from Age Group with respect to expiration was taken account of when it was statistically significant; even though the uncorrected p-values were also low due to inspiration (0.06 and 0.03 for with and without BMI correction at 5 kHz respectively).

Considering these results and the point that Age Group had a statistically significant effect both with respect to inspiration and expiration for the BLT position, we found that age has an influence on the ventilation-derived impedance signal in general but further studies are needed to consider it as a dependant variable of lung impedance change (%) due to ventilation using FIM where data will be collected from higher number of subjects.

5.3.4 Comparison of Change in Impedance (%) with Respect to Inspiration and Expiration

In Papers I and II, changes in impedance (%) were determined only with respect to expiration, whereas in the submitted Paper IV change in impedance (%) with respect to inspiration and

expiration were considered in order to run the study with broader approach. If the air volume that enters the lung during inspiration is high, a minimal change in impedance with respect to inspiration will be found, according to eq. 3.11, though it depends on lung capacity and physical condition of the lungs too.

Moreover, as lung condition can be influenced by the smoking habit and age (WHO report, 2008), it was assumed that these two factors influence the change in impedance (%) of lungs with respect to inspiration. Therefore, change in lung transfer impedance (%) with respect to inspiration can be considered in a similar study with FIM.

5.4 Lung disease detection with FIM and Present work

As the ultimate aim for the present work is to use FIM to detect lung disease, the pilot studies and the simulation studies presented in this thesis will guide the future research work in several ways despite having a few shortcomings as referred in the section 4.3 of Paper III.

In this simulation study it was found that even if we have good focus in a particular region, the contribution to the total transfer impedance is partly originating from outside the focus region, even for 4-electrode FIM, which is found to be the superior among all configurations.

Even though the studies with FIM were carried out as the other lung function monitoring techniques such as the widely used X-ray has radiation hazards, and MRI and PET have high installation costs. Commercial patent is also another challenge for the developing countries to deal with for manufacturing low cost lung detection tool.

On the other hand, in order to achieve the sub-goals mentioned in Section 2 the pilot studies and simulation study were executed. Several targets such as comparison of change in impedance of lungs due to ventilation at anterior and posterior plane of thorax using FIM was achieved by the third pilot study (Submitted Paper IV).

The results, where it was found that higher changes occurred at anterior plane, which supports the previous pilot study (Paper II), give a validation on FIM measurement for lung impedance change.

Determination of cardiac contribution on pulmonary impedance change due to ventilation (Paper II), gives us a brief idea on how heart located on the upper portion on the thorax can influence the result when measured using 6-electrode FIM (sub-goal 3 of section 2).

However, comparison between sum of change in impedance due to ventilation of column two and three of body mapping matrix and column four and five body mapping matrix also enhanced the knowledge in this regard.

In the present work, subjects were chosen from the age range 18-30 years. Women were also kept aside in these pilot studies. Fat tissues present on the anterior plane among the females possibly would influence the change in impedance due to ventilation when measured using FIM.

Nevertheless, measurement on women would be a large area of research for further studies. So to establish FIM as diagnosis tool, it is required to carry out experiments among babies, infants and aged subjects as well as women.

6. Conclusions

The following conclusions can be made after carrying out the pilot studies and simulation study on Focused Impedance Measurement (FIM) technique. They are as follows:

On Pilot Study (Paper II)

- The pilot study enhanced the fundamental understandings of lung impedance change due to ventilation with relatively simple and low-cost 6-electrode Focused Impedance Measurement (FIM) technique.
- It also supported the findings of Paper I where it was found that maximum change in impedance occurs at the anterior plane of the subject. However, the focused zone was ‘‘Diamond’’ in shape in Paper I.
- It directed us to explore more on various aspects and features of lung impedance change using FIM with different electrode configurations.

On Simulation Study (Paper III)

- The simulation study with Comsol Multiphysics (MPH) showed that MPH is a very useful FEM tool to investigate volume impedance measurement problems, especially when we consider models where there are large ratios between small and large objects and their inhomogeneities.

- Simulations allow us to explore the electrode configuration space and visualize and quantize alternative configurations. The simulations showed us that of the four configurations analysed here, the FIM4 configuration is superior in terms of SF and NF but when it is necessary to keep electrode size constant FIM4 should be given less priority. In addition 6-electrode FIM system shows asymmetry in the focused zone, which led us to choose a different configuration for further studies.

- The simulations also showed that the sensitivities in and beneath the electrodes were surprisingly high, but even so, the inhomogeneity beneath the electrodes did not affect the measurements as much as one might expect.

On Statistical Analysis (Paper IV)

- At the anterior plane of the human body, the maximum change in impedance (%) in terms of inspiration and expiration occurs at FLB (Front Left Bottom) when measured using 5kHz. At 50 kHz, the maximum change in impedance (%) in terms of inspiration occurs at FRB (Front Right Bottom).
- At the posterior plane of the human body, the maximum change in impedance (%) in terms of inspiration occurs at BRT (Back Right Top) at 5 kHz. However, maximum numbers of subjects have their maximum change in impedance (%) in terms of expiration at BRB (Back Right Bottom) when measured using 50 kHz at the posterior plane.
- In comparison of the anterior plane to the posterior plane at 5 kHz and 50 kHz, the anterior plane gives the maximum amount of change in impedance (%) due to ventilation among the highest number of subjects.
- Between two frequencies used in the present work, higher numbers of negative sensitive zones due to ventilation of thorax lie mostly at 50 kHz.

- Change in impedance (%) of lungs in terms of inspiration and expiration is affected by smoking status of the subjects and different age groups of the subjects.
- Thorax position BLT (Back Left Top) turned out be significant among the eight specified positions. It is influenced by smoking status and the age factor of the subjects according to this analytical study.

Therefore, it can be said that the sub-goals listed in Section 2 of this thesis, two objectives which include the effect of smoking habit and ages of the subjects on lung transfer impedance, are partly acquired from the statistical linear model. To determine the cardiac contribution in change in lung transfer impedance (sub-goal 2) and the suitable position to measure lung impedance changes in terms of inspiration and expiration, have been partially achieved as well. However, to establish age and smoking habit as variables of respiration-based impedance change more investigations are required with larger sample size and higher age span.

On the other hand 5 among 9 have been achieved such as comparison of change of lung transfer impedance (%) due to ventilation at anterior plane and posterior plane, developing a user friendly hand-held electric probe, comparing different configurations of FIM, to produce models providing current density and potentials at all points when applying FIM technique and to calculate transfer impedance using volume impedance density and sensitivity equations using Finite Element-based Multiphysics software programme.

7. Future Directions

The study of the present work on Focused Impedance Measurement (FIM) technique has left the research in a place with the following new ideas on which future studies can be executed.

To Collect Data from a Larger Sample for Better Result

Since the present work has been carried out among a small number of subjects (20), there is always an opportunity to have a larger sample which would minimize the errors in the result. Moreover, from Papers II and IV, it was found that lung problems depend on personal habits such as smoking behaviour and different age group.

So a large sample size of each category can have more in detail information related to transfer lung impedance change (in %) due to ventilation.

To Compare the Result with the Existing Methods

To establish FIM as pathological tool, it is important to compare the change in impedance (%) due to ventilation between FIM and other existing techniques such as EIT, X-ray, Ventiscan

etc. So with a large sample a comparison work can be performed between FIM and other existing techniques of lung disease detection.

To Determine the Cardiac Contribution of Change in Impedance (%) of Lungs

As it was seen from Paper II that change in impedance (%) due to ventilation varies from the anterior plane to the posterior plane of the subjects due to the location of the heart in the frontal plane, a further study can be carried out with FIM to determine the cardiac contribution in lung transfer impedance.

To Improve the User-friendly Handheld Probe

In the pilot study of Paper II, a spring loaded box-type hand-held electrode was used to measure the impedance change of the lungs due to ventilation. But at the curves of the human thorax, this handheld electrode probe experienced challenges due to its higher rigidity.

This problem was minimised by developing a pillow like electrode probe with more flexibility during probe placement on the thorax. However, to establish FIM for the mass it is necessary to have a very user-friendly electrode probe with which a wide range of thorax shapes can be measured with fewer hazards. This could also be an area of interest for future work on FIM.

To Compare Change in Impedance (%) with Larger PU Electrode Spacing

In the statistical study in Paper IV, the spacing between the voltage Pick Up (PU) electrodes was 2.8 cm. In the future, a study can be performed to look at how the change in impedance varies with the spacing between the PU electrodes in the electrode configuration. Although simulation software enables us to see the features for larger spacing between PU electrodes, comparing them with real life results would be another dimension of lung impedance study.

8. Appendix

Chapter Contents

8.1 General Definitions and Definitions Related to Impedance & Admittance Model

Table for General definitions and definitions related to impedance & admittance model

General Definitions			Definitions Related to Impedance Model (Z)	Definitions Related to Admittance Model (Y)
Physical Property	Symbol	Unit		
Current	I	[A]	$Z = \frac{U}{I}$ [Ω]	$Y = \frac{I}{U} = Z^{-1}$ [S]
Potential	U	[V]		
Resistivity	ρ	[Ωm]	$Z = R + jX$	$Y = G + jB$
Time	t	[s]		
Frequency	f	[Hz]	$X = -\frac{1}{\omega C}$	$B = \omega C$
Angular Frequency. (2πf)	ω	[Hz]		
Resistance	R	[Ω]	$\lvert Z\rvert = \sqrt{R^2 + X^2}$	$\lvert Y\rvert = \sqrt{G^2 + B^2})$
Reactance	X	[Ω]		
Capacitance	C	F	$Z = \lvert Z\rvert e^{i\varphi}$	$Y = \lvert Y\rvert e^{i\varphi}$
Conductance	G	[S]		
Susceptance	B	[S]	$\varphi = arctan\frac{X}{R}$	$\varphi = arctan\frac{B}{G}$
Imaginary Unit	**j**	$j = \sqrt{-1}$		

Table 8.1.1

8.2 Electrical Impedance of lungs using Focused Impedance Measurement (FIM) technique during inspiration and expiration

8.2.1 Electrical Impedance of lungs of the Non-Smokers aged between 23-26 years

Non-Smoker, Age 23-26years							
				Frequency = 5 kHz		Frequency = 50 kHz	
Subject 1	Weight 92 kg	Height 170,2 cm	Electrode Position	Z_{in} (ohms)	Z_{out} (ohms)	Z_{in} (ohms)	Z_{out} (ohms)
			FRT	70,65	46,4	25,3	25,95
			FRB	29,9	31,6	18,1	10,65
			FLT	11,15	15,9	22,8	25,65
			FLB	82,95	42,2	46,2	15,2
			BRT	24	9,9	16,1	16,45
			BRB	14,1	14,3	14,55	12,75
			BLT	11,7	13,9	14,1	17,1
			BLB	16,05	14,4	11,8	10,65
Subject 2	Weight 115 kg	Height 177,8 cm	Electrode Position	Z_{in} (ohms)	Z_{out} (ohms)	Z_{in} (ohms)	Z_{out} (ohms)
			FRT	42,45	37,25	20,9	16,2
			FRB	46,1	28,7	22,65	16,95
			FLT	38,15	15,05	16,75	18,05
			FLB	130	108	17,2	26,55
			BRT	59,2	42,25	10,85	9,3
			BRB	30,55	13,75	12,8	14,4
			BLT	18,45	9,25	12,7	12,2
			BLB	13,4	25	15,7	16,45
Subject 3	Weight 85 kg	Height 165,1 cm	Electrode Position	Z_{in} (ohms)	Z_{out} (ohms)	Z_{in} (ohms)	Z_{out} (ohms)
			FRT	49,05	44,15	55,75	17,15
			FRB	101,65	115,8	54,7	27,1
			FLT	48,25	42,9	35	23,75
			FLB	41,95	27,5	13,45	28,4
			BRT	16,6	16,7	8,55	16,25
			BRB	18,05	13,9	11,55	12,75
			BLT	34,8	24,45	10,6	12,1
			BLB	31,3	35,5	12,6	7,35
Subject 4	Weight 78 kg	Height 172,7 cm	Electrode Position	Z_{in} (ohms)	Z_{out} (ohms)	Z_{in} (ohms)	Z_{out} (ohms)
			FRT	19,8	11,35	20,7	16,95
			FRB	29,25	32,6	11,1	13,45
			FLT	67,65	50,3	17,05	16,25
			FLB	70,7	22,3	16	42,85
			BRT	96,25	67,1	26,35	20,95
			BRB	38,15	18,7	11,85	8,9
			BLT	33,25	20,75	10	10,35
			BLB	25,25	42,4	11	11,5
Subject 5	Weight 56 kg	Height 165,1	Electrode Position	Z_{in} (ohms)	Z_{out} (ohms)	Z_{in} (ohms)	Z_{out} (ohms)
			FRT	90,8	51,45	87,25	46,4
			FRB	44,85	49,8	141,9	127,85
			FLT	72,4	46,7	45,35	38,2
			FLB	55,35	115	55,75	53,2
			BRT	53,5	51,8	45,25	30,1
			BRB	100	46,05	54,15	30,7
			BLT	78,95	49,8	37,5	37,4
			BLB	46,05	37,95	64,15	57,55

Table 8.2.1

8.2.2 Electrical Impedance of lungs of the Non-Smokers aged between 27-30 years

Non-Smoker, Age 27-30years							
				Frequency = 5 kHz		Frequency = 50 kHz	
Subject 1	Weight 95 kg	Height 172,72 cm	Electrode Position	Z_{in} (ohms)	Z_{out} (ohms)	Z_{in} (ohms)	Z_{out} (ohms)
			FRT	113,85	103,15	57,65	19,25
			FRB	31,2	16,85	119,8	72,55
			FLT	72,1	35,6	38,55	37,1
			FLB	111,15	87,35	71,6	71,5
			BRT	38,7	57,2	65,15	16,3
			BRB	73,05	72,8	86,5	26,75
			BLT	46,1	60,65	28	28,65
			BLB	38,35	34,05	14,45	12,6
Subject 2	Weight 95 kg	Height 166,37 cm	Electrode Position	Z_{in} (ohms)	Z_{out} (ohms)	Z_{in} (ohms)	Z_{out} (ohms)
			FRT	37,75	53,9	22,8	26,6
			FRB	35,9	25,05	23,9	21,05
			FLT	23,35	15,15	23,7	18,05
			FLB	19,2	13	21	17,2
			BRT	10,65	10,45	18,15	18,3
			BRB	22,9	19,8	18,5	18,4
			BLT	11,7	13,45	16,95	17,6
			BLB	20,25	21,05	17,15	16,45
Subject 3	Weight 64 kg	Height 165 cm	Electrode Position	Z_{in} (ohms)	Z_{out} (ohms)	Z_{in} (ohms)	Z_{out} (ohms)
			FRT	12,3	48,3	12,9	15,35
			FRB	66,85	65,1	63,6	36,5
			FLT	97	55,4	66,15	27,75
			FLB	126,85	100,15	115,8	69,15
			BRT	92,05	47,1	21,65	21
			BRB	29,95	57,35	32,85	19,85
			BLT	31,95	41,85	26,6	16,1
			BLB	78,45	40,5	67,55	62,6
Subject 4	Weight 84 kg	Height 177,8	Electrode Position	Z_{in} (ohms)	Z_{out} (ohms)	Z_{in} (ohms)	Z_{out} (ohms)
			FRT	26,5	26,25	20	19,25
			FRB	22,95	31,95	17,1	82,55
			FLT	46,05	54,9	25,85	28,1
			FLB	44,6	29,7	31,5	28,35
			BRT	13,9	17,2	12,55	11,35
			BRB	27,75	16,7	21,8	13,75
			BLT	15,75	28,8	15,4	15,8
			BLB	39,2	17,85	21,75	19,35
Subject 5	Weight 92 kg	Height 172,7 cm	Electrode Position	Z_{in} (ohms)	Z_{out} (ohms)	Z_{in} (ohms)	Z_{out} (ohms)
			FRT	46,55	48,55	27,15	21,7
			FRB	11,9	12,4	41	17,4
			FLT	14,3	14,05	42,25	24,2
			FLB	112,25	65,6	19,3	15,55
			BRT	9,05	13,3	11,6	7,75
			BRB	11,35	10,65	20,3	10,15
			BLT	9,25	8,05	16,75	11,1
			BLB	12,55	14,35	64,85	12,25

Table 8.2.2

8.2.3 Electrical Impedance of lungs of the Smokers aged between 23-26 years

Smoker, Age 23-26y							
				Frequency = 5 kHz		Frequency = 50 kHz	
Subject 1	Weight 60,5 kg	Height 163,8 cm	Electrode Position	Z_{in} (ohms)	Z_{out} (ohms)	Z_{in} (ohms)	Z_{out} (ohms)
			FRT	92,8	70,5	17,15	15,45
			FRB	112,5	51,35	17,05	37,15
			FLT	95,95	11,45	11,7	10,6
			FLB	89,75	71,9	21,55	8,8
			BRT	16,15	14,9	13,75	7,65
			BRB	35,5	13,95	7,85	9,15
			BLT	24,95	10,1	8,7	7,45
			BLB	40,95	33,6	8,9	9,95
Subject 2	Weight 70,3 kg	Height 172,72 cm	Electrode Position	Z_{in} (ohms)	Z_{out} (ohms)	Z_{in} (ohms)	Z_{out} (ohms)
			FRT	157	60,5	26,3	16,7
			FRB	48,6	56,95	76	117,35
			FLT	140,9	112	15,5	15,2
			FLB	76,95	51,45	44,55	37,05
			BRT	20,85	21,75	6,5	5,65
			BRB	57,05	58,2	13,05	7,3
			BLT	34,6	15,4	8,1	8,05
			BLB	24,25	10,9	8,95	8,25
Subject 3	Weight 78 kg	Height 165,1 cm	Electrode Position	Z_{in} (ohms)	Z_{out} (ohms)	Z_{in} (ohms)	Z_{out} (ohms)
			FRT	21,4	18,7	20,55	12,55
			FRB	26,3	23,25	20,5	18,25
			FLT	15,75	16,1	24,35	22,05
			FLB	34,9	26,8	25,35	42,7
			BRT	44	11,6	9,15	16,95
			BRB	15,8	9,85	10,7	10,2
			BLT	12,6	8,5	19,05	10,9
			BLB	62,7	41,1	11	13,35
Subject 4	Weight 59 kg	Height 167,64 cm	Electrode Position	Z_{in} (ohms)	Z_{out} (ohms)	Z_{in} (ohms)	Z_{out} (ohms)
			FRT	79,85	69,2	30,15	19,25
			FRB	25,3	20,55	46,85	17,95
			FLT	52,7	45,95	5,65	4,15
			FLB	78,55	62,15	50,7	5,35
			BRT	37	10,55	8,3	7,75
			BRB	22,65	2,5	9	9,4
			BLT	45,9	31,9	5,9	6,05
			BLB	17,85	16,05	25,9	26,95
Subject 5	Weight 57 kg	Height 166,4 cm	Electrode Position	Z_{in} (ohms)	Z_{out} (ohms)	Z_{in} (ohms)	Z_{out} (ohms)
			FRT	43,25	50,3	111,5	69,5
			FRB	101,6	46	106,55	61,3
			FLT	51,1	44,6	34,25	38,1
			FLB	58,3	40,8	47,5	21,35
			BRT	61,35	15,2	37,25	51,65
			BRB	85	36	26,6	25,7
			BLT	115,8	103,1	56,9	51,4
			BLB	55,4	47,85	34,6	22,45

Table 8.2.3

8.2.4 Electrical Impedance of lungs of the Smokers aged between 27-30 years

Smoker, Age 27-30 years							
				Frequency = 5 kHz		Frequency = 50 kHz	
			Electrode Position	Z_{in} (ohms)	Z_{out} (ohms)	Z_{in} (ohms)	Z_{out} (ohms)
Subject 1	Weight 56,4 kg	Height 175,26 cm	FRT	164,65	156,1	46,5	31,1
			FRB	25,4	30,06	64,35	49,5
			FLT	69,45	29,91	73,85	64,1
			FLB	180,05	149,34	73	60,95
			BRT	71,5	43,96	10,2	7,45
			BRB	33,25	43,06	14,65	6,95
			BLT	29	23,79	11,1	6,3
			BLB	49,05	25,29	40,55	41,25
Subject 2	Weight 58 kg	Height 177,8 cm	Electrode Position	Z_{in} (ohms)	Z_{out} (ohms)	Z_{in} (ohms)	Z_{out} (ohms)
			FRT	104,65	121	128,5	103,7
			FRB	283,5	299,5	28,9	18,45
			FLT	323	277,5	398	403,5
			FLB	104	82,1	14,85	17,85
			BRT	137,2	35,35	32,9	15,65
			BRB	87	56,3	21,4	22,1
			BLT	44,5	32,6	18,85	16,75
			BLB	147,5	121,5	84,2	85,35
Subject 3	Weight 68,2 kg	Height 160,02 cm	Electrode Position	Z_{in} (ohms)	Z_{out} (ohms)	Z_{in} (ohms)	Z_{out} (ohms)
			FRT	29,2	17,2	14,4	15,95
			FRB	40,9	32,65	43,7	15
			FLT	10,6	10,5	17	15,4
			FLB	90,5	39,45	57,35	47,3
			BRT	29,65	16,9	11	13,4
			BRB	10,6	8,05	8,25	11,7
			BLT	12,65	10,85	10,65	11,2
			BLB	21,4	15,4	9,85	9,35
Subject 4	Weight 72,1 kg	Height 170,2 cm	Electrode Position	Z_{in} (ohms)	Z_{out} (ohms)	Z_{in} (ohms)	Z_{out} (ohms)
			FRT	63,7	46,75	8,75	11,55
			FRB	68,9	29,1	11,15	10,75
			FLT	14,3	29,3	8,85	11,5
			FLB	11,95	15,25	40,45	20,55
			BRT	9,65	9,55	10,3	7,2
			BRB	23,55	17,2	6,6	4,45
			BLT	19,65	12,15	6,4	7,7
			BLB	18,4	11,7	8,8	8,3
Subject 5	Weight 76 kg	Height 167,6 cm	Electrode Position	Z_{in} (ohms)	Z_{out} (ohms)	Z_{in} (ohms)	Z_{out} (ohms)
			FRT	104	73	132,25	111,35
			FRB	366	155,9	77,2	46,9
			FLT	150,9	143	62,6	57,95
			FLB	107	91,85	257	195,5
			BRT	43,1	32,5	8,75	6,9
			BRB	63,2	43,35	35	37,7
			BLT	42,4	25,05	12,25	10,15
			BLB	18,95	12,75	15,4	11,75

Table 8.2.4

8.3 Tables for Change of Impedance (%) due to Ventilation Using 8-electrode FIM

8.3.1: Change of Impedance (%) with Respect to Inspiration

	Subjects	No of Obs.	BMI	change of Impedance (%) in Electrode Position (Inspiration)							
				FRT	FRB	FLT	FLB	BRT	BRB	BLT	BLB
Frequency =5 kHz	Age 23-26y, Non-Smoker	1,0	31,8	34,3	-5,7	-42,6	49,1	58,8	-1,4	-18,8	10,3
		2,0	36,3	12,2	37,7	60,6	16,9	28,6	55,0	49,9	-86,6
		3,0	31,2	10,0	-13,9	11,1	34,4	-0,6	23,0	29,7	-13,4
		4,0	26,0	42,7	-11,5	25,6	68,5	30,3	51,0	37,6	-67,9
		5,0	20,0	43,3	-11,0	35,5	-107,8	3,2	54,0	36,9	17,6
	Age 27-30y, Non-Smoker	1,0	32,1	9,4	46,0	50,6	21,4	-47,8	0,3	-31,6	11,2
		2,0	34,5	-42,8	30,2	35,1	32,3	1,9	13,5	-15,0	-4,0
		3,0	23,5	-292,7	2,6	42,9	21,0	48,8	-91,5	-31,0	48,4
		4,0	26,5	0,9	-39,2	-19,2	33,4	-23,7	39,8	-82,9	54,5
		5,0	30,7	-4,3	-4,2	1,7	41,6	-47,0	6,2	13,0	-14,3
	Age 23-26y, Smoker	1,0	22,1	24,0	54,4	88,1	19,9	7,7	60,7	59,5	17,9
		2,0	23,8	61,5	-17,2	20,5	33,1	-4,3	-2,0	55,5	55,1
		3,0	28,7	12,6	11,6	-2,2	23,2	73,6	37,7	32,5	34,4
		4,0	20,1	13,3	18,8	12,8	20,9	71,5	89,0	30,5	10,1
		5,0	20,7	-16,3	54,7	12,7	30,0	75,2	57,6	11,0	13,6
	Age 27-30y, Smoker	1,0	32,2	5,2	-18,3	56,9	17,1	38,5	-29,5	18,0	48,4
		2,0	18,3	-15,6	-5,6	14,1	21,1	74,2	35,3	26,7	17,6
		3,0	26,6	41,1	20,2	0,9	56,4	43,0	24,1	14,2	28,0
		4,0	24,9	26,6	57,8	-104,9	-27,6	1,0	27,0	38,2	36,4
		5,0	27,2	29,8	57,4	5,2	14,2	24,6	31,4	40,9	32,7
Frequency =50KHz	Age 23-26y, Non-Smoker	1,0	31,8	-2,6	41,2	-12,5	67,1	-2,2	12,4	-21,3	9,7
		2,0	36,3	18,6	31,5	-5,7	-20,2	9,6	-11,0	3,5	-6,4
		3,0	31,2	69,2	50,5	32,1	-111,2	-90,1	-10,4	-14,2	41,7
		4,0	26,0	18,1	-21,2	4,7	-167,8	20,5	24,9	-3,5	-4,5
		5,0	20,0	46,8	9,9	15,8	4,6	33,5	43,3	0,3	10,3
	Age 27-30y, Non-Smoker	1,0	32,1	66,6	39,4	3,8	0,1	75,0	69,1	-2,3	12,8
		2,0	34,5	-16,7	11,9	23,8	18,1	-0,8	0,5	-3,8	4,1
		3,0	23,5	-19,0	42,6	58,0	40,3	3,0	39,6	39,5	7,3
		4,0	26,5	3,8	-382,7	-8,7	10,0	9,6	36,9	-2,6	11,0
		5,0	30,7	20,1	57,6	42,7	19,4	33,2	50,0	33,7	81,1
	Age23-26y, Smoker	1,0	22,1	9,9	-117,9	9,4	59,2	44,4	-16,6	14,4	-11,8
		2,0	23,8	36,5	-54,4	1,9	16,8	13,1	44,1	0,6	7,8
		3,0	28,7	38,9	11,0	9,4	-68,4	-85,2	4,7	42,8	-21,4
		4,0	20,1	36,2	61,7	26,5	89,4	6,6	-4,4	-2,5	-4,1
		5,0	20,7	37,7	42,5	-11,2	55,1	-38,7	3,4	9,7	35,1
	Age27-30y, Smoker	1,0	32,2	33,1	23,1	13,2	16,5	27,0	52,6	43,2	-1,7
		2,0	18,3	19,3	36,2	-1,4	-20,2	52,4	-3,3	11,1	-1,4
		3,0	26,6	-10,8	65,7	9,4	17,5	-21,8	-41,8	-5,2	5,1
		4,0	24,9	-32,0	3,6	-29,9	49,2	30,1	32,6	-20,3	5,7
		5,0	27,2	15,8	39,2	7,4	23,9	21,1	-7,7	17,1	23,7

Table 8.3.1

8.3.2: Change of Impedance (%) with Respect to Expiration

	Subjects	No of Obs.	BMI	change of Impedance (%) in Electrode Position (Expiration)							
				FRT	FRB	FLT	FLB	BRT	BRB	BLT	BLB
Frequency =5 kHz	Age 23-26y, Non-Smoker	1,0	31,8	52,3	-5,4	-29,9	96,6	142,4	-1,4	-15,8	11,5
		2,0	36,3	14,0	60,6	153,5	20,4	40,1	122,2	99,5	-46,4
		3,0	31,2	11,1	-12,2	12,5	52,5	-0,6	29,9	42,3	-11,8
		4,0	26,0	74,4	-10,3	34,5	217,0	43,4	104,0	60,2	-40,4
		5,0	20,0	76,5	-9,9	55,0	-51,9	3,3	117,2	58,5	21,3
	Age 27-30y, Non-Smoker	1,0	32,1	10,4	85,2	102,5	27,2	-32,3	0,3	-24,0	12,6
		2,0	34,5	-30,0	43,3	54,1	47,7	1,9	15,7	-13,0	-3,8
		3,0	23,5	-74,5	2,7	75,1	26,7	95,4	-47,8	-23,7	93,7
		4,0	26,5	1,0	-28,2	-16,1	50,2	-19,2	66,2	-45,3	119,6
		5,0	30,7	-4,1	-4,0	1,8	71,1	-32,0	6,6	14,9	-12,5
	Age 23-26y, Smoker	1,0	22,1	31,6	119,1	738,0	24,8	8,4	154,5	147,0	21,9
		2,0	23,8	159,5	-14,7	25,8	49,6	-4,1	-2,0	124,7	122,5
		3,0	28,7	14,4	13,1	-2,2	30,2	279,3	60,4	48,2	52,6
		4,0	20,1	15,4	23,1	14,7	26,4	250,7	806,0	43,9	11,2
		5,0	20,7	-14,0	120,9	14,6	42,9	303,6	136,1	12,3	15,8
	Age 27-30y, Smoker	1,0	32,2	5,5	-15,5	132,2	20,6	62,7	-22,8	21,9	94,0
		2,0	18,3	-13,5	-5,3	16,4	26,7	288,1	54,5	36,5	21,4
		3,0	26,6	69,8	25,3	1,0	129,4	75,4	31,7	16,6	39,0
		4,0	24,9	36,3	136,8	-51,2	-21,6	1,0	36,9	61,7	57,3
		5,0	27,2	42,5	134,8	5,5	16,5	32,6	45,8	69,3	48,6
Frequency =50KHz	Age 23-26y, Non-Smoker	1,0	31,8	-2,5	70,0	-11,1	203,9	-2,1	14,1	-17,5	10,8
		2,0	36,3	18,1	53,5	-5,1	-61,5	9,4	-12,5	2,9	-7,0
		3,0	31,2	225,1	101,8	47,4	-52,6	-47,4	-9,4	-12,4	71,4
		4,0	26,0	22,1	-17,5	4,9	-62,7	25,8	33,1	-3,4	-4,3
		5,0	20,0	88,0	11,0	18,7	4,8	50,3	76,4	0,3	11,5
	Age 27-30y, Non-Smoker	1,0	32,1	199,5	65,1	3,9	0,1	299,7	223,4	-2,3	14,7
		2,0	34,5	-14,3	13,5	31,3	22,1	-0,8	0,5	-3,7	4,3
		3,0	23,5	-16,0	74,2	138,4	67,5	3,1	65,5	65,2	7,9
		4,0	26,5	3,9	-79,3	-8,0	11,1	10,6	58,5	-2,5	12,4
		5,0	30,7	25,1	135,6	74,6	24,1	49,7	100,0	50,9	429,4
	Age 23-26y, Smoker	1,0	22,1	11,0	-54,1	10,4	144,9	79,7	-14,2	16,8	-10,6
		2,0	23,8	57,5	-35,2	2,0	20,2	15,0	78,8	0,6	8,5
		3,0	28,7	63,7	12,3	10,4	-40,6	-46,0	4,9	74,8	-17,6
		4,0	20,1	56,6	161,0	36,1	847,7	7,1	-4,3	-2,5	-3,9
		5,0	20,7	60,4	73,8	-10,1	122,5	-27,9	3,5	10,7	54,1
	Age 27-30y, Smoker	1,0	32,2	49,5	30,0	15,2	19,8	36,9	110,8	76,2	-1,7
		2,0	18,3	23,9	56,6	-1,4	-16,8	110,2	-3,2	12,5	-1,3
		3,0	26,6	-9,7	191,3	10,4	21,2	-17,9	-29,5	-4,9	5,3
		4,0	24,9	-24,2	3,7	-23,0	96,8	43,1	48,3	-16,9	6,0
		5,0	27,2	18,8	64,6	8,0	31,5	26,8	-7,2	20,7	31,1

Table 8.3.2

References

A

Abir R, Pettersen F J, Martinsen O G and Rabbani K S (2013) Effect of a spherical object in 4 electrode focused impedance method (FIM): measurement and simulation. *J. Phys.: Conf. Ser.* **434** 012009

Ahmed OB, Lopez AD , Inoune M (2000) The decline in child mortality: a reappraisal. *Bull World Health Organ.* **78** 1175–91

Amin A A, Parvin S, Kadir M A, Tahmid T, Kaisar S A, Rabbani K S (2014) Classification of breast tumour using electrical impedance and machine learning techniques. *Physiol. Meas.* **35** 965–974 doi:10.1088/0967-3334/35/6/965

B

Bangladesh Demographic Health Survey (2004) National Institute of Population Research and Training. Dhaka/Calverton (2005) MD: Mitra and Associates/ORC Macro

Barber DC, Brown, B.H (1984) Applied Potential Tomography. *J. Phys. E:Sci. Instrum* **17 (9)** 723–733 doi:10.1088/0022-3735/17/9/002

Baqui AH, Sabir AA, Begum N, Arifeen SE, Mitra SN, Black RE (2001) Causes of childhood deaths in Bangladesh: an update. *Acta Paediatr* **90** 682–90

Black RE, Morris SS, Bryce J (2003) Where and why are 10 million children dying every year? *Lancet* **361** 2226–34

Bordi F, Cametti C and Gili T (2001) Reduction of the contribution of electrode polarization effects in the radiowave dielectric measurement of highly conductive biological cell suspensions. *Bioelectrochem* **54** 53-61

Brooks WA, Santosham M, Naheed A (2005) Effect of weekly zinc supplements on incidence of pneumonia and diarrhoea in children younger than 2 years in an urban, low-income population in Bangladesh: randomised controlled trial. *Lancet* **366** 999–1004

Brown BH, Wilson A J and Bertemes-Filho P (2000) Bipolar and tetrapolar transfer impedance measurements from volume conductor. *Electron. Lett.* **36** 2060

Bryce J, Boschi-Pinto C, Shibuya K, Black RE (2005) WHO estimates of the causes of death in children. *Lancet*; **365** 1147–52

C

Cole KS (1928a) Electrical impedance of suspension of spheres. *J Gen Physiol* **12** 29-36

Cole KS (1928b) Electrical impedance of suspension of arbacia cells. *J Gen Physiol* **12** 37-54

Cole KS (1934) Alternating current conductance and direct current excitation of nerve. *Science* **79** 164-165

Cole KS (1940) Permeability and impermeability of cell membranes for ions. *Cold Spring Harbor Sympos Quant Biol* **8** 110-122

Cole KS & Cole RH (1941) Dispersion and absorption in dielectrics .I. Alternating current characteristics. *J Chem. Pys* **9** 341-351

COMSOL (2013) COMSOL Multiphysics Reference Manual. Part of software package.

Crile G W, Hosmer R H, Rowland A F (1922) The electrical conductivity of animal tissue under normal and pathological conditions. *American Journal of Physiology* **60** 59-106

F

Ferdous H, Baig T N & Rabbani K S (2013) Thorax mapping for localised lung Impedance change using focused impedance measurement (FIM): A pilot study. *Journal of Electrical Bioimpedance* **4** 57-61. doi:10.5617/jeb.778

Fricke H (1932) The theory of electrolytic polarization. *Phil.Mag.* **14** 310-318

Frerichs I, Hahn G, Schroder T, Hellige G (1998) Electrical impedance tomography in monitoring experimental lung injury. *Intensive Care Med* **24** 829-836

Funatogawa I, Funatogawa T, Yano E (2012) Impacts of early smoking initiation: long-term trends of lung cancer mortality and smoking initiation from repeated cross-sectional surveys in Great Britain. *BMJ Open* **2**:e001676 doi:10.1136/bmjopen-2012-001676

G

Gabriel C and Gabriel S (1996) Compilation of the dielectric properties of body tissues at RF and microwave frequencies. *Report No AL/OE-TR-1996–0037* (Armstrong Laboratory (AFMC), Brooks Air Force Base, TX, USA)

Geselowitz DB (1971) An application of electrocardiographic lead theory to impedance plethysmography. *IEEE Trans. Biomed. Eng.* **18** 38–41

Griffiths H, Ahmed A (1987) Applied Potential Tomography for non-invasive temperature mapping in hyperthermia. *Clin Phys Physiol Meas* **8 (suppl A)** 147-153

Grimnes S and Martinsen ØG (2008) *Bioimpedance and Bioelectricity Basics* 2nd ed (San Diego: Academic)

Grimnes S and Martinsen ØG (2007) Sources of errors in tetrapolar impedance measurements on biomaterials and other ionic conductors. *J. Phys. D: Appl. Phys.* **40** 9

H

Haowlader S, Baig T N, Rabbani K S (2010) Abdominal fat thickness measurement using Focused Impedance Method (FIM) - phantom study. *J. Phys. Conf. Ser.* (IOP Publishing) **224** doi:10.1088/1742-6596/224/1/012061

Harris ND, Sugget AJ, Barber DC, Brown BH (1987) Application of applied potential tomography (APT) in respiratory medicine. *Clin Phys Physiol Meas* **8 (Suppl A)** 155-165

Holder DS (1992) Detection of cortical spreading depression in anesthetised rat by impedance measurement with scalp electrodes-implications for noninvasive imaging in the brain with electrical impedance tomography. *Clin Phys Physiol Meas* **13 (1)** 77-86

Humphries S J (1997) *Field Solution on Computers* (Boca Raton, FL: CRC Press)

I

Islam, Naimul, Rabbani, K Siddique-e and Wilson, Adrian J (2010) The sensitivity of focused electrical impedance measurements. *Phys. Meas.* **31** S97-S109

Iquebal A H M, Rabbani K S (2010) 3D sensitivity of 6-electrode Focused Impedance Method (FIM). *J. Phys.: Conf. Ser* **224** 012156

J

Jossinet J, Schmitt M (1998) Alternative parameters for the characterisation for breast tissue. *Proceedings of the X International Conference on Electrical Bioimpedance* pp 45-48

K

Kadir MA , Baig TN, Rabbani KS (2009) Application of 6-electrode Focused Impedance Method (FIM) to study lungs ventilation. *Proceedings, 10th International Conference on Biomedical Applications of Electrical Impedance Tomography,* Manchester, UK.

Kadir MA, Ferdous H, Baig TN and Rabbani KS (2010) Ventilation mapping of chest using Focused Impedance Method (FIM). *J. Phys.: Conf. Ser.* (IOP Publishing) **224** 012031

Karal MAS, Rabbani KS (2008) Sensitivity of Four-electrode Focused Impedance Measurement (FIM) for objects with different conductivity. *Annals of biomedical engineering* **36** 1072-7

Khambete N D, Shashidhara J, Bhuvaneshwar GS and Sivakumar R (1995) Impedance Measurement system for concentric needle electrodes. *Proc. RC IEEE-EMBS and 14th* 1.1-1.2

Khambete N, Metherall P, Brown BH, Smallwood RH and Hose R (1999) Can we optimize electrode placement for impedance Pneumography ? *Annals of the New York Academy of Science,* **873** 534-542

Khambete ND, Brown BH, Smallwood RH (2000) Movement artefact rejection in impedance pneumography using six strategically placed electrodes. *Physiol. Meas*. **21(1)** 79-88

M

McAdams ET, Jossinet J (1994) The detection of the onset of electrode-electrolyte interphase impedance nonlinearity: a theoretical study. *IEEE Trans Biomed Eng* **41(5)** 498-500

Mangnall YF, Baxter AJ, Avill R, Brid NC, brown BH, Barber DC, Seagar AD, Jhonson AG, Read NW (1987) Applied potential tomography: a new non-invasive technique for assessing gastric function. *Clin Phys Physiol Meas* **8 (suppl A)** 1999-130

Martinsen Ø.G, Nordbotten B, Grimnes S, Fossan H, Eilevstjønn J (2014) Bioimpedance based respiration monitoring with a defibrillator. *IEEE Trans. Biomed. Eng.* **61** 1858-1862

Mulholland K (2003) Global burden of acute respiratory infections in children: implications of interventions. *Pediatr Pulmonol* **36** 469–74

Murphy D, Burton P, Coombs R, Tarassenko L, Rolfe P (1987) Impedance imaging in newborn. *Clin Phys Physiol Meas* **8 (Supp A)** 131-140

N

Nopp P, Rapp E, Pfutzner H, Nakesch H and Ruhsam C (1993) Dielectric properties of lung tissue as a function of air content *Phys. Med. Biol*. **38** 699-719. http://dx.doi.org/ 10.1088/0031-9155/38/6/005

P

Pettersen F-J, Ferdous H, Kalvøy H, Martinsen Ø G, Høgetveit JO (2014) Comparison of four different FIM configurations—a simulation study. *Physiol. Meas,*. **35** 1067–1082. doi:10.1088/0967-3334/35/6/1067

Pettersen F-J and Høgetveit JO (2011) From 3D tissue data to impedance using Simpleware Scan FE+IP and COMSOL Multiphysics-a tutorial. *J. Electr. Bioimp.* **2** 13-32

Phelps ME, Hoffman EJ, Mullani NA, Ter-Pogossian MM (1975) Application of annihilation coincidence detection to transaxial reconstruction tomography. *Journal of Nuclear Medicine* **16 (3)** 210–224

R

Rabbani KS, Sarker M, Akond MHR and Akter T (1998) Focused Impedance Measurement (FIM) a new technique with zone localization. *Proceeding of the X International conference on Electrical Bioimpedance*, Barcelona, Spain 31-34

Rabbani KS, Sarker M, Akond MHR and Akter T (1999) Focused Impedance Measurement (FIM) a new technique with improved zone localization. *Ann. N Y Acad. Sci.* **873** 408-420 http://dx.doi.org/10.1111/j.1749-6632.1999.tb09490.x

Rabbani KS (2010) Focused Impedance Method (FIM) and Pigeon Hole Imaging (PHI) for localized measurements – a review. *J. Phys. Conf.* Ser. **224** 012003 doi:10.1088/1742-6596/224/1/012003

Rabbani KS and Kadir MA (2011) Possible applications of Focused Impedance Method (FIM) in biomedical and other areas of study. *Bangladesh Journal of Medical Physics*, **4(1)** 67-74

Russel WMS and Burch RL (1959) The principles of human experimental technique. (London: Methuen)

Raicu V, Saibara T and Irimajiri A (1998) Dielectric properties of Rat liver in vivo: a noninvassive using open ended coaxial probe at audio/radio frequencies. *Bioelectrochem. Bioener*. **47** 325-332

Rosell J, Murphy D, Pallas-Areny R, Rolfe P (1988b) Analysis and Assessment of errors in parallel data acquisition system for electrical impedance tomography. *Clin Phys Physiol Meas* **9 (supp A)** 93-100

S

Schwan HP (1954) Die elektrischen Eigenschaften von Muskelgewebe bei Niederfrequenz. *Z Naturfor* **9b**, 245

Schwan HP (1957) Electrical Properties of tissue and cell suspensions. In: Lawrence JH, Tobias CA (Eds). *Advances in biological and medical physics* **Vol V** Academic Press pp 147-209

Schwan HP (1957) The conductivity of living tissue. *Ann NY Acad Sci*, **65**, 1007

Schwan HP (1962) Electrical Properties of the membranes of the pleuro-pneumonia-like organism A5969. *Biophys J* **2,** 295

Schwan HP (1963) Determination of biological impedances. In: Nastuk WL (ed.). *Physical techniques in biological research* **Vol 6** Academica Press pp 323-406

Schwan HP (1992) Linear and Nonlinear Electrode Polarization and Biological Materials. *Ann Biomed. Eng*. **20** 269-288

Scott JE (2004) The Pulmonary Surfactant: Impact of Tobacco Smoke and Related Compounds on Surfactant and Lung Development. *Tobacco Induced Diseases* **2 (1)** 3-25, 2004 . doi:10.1186/1617-9625-2-1

Smallwood RH, Mangnallm YF, Leathard AD (1994) Transport of gastric contents. *Physiol Meas* **15 (suppl 2A)** 175-188

Surovy N J, Billah M MD, Haowlader S, Al-Quaderi G D, Rabbani K S (2012) Determination of abdominal fat thickness using dual electrode separation in the focused impedance method (FIM). *Phys. Meas*. **33** 707–718

T

Ter-Pogossian MM, Phelps ME, Hoffman EJ, Mullani NA (1975) A positron-emission transaxial tomograph for nuclear imaging (PET). *Radiology* **114** (1): 89-98.

W

World Health Organization. WHO report on the global tobacco epidemic: The MPOWER package. Geneva: World Health Organization, 2008.

Z

Zaman K, Baqui AH, Yunus M (1997) Acute respiratory infections in children: a community-based longitudinal study in rural Bangladesh. *J Trop Pediatr* **43** 133–7

I

Ventilation mapping of chest using Focused Impedance Method (FIM)

M Abdul Kadir[1], Humayra Ferdous[2], Tanvir Noor Baig[2] and K Siddique-e-Rabbani[1]
[1]Department of Biomedical Physics & Technology, University of Dhaka, Dhaka-1000, Bangladesh
[2]Department of Physics, University of Dhaka, Dhaka-1000, Bangladesh

email: rabbani@univdhaka.edu

Abstract: Focused Impedance Method (FIM) provides an opportunity for localized impedance measurement down to reasonable depths within the body using surface electrodes, and has a potential application in localized lung ventilation study. This however needs assessment of normal values for healthy individuals. In this study, localized ventilation maps in terms of electrical impedance in a matrix formation around the thorax, both from the front and the back, were obtained from two normal male subjects using a modified configuration of FIM. For this the focused impedance values at full inspiration and full expiration were measured and the percentage difference with respect to the latter was used. Some of the measured values would have artefacts due to movements of the heart and the diaphragm in the relevant anatomical positions which needs to be considered with due care in any interpretation.

1. Introduction

Monitoring of physiological events by impedance has become a subject matter of great interest for the last few decades. Dielectric properties of lungs tissue change as a function of air content [1], therefore lungs ventilation makes a potential area of application of electrical impedance techniques. Electrical Impedance Tomography (EIT) has been applied in the study of lungs ventilation successfully to explore lungs physiology as well as to monitor and diagnose lungs disorders and injury [2][3]. A relatively new development in the field of bio-impedance measurement is the Focused Impedance Method (FIM) [4][5], developed at the authors' laboratory at Dhaka University, in which two pairs of current drive electrodes perpendicular to each other over a common zone at the center are used to apply alternating currents of constant amplitude separately. Two potential measuring electrodes with a smaller separation, placed at the centre at an angle of 45^0 to either of the current drive directions, are used to measure the potentials resulting from each of the current drives. The sum of the two measured potentials has a dominant contribution from the central region, approximately a square with the potential electrodes at the diagonal points. Therefore this gives localized sensitivity at the central region which has been termed as the focused region. Because of a 3D sensitivity, FIM electrodes, placed on the skin surface, may be used to monitor changes at a depth, and has been successful in measuring gastric emptying [5]. FIM applied to a localized region of lung showed a linear relationship to change in expired volume of air in a subject [6]. It needs to be seen if FIM could be used to detect and quantify changes in localised lung ventilation, for potential use in detection and diagnosis of localized lung ventilation disorders. In this preliminary study, the FIM impedance change between

maximum inspiration and maximum expiration at different localized segments of the thorax of some healthy human subjects was measured using the 6 electrode FIM system to get a ventilation mapping matrix, with the above aim.

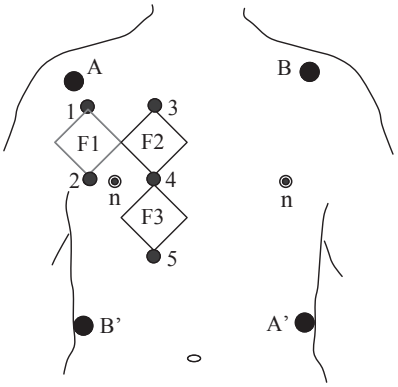

Figure 1. Electrode configuration and focused zones for ventilation mapping of human thorax. Current electrode pairs: A-A', B-B'. Potential electrodes pairs: 1-2, 3-4, 4-5, etc. giving focused zones F1, F2, F3, etc. respectively.

2. Methods and Measurements

Here the FIM has been applied with some modifications in order to facilitate measurement and standardization as shown in figure 1. A 10kHz alternating current of constant amplitude (approx. 0.5mA) was passed, in sequence, through two orthogonal electrode drive pairs A-A' and B-B' as shown, by switching the pairs manually. These electrodes were placed such that they make the largest possible approximate square on the chest. Using a hand-held probe, two potential measuring electrodes, 10cm apart, were then placed vertically at different places, such as at 1&2, 3&4, etc. on the chest. For each placement, the two potentials developed due to the two orthogonal current drives were recorded and summed, which essentially gave a value proportional to the focused impedance within the respective zones F1, F2, etc., since the current amplitudes were constant. Measurements were taken with the subject taking a deep breath (maximum inspiration) and then with the subject breathing out as much as possible (maximum expiration). The difference was expressed as a percentage of the value at maximum expiration, which is described as the %change of focused impedance in this work. Each measurement was repeated once and averaged to minimise the effect of changing blood volume in the heart. This %change in impedance is essentially a ventilation parameter of the lungs in the respective focused region, down to a certain depth. The procedure was then repeated with the potential electrode pair placed at different points on the chest in a predefined matrix. Similar measurements were carried out on the back as well. The breast nipple level (indicated by n-n) was taken as an anatomical reference for placement of potential electrodes. Measurements were made with the subject standing upright. The total volume of air exhaled by the subject in each of these procedures is a function of the lungs volume and is known as the Vital Capacity (VC), which was measured using a bellows type spirometer and recorded. Measurements were carried out on two normal healthy young male subjects having no complaints regarding respiration.

3. Results and observations

The %change of focused impedance between maximum inspiration and maximum expiration at localized segments of the thorax were calculated for each subject to get the ventilation mapping matrix, from the front and from the back, and are presented in figures 2 and 3 respectively. These are superimposed on the outline of a human thorax giving the outline of the lungs and the heart as well. The positions of the current electrodes are shown as grey circles. The matrix positions obtained from the back were flipped horizontally to give the same right and left orientation. Some relevant subject

information including their vital capacity (VC) are given in the respective figure captions. Two extreme left and right regions on ventilation mapping matrix represent the impedance changes on lateral curved parts of the thorax. The back side offered measurements on a few extra matrices at the top, and are also shown. The positions of the nipples of the breasts are shown as black dots.

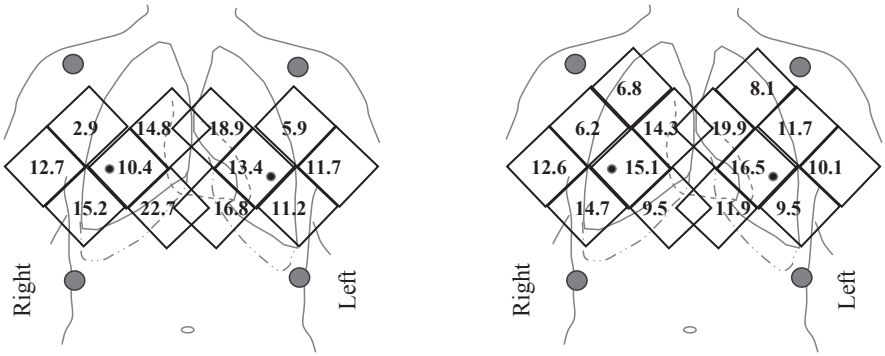

a) measured from front b) measured from back

Figure 2. Ventilation mapping of a subject from front (a) and back (b). Matrices from back has been arranged to match the view from the front. Subject age: 26 yrs, height: 1.71m, weight: 52 kg, Vital Capacity: 4.8 litres, non-smoker.

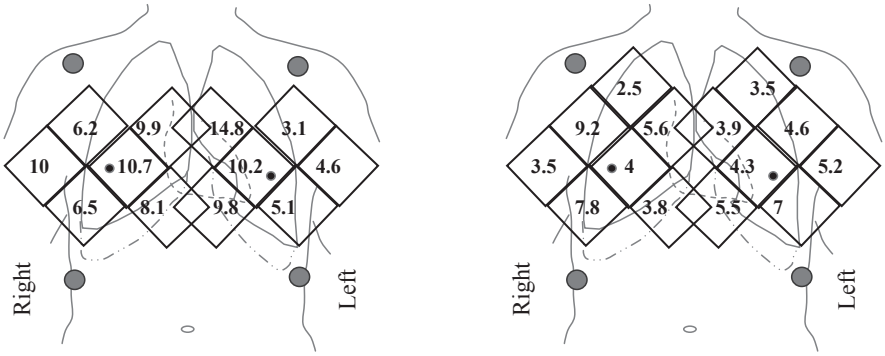

a) measured from front b) measured from back

Figure 3. Ventilation mapping of another subject from front (a) and back (b). Subject age: 20yrs, height: 1.68m, weight: 56 kg, Vital Capacity: 4.1 litres, non-smoker.

4. Discussions

The present work was taken up to have an overall idea of localized impedance change throughout the thorax due to lung ventilation using the newly developed 6-electrode FIM system. It is expected that the change in air content will be reduced if part of the lung is filled with water, blood of injury, or any

other substance. In such cases, the impedance change measured in that region would be significantly reduced and this can possibly be detected by FIM. However to predict such distinction between localized zones of a healthy lung and a diseased lung a standard set of values are needed, and this should be based on measurements taken on a large number of healthy normal subjects.

The changes in air contents during ventilation in different regions of the lungs are different depending on the anatomical structure of the lungs. The expected change of impedance due to change in air content is visible from the maps in figures 2 and 3. The values in the corresponding matrices along the level of the nipple in the frontal measurement are similar for both the subjects; however for matrices above and below, there appears to be some difference. For subject 1 values of corresponding zones from the front and from the back are similar for nipple level, but are different at other levels. On the other hand, values from the front and back for subject 2 are different even at nipple level. Further work is required to resolve, or understand the cause for such discrepancies. The differences in VC between the two subjects need to be noted. Besides, there could be experimental error due to variation in the effort a person exerts in full inspiration and full expiration and posture of the subject. The inter-electrode separation plays a big role in the measurement [7] and has to be considered to set up a standard. The contribution of perfused blood should also be taken into account, however, by averaging the readings over a few seconds with breath-hold, this effect may be eliminated.

FIM looks at a limited region of the lungs, however, there is some spread in sensitivity including negative values beyond the focused zone [7] which may become significant in certain situations, and should be considered to get an improved result and standardization. Again, if the sensitive zone includes a boundary of the lungs, particularly on the lower side, it may cause a large error since the changes will be due to several factors including the movement of the diaphragm, besides lung ventilation. Therefore these areas need to be avoided. Similarly the cardiac region is best avoided because of the movement of the heart between the breathing cycles. Measurements from the sides and back may be useful for measurements around the heart. Again for female subjects, frontal measurements of lungs may be difficult because of fatty tissues, and measurement from the back may be desired.

Although EIT appears to offer pixel level resolution, 2D EIT images are cluttered by objects in 3D, and have limited accuracy. Therefore, for applications such as studies of lungs, the much simpler FIM may offer an acceptable solution for clinical applications, and therefore it seems justified to take up further study in this direction.

5. Acknowledgements

Acknowledgements are due to the two volunteers who took part in this study.

6. References:

[1] Nopp P, Rapp E, Pfutzner H, Nakesch H and Ruhsam C 1993 *Phys Med Biol* **38**:699-716
[2] Harris ND, Suggett AJ, Barber DC and Brown BH 1987 *Clin. Phys. Physiol. Meas.* ***8 Sup1.A*** 155-165
[3] Frerichs I., Hahn G., Schroder T., Hellige G 1998 *Intensive Care Med* **24**: 829-836
[4] Rabbani KS, Sarker M, Akond MHR. and Akter T 1998 *Proceedings of the X International conference on Electrical Bioimpedance,* Barcelona, Spain. 31-34
[5] Rabbani KS, Sarker M, Akond MHR. and Akter T 1999 *Ann. N Y Acad. Sci*. **873**: 408-420
[6] Kadir MA, Baig TN and Rabbani KS 2009 *Proceedings (on-line), 10th International Conference on Biomedical Applications of Electrical Impedance Tomography (EIT 2009), Manchester, UK,* http://www.maths.manchester.ac.uk/eit2009/abstracts/kadir.pdf
[7] Howlader S, Baig TN and Rabbani KS 2010 *Proceedings, International Conference on Electrical Bioimpedance,* Florida, USA

.

II

Journal of Electrical Bioimpedance
www.bioimpedance.net

J Electr Bioimp, vol. 4, pp. 57–61, 2013
Received: 04 Dec 2013, published: 28 Dec 2013
doi:10.5617/jeb.778

Thorax mapping for localized lung impedance change using focused impedance measurement (FIM): A pilot study

Humayra Ferdous [1,3], Tanvir Noor Baig [2] and K. Siddique-e Rabbani [2,3]

1. *Department of Physics, University of Oslo, Oslo, Norway*
2. *Department of Biomedical Physics and Technology, University of Dhaka, Dhaka-1000, Bangladesh*
3. *E-mail any correspondence to: humayraf@student.matnat.uio.no or rabbani@univdhaka.edu*

Abstract
Focused impedance measurement (FIM) is a technique where impedance can be measured with the optimum level of localization without much increase in complexity of measuring instrument. The electrodes are applied on the skin surface while the organs inside also contribute to the measurement, as the body is a volume conductor. In a healthy and disease free lung region, the air enters at breathe-in, increases the impedance of the lung, and impedance reduces during breathe-out. In contrast, for a diseased lung, where part of the lungs is filled with water or some fluid, air will not enter into this zone reducing impedance change between inspiration and expiration. With this idea, the current work had been executed to have general view of localized impedance change throughout thorax using 6-electrode FIM. This generated a matrix mapping from both the front and from the back of the thorax, which showed how impedance change due to ventilation varies from frontal plane to back plane of human bodies.

Keywords: Focused impedance measurements, FIM, lung impedance, bioimpedance

Introduction

Focused impedance measurement (FIM) [1, 2] is a comparatively new technique that had been developed at the Department of Biomedical Physics and Technology (BMPT) of the University of Dhaka for measuring impedance. It has three versions having 8, 6 and 4 electrodes in special configurations. In a 6-elctrode-FIM, current is driven through two concentric pairs of orthogonal electrodes while another pair of electrodes with a smaller separation is placed at 45° to either of the current drive directions at the central zone for potential measurement. The resultant potential measurement possesses has a dominant influence from the central zone, which is nearly a square with the potential electrodes at the diagonal points. Thus it localizes the sensitivity at the central area, which has been termed the "focused zone."

FIM with its 3D sensitivity had been effective in the study of measuring gastric emptying [2]. A linear relationship to change in expired volume of air was found in a previous study when implemented to a focused zone of the lung in a subject [3]. In principle, the dielectric properties of lung tissue varies greatly as a result of air ventilation, between expiration and inspiration [4], which ultimately offers an area of opportunity to implement electrical impedance measurement systems for further study, such as for lung disease detection. However, to apply FIM for lung impedance study and disorder detection, it is essential to verify whether FIM can be applied to measure the changes of lung impedance due to ventilation in localized regions. In the current work the 6-electrode FIM had been applied to some healthy human subjects to measure the change in impedance in between full inspiration and full expiration.

Materials and methods

Instrumentation

Instrumentation for FIM developed earlier at BMPT was used for the present study. A simplified block diagram is shown in Figure 1 [2]. A sinusoidal signal, 10 kHz, is split up into two isolated current drives (AA' and BB'). This was done through appropriate voltage to current converters and isolating transformers. The circle in Figure 1 represents an object under test, which could be a human body. Amplitudes of each of the current drives were adjusted to have two equal perpendicular driving currents. The phases of the current drives were adjusted through the electrode connections such that the output signal at u and v of both the orthogonal drives appear in phase. Thus a single measurement of potential across u and v gives the sum of the combined transfer impedance in both the orthogonal directions. Subsequent amplification and signal conditioning circuitry gives a dc signal that is proportional to the combined impedance. This dc output voltage was measured using a digital voltmeter.

Subject selection

The present work was performed at BMPT and volunteers were mainly students of this department, with no known acute or chronic lungs disease and with no previous complaint of respiratory problems. All of them were non-smokers and their ages ranged from 17 to 26 years.

Electrode Configuration

The electrode arrangement was indicated in Figure 1, where electrode pairs AA' and BB' were the current drives while the potential was measured across the pair uv. In the present experiment this electrode configuration was used to

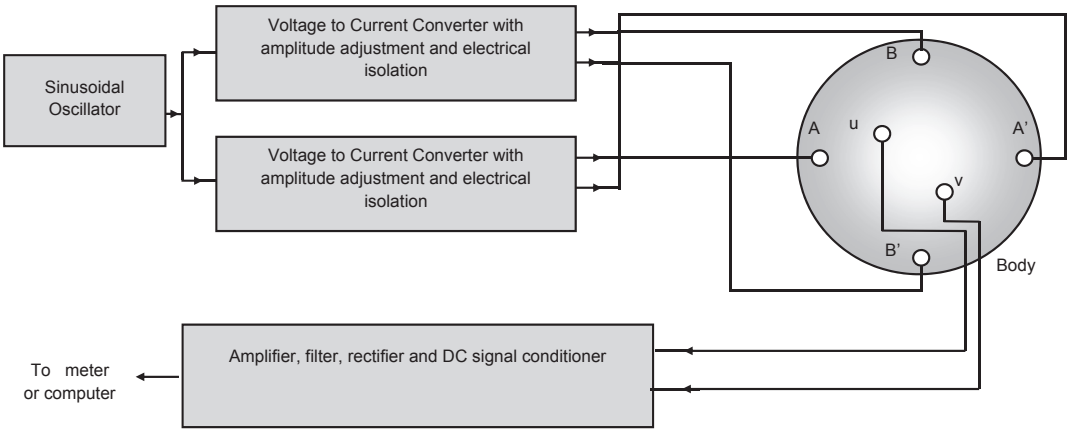

Fig. 1: A block diagram of the 6-electrode FIM instrumentation

map the lungs both from the front and from the back of the thorax. In this electrode configuration the focused region is defined by a square with uv as the diagonal, shown shaded in Figure 2.

To map consecutive focused zones on the thorax we placed the electrodes in a 'diamond' configuration, as shown in Figure 2, since the focused zone is tilted at 45° to the sides of the larger square formed by the current drive electrodes. As shown, the sides of the larger square were 4 inches (~10cm) while the diagonal of the smaller square was 2 inches (~5cm), corresponding to sides of about 1.4 inches (~3.5cm). The measurement required a common reference electrode, which was placed at the center (small black circle). The colors red and black are used for the two current drive pairs of electrodes in Figure 2 to indicate the relative phases (red indicating positive polarity at an instant). Figure 3 shows a picture of the hand held electrode probe used. Wet cotton wool is inserted into cylindrical recesses touching the metallic electrode inside an insulated cylindrical structure. Each electrode has a spring-loaded stem allowing perpendicular movement in order to ensure good connections at curved body surfaces.

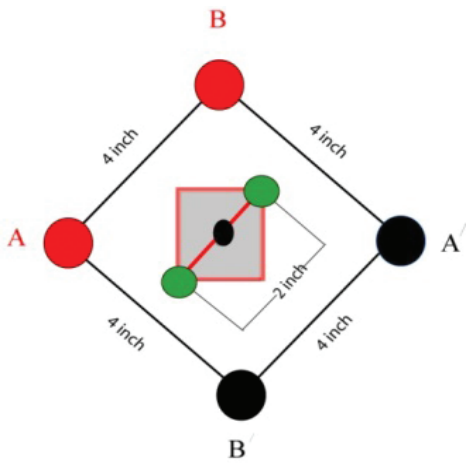

Fig. 2: The schematic diagram of 'diamond' type electrode configuration for the 6-electrode FIM system, the shaded square region bounded by red color represents the focused zone.

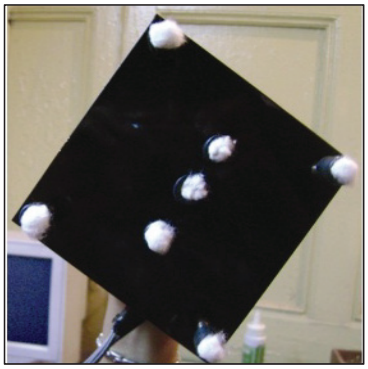

Fig. 3: The handheld electrode probe, seen from the electrode side. Wet cotton wool is inserted into recesses touching the metallic electrode inside. The stems of the electrodes are spring-loaded to ensure good contact at curved body surfaces.

Body mapping Matrix

As mentioned above, the side of the focused region is about 1.4 inches (~3.5cm). Therefore, to obtain the lung impedance map at successive square regions in a matrix as shown in Figure 4, we moved the electrode by the same distance horizontally and vertically, as indicated in Figure 5. To facilitate measurement on human subjects guiding points were marked out on the front and back of the thorax using a paper template as shown in the photographs of Figure 6. The cell numbers shown in the last two photographs were superimposed in computer later; these were not marked on the human subjects. Thus a standard design was developed so that the impedance changes at individual matrix locations can be compared among subjects of similar body size. Figure 4 also shows the

reference matrix numbers that were used in the analyses presented later.

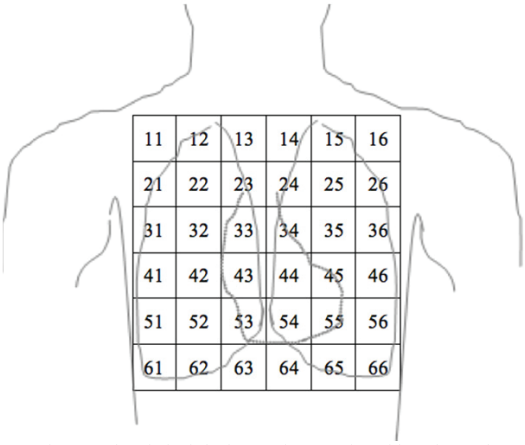

Fig. 4: The desired body-mapping matrix with values of impedance. The measurements are performed both from the front and the back.

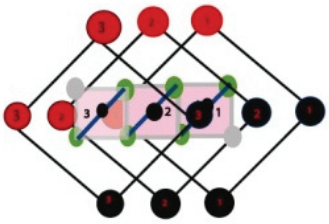

Fig. 5: Movement of hand held electrode probe to obtain the desired body mapping matrix.

Measurement of ventilation

Measurements were made with the subject standing straight. The output voltage of the FIM system, which was measured using a digital multi-meter, is proportional to the impedance of the focused region defined before. For each position of the electrode, a reading of the focused impedance was taken with the subject breathing in fully (forced maximum inspiration) and another reading with the subject breathing out as much as possible (forced maximum expiration). The difference was expressed as a percentage of the value at forced maximum expiration at that location. Measurements were taken from both the front and the back according to the matrix described before. Figure 7 shows typical measurement procedures from the front and from the back. The spring-loaded electrode stem allowed a good contact even at curved regions. The total volume of air between forced maximum inspiration and forced maximum expiration is known as forced vital capacity (FVC), which was measured using a bellows type spirometer.

Results

The results of the study on four subjects are presented in Table 1. The left major column shows the localized percentage change in impedance in each matrix location measured from the front of the thorax while the right major column shows the same as measured from the back. The right-left orientation of the measured values from the back was rearranged in the matrices to match that from the front, to enable a simple visual comparison. The age, height, weight, and forced vital capacity of the subjects are all indicated in the tables.

The values at each matrix element are assumed to correspond to localized ventilation within that region. It needs to be appreciated that the measured impedance values have the major contribution from the soft tissue underlying the skin, which does not change with ventilation. The depth sensitivity of the FIM decreases sharply with depth [5, 6], therefore, a small contribution comes from the ventilating lungs. Subtraction of the two values of impedance on inspiration and on expiration accentuated the ventilation, which was the justification of these attempts at measurement of ventilation.

Table 2 shows the comparison between the impedance percentages changes at frontal plane and backplane of the human bodies. However, the measured values near the edges were expected to be erroneous, because of two reasons: i) large curvatures at the sides making it difficult, even impossible for all electrodes of the probe to touch the skin properly, and ii) the movement of the edges of the expanding and contracting lungs falling within the measured regions, contributing to the measurement significantly. Therefore, the central matrix elements numbered 22 to 45 were considered for the present analysis.

Table 3 was developed to represent the comparison of impedance percentage change between the right side and the left side of each plane. In this particular comparison column 2 and 3 of each plane were considered the right side of the body whereas column 4 and 5 were considered the

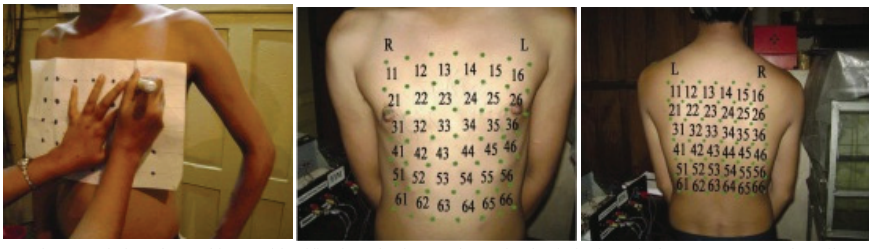

Fig. 6: Technique for marking out identification of points on thorax for the desired matrix for measurement. The cell numbers shown were superimposed later on the photographs.

left side of the body leaving out 1 and 6 column at each plane due to it erroneousness, as mentioned earlier. The second row in each plane is deemed ''top'' in Table 3. Similarly, the third and fourth rows of each plane are referred to as "mid" and "low," respectively in Table 3, for understanding the comparison at a glance.

Fig. 7: Measurement of localized ventilation using the hand held probe with spring loaded electrodes.

Table 1: Percentage change in localized impedance in each individual matrix, as measured from the front and from back. The right-left orientation are arranged to be the same on both views, for easy visual comparison.

Measurement from Front							Measurement from Back					
Right				Left			Right				Left	
***Subject-1**: age: 26 y, Height: 179 cm, Weight: 67 kg, F Vital capacity: 3.8 L*												
3.5	6.7	13.9	9.5	3.3	1.9		2.6	7.6	1.8	1.9	2.2	1.5
0	6.8	11.6	5.5	8.5	0		1.8	2.8	2.1	6.1	1.2	1.7
14.1	8.2	6.5	5.5	7.1	6.4		3.9	2.5	1.9	2.1	2.6	3.3
0	6.5	5.8	8.6	6.7	0		0	2.2	1.3	4	3.2	6.
0	4.3	2.8	4.7	2.1	0		0	3.3	2.7	2.2	4.7	0
4.1	0	2.7	0	3.9	7.1		0	0	3.4	2.2	3.8	0
***Subject -2:** age: 18 y, Height: 174 cm, Weight: 70 kg, F Vital capacity: 4.4 L*												
7.7	5.3	15.1	6.8	4.8	2.4		3.8	7.8	4.8	2.6	4.6	7.6
8.1	11.7	14.3	6.7	4.5	3.8		1.5	1.6	4.4	7.2	4.4	7.6
11.3	15	16.7	12.4	13.6	6.3		3.3	10.7	4.8	5	10.5	6
.5	12.1	10.6	4.8	12.7	20.4		9.4	7.1	3.3	4.3	3.6	9.5
19.1	12.9	4.1	8.2	12.4	16		14.1	6	4.3	3.3	3.7	5.8
***Subject-3:** age: 26 y, Height: 169 cm, Weight: 65 kg, F Vital capacity: 3 L*												
8.5	10.9	10.5	10.5	12.8	8.8		0	0	0	0	0	0
14.9	13.3	30.6	14.6	6.3	0		6.3	7.4	11.1	3.8	13.2	12.7
0	14.8	15.9	15.2	14.5	15.4		8.2	15.4	5.7	3.6	5	9.7
12.3	12.2	12.5	10.1	7.3	15.5		5.4	8.3	3.7	4.5	4.7	10
21.1	17.2	12	8.1	26.2	21.7		4.8	2	0	0	7.3	8.9
4.5	12	7.7	5.3	2	10.6		0	0	0	0	0	0
***Subject-4:** age: 20y, Height: 172 cm, Weight: 74 kg F Vital capacity: 3 L*												
2	2.6	4.2	7.1	2.8	1.1		1.6	1	3	3.1	2.8	1.2
4.5	3	7.2	3.6	1.7	6		6.8	2.2	2.3	2.7	1.7	1.7
5.6	4.7	8.6	3.1	1.7	6		1.6	0.9	2.6	4	4.1	2.3
2.7	4.4	5.7	3.8	4.2	2.2		0.9	1.3	2.1	4.6	3.5	6.1
4.9	2.14	1.97	3.6	5.7	4.8		2.3	0.9	0.8	4.2	5.3	3
1.8	4.7	2.6	0	0	0		5	1.8	2.5	3.9	1.2	1.7

After summing up the impedance percentage change of column 2 and 3 for each level [top (22, 23), mid (32, 33), and low (42, 43)], the values for right (Rt) in the Table 3 were obtained. A similar process is followed for achieving left (Lt) values in Table 3. In the former case matrix elements 24 and 25 are used in summing up impedance percentage change at top level of each plane. For mid-level, the impedance percentage change of matrix elements 34 and 35 are summed up and for the low level, matrix elements 44 and 45 are taken into account for each plane.

The ratio between Rt and Lt for each level of each plane was calculated. The mean value of these ratios for frontal and backplane gives an idea how impedance varies from right to left side of each plane.

Table 2: Comparison of summed values from front and back for 12 matrix elements, 22 to 45.

Subject	Location	Sum of change in Impedance (%)	Forced Vital Capacity (FVC) L	Sum/FVC	Ratio front/back
Subj-1	front (elem. 22-45)	87.3	3.8	23	2.73
	back (elem.22-45)	32		8.4	
Subj-2	front (elem.22-45)	135.1	4.4	30.7	2.02
	back (elem.22-45)	66.9		15.2	
Subj-3	front (elem.22-45)	167.3	3	55.7	1.94
	back (elem.22-45)	86.35		28.7	
Subj-4	front (elem.22-45)	51.7	3	17.2	1.61
	back (elem.22-45)	32		10.67	
				Average of front/back ratio=	2.1±0.47

Table 3: Comparison of summed values between right and left sides, for three horizontal levels for 12 matrix elements, 22 to 45 of front plane and back plane

Subject	Location	Frontal Plane				Back Plane			
		Right (Rt) [Column 2 and 3]	Left (Lt) [Column 4 and 5]	Ratio, Rt/Lt F	Mean F	Right (Rt) [Column 2 and 3]	Left (Lt) [Column 4 and 5]	Ratio, Rt/Lt B	Mean B
Subject 1	top (elem. 22-25)	18.4	14	1.31	1.55±0.6	4.9	7.3	0.67	0.96±0.6
	mid (elem. 32-35)	14.7	12.6	1.17		4.4	4.7	0.94	
	low (elem. 42-45)	12.3	15.3	0.80		3.5	7.2	0.49	
Subject 2	top (elem. 22-25)	26	11.2	2.32		6	11.6	0.52	
	mid (elem. 32-35)	31.7	26	1.22		15.5	15.5	1.00	
	low (elem. 42-45)	22.7	17.5	1.30		10.4	7.9	1.31	
Subject 3	top (elem. 22-25)	43.9	20.9	2.10		18.5	17	1.09	
	mid (elem. 32-35)	30.7	29.7	1.03		21.1	8.6	2.45	
	low (elem. 42-45)	24.7	17.4	1.42		11	9.2	1.19	
Subject 4	top (elem. 22-25)	10.2	5.3	1.92		4.5	4.4	1.02	
	mid (elem. 32-35)	13.3	4.8	2.77		3.5	8.1	0.43	
	low (elem. 42-45)	10.1	8	1.26		3.4	8.1	0.41	

Discussion

Primarily, this study was carried out to have a generalized view of localized impedance change across the thorax of human body due to breathing using 6-electrode FIM system. The ultimate objective was to employ the non-invasive FIM to detect lung disease based on the idea that the change in impedance measurement of diseased lung during breathe in and breathe out would be significantly less compared to that of a healthy one since air content will be reduced by the presence of water, blood, fluid, other substance or any other injury. This indication can only be functional and influential when the study on the large number of normal lungs takes place and a standard set of values are available to compare with the diseased lungs of different category. Furthermore the changes in impedance at different region at each plane (both front and back) are also dependent on anatomical structure of the lung as well as the body structure of the subjects, which led to use at times 6×6 matrix or 6×5 matrix.

It is noticeable from the Table 1 that the changes in impedance are greater when it is measured from the anterior plane than that of the posterior plane. For the ***Subject-1*** in

Table 1, the maximum change occurred in the frontal plane (14.1%) with a second maximum change of 13.9%, whereas the maximum change in impedance in the back plane for the same subject was 7.6% with a second maximum of 6.1%.

For the next subject (***Subject-2*** in Table 1), the maximum change of impedance was 20.4% and a second maximum change of impedance is 19.1% for frontal plane, whereas when measured from the back the maximum and the second maximum change in impedance shrunk to 14.1% and 10.7%, respectively.

Analyzing ***Subject-3*** in Table 1, it was found that the maximum change of impedance was 30.6% and the second maximum change of impedance was 26.2% for the frontal plane. When it was measured from the back, the maximum and the second maximum change in impedance were 15.4% and 13.2%, respectively.

Subject-4 in Table 1 also supports us in this conclusion, as the maximum change of impedance in this subject was 8.6% with a second maximum change of impedance of 7.2% for the frontal plane. When it was measured from the back, the maximum and the second maximum change in impedance became 6.8% and 6.1%, respectively. This may be because the sensitivity of the focused zone decreases with depth.

Moreover, the right most and the left most column at each plane usually possess larger values compared to the other column. Here also the change in impedance (%) in frontal plane remained higher than that of the back plane. One of the reasons for this could be due to the presence of solid bones right under these focused zones. Differences in vital capacity for each subject should be taken into account too. The human error of in regards to the instructions of full expiration and full inspiration may also cause to this result.

There are some cases when negative values do occur – though not considered in this study to avoid complication – and are needed to develop advanced FIM applications. The change in impedance at lower side (the bottom most row in each matrix) of the lungs of each plane varies abruptly in some cases such as the frontal and backplane of ***Subject-2*** and back plan of ***Subject-4*** in Table 1. The possible reason could be the diaphragm of the lungs, which expands and shrinks due to ventilation in this region and contributes to the impedance change to great extent.

In addition, it is seen from Table 2 that the average ratio between total impedance percentage change of the frontal plane and back plane is 2.1 (Table 2) i.e., on average the total impedance percentage changes at the frontal plane is twice as much as that of the backplane for each subject. This leaves another field to explore with more detail approach.

The potential reason for such higher values of impedance percentage change at the front plane might be the existence of heart at the frontal plane. The matrix column 2, 3, 4, 5 at frontal plane resembles cardiac region of human body and from Table 1 it is seen that the impedance percentage change in these focused zones varied significantly, especially when measured from the front, as mentioned earlier. So the ratio value from Table 2 also insinuates how heart and solid ribs contribute to the impedance change, though experiments with larger number of subjects are required to establish this result.

From Table 3, it is found that the impedance percentage change of the right side of frontal plane of human body is ~1.6 times that of left side of the same plane. The same value shrinks to ~1 when the comparison of right and left side of back plane is considered. The possible reason for such difference might be the same as mentioned earlier, i.e., contribution of heart at frontal plane and existence of muscle at back plane.

Nevertheless, it becomes more critical for the female subjects in terms of impedance change measurement due to the presence of fat tissue on anterior plane of thorax providing the same result found when the change in impedance was measured using the dice or diamond shape localized zone [7].

Conclusion

This present work has enhanced our understanding on lung impedance change due to ventilation with relatively simple and low-cost instrumental FIM setup. Consequently, advance study in this direction should explore different aspects and features.

Acknowledgement

The authors would like to express their gratitude to the volunteers for their participation in the study.

References

1. Rabbani KS, Sarker M, Akond MHR and Akter T. Proceeding of the X International Conference on Electrical Bioimpedance, Barcelona, Spain. 1998:31-34.
2. Rabbani KS, Sarker M, Akond MHR, Akter T. Ann. N.Y. Acad. Sci. 1999;873:408-420. http://dx.doi.org/10.1111/j.1749-6632.1999.tb09490.x
3. Rabbani KS, Kadir MA. Possible applications of Focused Impedance Method (FIM) in biomedical and other areas of study. Bangladesh J. Med. Phys. 2011;4(1):67-74.
4. Nopp P, Rapp E, Pfutzner H, Nakesch H and Ruhsam C. Phys. Med. Biol. 1993;38:699-719. http://dx.doi.org/10.1088/0031-9155/38/6/005
5. Islam, N, Rabbani, KS, Wilson A. The sensitivity of focused electrical impedance measurements. Physiol. Meas. 2010;31: S97-109. http://dx.doi.org/10.1088/0967-3334/31/8/S08
6. Iquebal AH Masum, Rabbani KS. 3D sensitivity of 6-electrode Focused Impedance Method. J. Phys. Conf. Ser. 2010;224:012156. http://dx.doi.org/10.1088/1742-6596/224/1/012156
7. Kadir MA, Ferdous H, Baig TN, Rabbani KS 2010. Ventilation mapping of chest using Focused Impedance Method (FIM). J. Phys. Conf. Ser. 2010;224: 012031. http://dx.doi.org/10.1088/1742-6596/224/1/012031

III

IOP Publishing | Institute of Physics and Engineering in Medicine Physiological Measurement
Physiol. Meas. **35** (2014) 1067–1082 doi:10.1088/0967-3334/35/6/1067

Comparison of four different FIM configurations—a simulation study

F J Pettersen[1,2], H Ferdous[2], H Kalvøy[1,2], Ø G Martinsen[1,2] and J O Høgetveit[1,2]

[1] Department of Clinical and Biomedical Engineering, Oslo University Hospital, Norway
[2] Department of Physics, University of Oslo, Norway

E-mail: fred.johan.pettersen@ous-hf.no

Received 30 November 2013, revised 9 March 2014
Accepted for publication 14 March 2014
Published 20 May 2014

Abstract
Focused impedance measurements (FIM) are used in several fields, and address the problem of measuring the volume impedance of an object within a volume conductor. Several electrode configurations are possible, and these have different properties. Sensitivity fields of four configurations have been investigated. We present one new development of an existing FIM configuration, and we made finite element models of the configurations to analyse and compare them both graphically and numerically. The models developed have a variable-sized mesh that allows us to build complex models that fit easily in computer memory. We found that one configuration in particular, FIM4, was superior to the others in most aspects. We also analysed the effects of very high sensitivities in and under the electrodes. We found that even if the sensitivity is very high under the electrodes, the effects of inhomogeneities were not as high as one might expect.

Keywords: focused impedance measurement, finite element model, simulation, three Rs

(Some figures may appear in colour only in the online journal)

1. Introduction

Electrical impedance in volume conductors is measured in many ways. For all but the simplest cases, it is difficult to know to what degree different sub-volumes in the conductor contribute to the measured result, i.e. the sensitivity field distribution. This means that in many volume impedance measurements, the understanding of the complete measurement problem is too low. An extension to this problem is the cases where we want to measure the impedance in a

specific volume with as uniform sensitivity in our target volume and as little influence from other volumes as possible.

Focused impedance measurement (FIM) using four, six, and eight electrodes has been presented in Rabbani *et al* (1999) and Rabbani and Karal (2008). These methods are focusing the sensitivity to a region roughly shaped as a half-sphere below a flat surface.

The FIM techniques may be applied for a wide range of applications such as cancer diagnosis, bladder emptying, and lung ventilation (Rabbani and Kadir 2011). FIM can be useful since it enables us to target the measurement in tissues or organs of interest. In the study of measuring gastric emptying, FIM along with its 3D sensitivity was found effective (Rabbani *et al* 1999). A linear relationship to change in expired volume of air was found in a previous study when implemented to a focused zone of the lung in a subject (Rabbani and Kadir 2011). In principle, the dielectric properties of lung tissue varies greatly as a result of air ventilation, between expiration and inspiration (Nopp *et al* 1993), which ultimately offers an area of opportunity to implement electrical impedance measurement systems for further study with FIM (Kadir *et al* 2010). One such pilot study showed that to have a thorax mapping in terms of transfer impedance an appropriate model is required before FIM technique is implemented (Ferdous *et al* 2013). One of the appealing properties of the technique is that it is possible to make simple and low-cost equipment based on FIM. A FIM based instrument is typically based on a low-end microcontroller and a handful of analogue components. This is in contrast to more advanced systems like EIT, x-ray, MRI, and ultrasound. Since the equipment is low-cost, it is especially suited for use in poor countries.

Brown *et al*, and Islam *et al* have addressed the problem of analysing the sensitivity field distribution using Matlab simulations based on Geselowitz' lead field theory (Geselowitz 1971). These analyses were done for points in a mesh with 1mm distance in the x, y, and z-directions. The models consisted of 343 000 and 8000 000 points, respectively. The models can be used to calculate sensitivity in each point. Our approach is also based on the Geselowitz theory, but we realize it in COMSOL Multiphysics (MPH) finite element models (FEM) that gives us some extra possibilities such as a variable mesh that can be made finer, i.e. the distance between nodes is smallest around small geometrical objects, around regions of special interest. For instance, in our models the highly interesting electrodes are made as 372 tetrahedra instead of only a point in the previous work. In addition to this, the Matlab models only gave sensitivity while our models have current density vectors and potentials available for all points. Expressions for sensitivity (equation (5)) and volume impedance density (equation (6)) are added to enable us to graphically display sensitivities and to enable us to calculate transfer impedance. The previous work is limited to semi-infinite homogenous volumes while the presented FEM models do not have this limitation. In addition, the FEM model allows us to model almost any geometrical shape. The larger feature-set of the FEM-tool enables us to extract more interesting information out of the model. Furthermore, we present some new metrics that should be taken into account when evaluating a given measurement configuration.

The software models were used to analyse the different FIM set-ups *in silico*. Using the models described in the paper we are able to measure with the different electrode configurations and determine how they are influencing the measurement results. The sensitivity field distribution can be crucial when measuring in biological tissue or other sample of non-homogenous nature.

Different configurations of electrodes have been used to measure impedance. FIM is a special set-up for impedance measurement where two or four electrodes are current carrying (CC), and two or four electrodes are used for voltage pick-up (PU). Some configurations have two steps where the electrode usage is changed. In these cases, the configuration requires

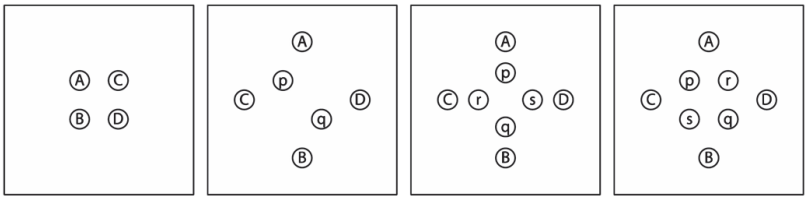

(a) (b) (c) (d)

Figure 1. Top view of electrode configurations. Dimensions are not to scale. (a) FIM4, (b) FIM6, (c) FIM8a, (d) FIM8b.

simple post-processing. The benefit of FIM is that simple circuitry allows us to measure in the region of interest (Rabbani *et al* 1999).

However, one of the major problems of such impedance studies is that unless real life experiments have been executed it is difficult to avail information beforehand, which is obviously time-consuming and challenging to rectify if necessary. To solve these problems, the experiments can be done *in silico* using FEM software for modelling. Another benefit of *in silico* experiments is replacement of animal experiments in accordance with the three Rs of animal welfare (Russel and Burch 1959).

We are presenting a new tool for selecting the optimal electrode configuration for a given FIM problem. Examples of such problems are the thoracic mapping where the use of a FEM-tool could aid in choosing the best FIM configuration, and to improve understanding of the measurement results.

2. Method

2.1. Model descriptions

All models are 50 cm wide $\times$ 50 cm long $\times$ 25 cm high. The height is set to half the width since previous work (Brown *et al* 2000, Islam *et al* 2010) have shown that sensitivity is decreasing rapidly when moving away from the electrode plane. The electrodes are placed on top of the models. Electrode radius is varied according to column 2 in table 4. The electrode height is equal to electrode radius. In addition to the electrode itself, a half-sphere is made under the electrode. The half-sphere has the same electrical properties as the bulk material, and is used to (a) force the FEM tool to make the mesh finer in these regions, and (b) to define a region for volume integration. The radius of this half-sphere is varied from the same radius as the electrode and up to 10 mm in 2 mm steps. The inner electrodes for all models form a square with 4 cm sides. For FIM6, FIM8a, and FIM8b, the CC electrodes form a square with 12 cm sides. Configurations are shown in figure 1. A sphere is placed just underneath the surface for the same reasons as for the half-spheres. The sphere has the same electrical properties as the bulk material. The sphere radius is 1/3 of the spacing between the inner electrodes, i.e. 1.33 cm, and is touching the top surface of the model. The works presented in Brown *et al* (2000) and Islam *et al* (2010) suggest that this is a depth where sensitivity might be high.

To simulate the effect of an inhomogeneous material under an electrode, two ellipsoids were placed under one CC-electrode in the FIM8a-model. One ellipsoid was placed in the region with positive sensitivity, and the other in the region with negative sensitivity. The regions of positive and negative sensitivity were determined in the previous simulations. The ellipsoid has radius identical to the radius of the electrode in x-direction, and y-direction, and radius identical to half the electrode radius in the z-direction, which is shown in figure 2.

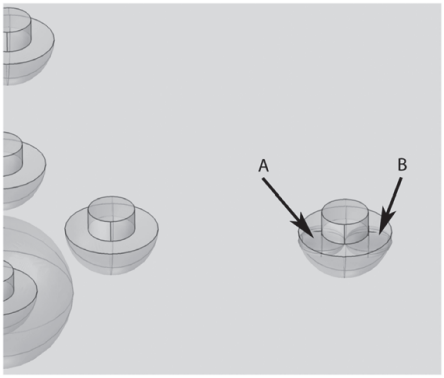

Figure 2. Placement of ellipsoids beneath one electrode. The one marked A is in the region of negative sensitivity, while the one marked B is in the region of positive sensitivity.

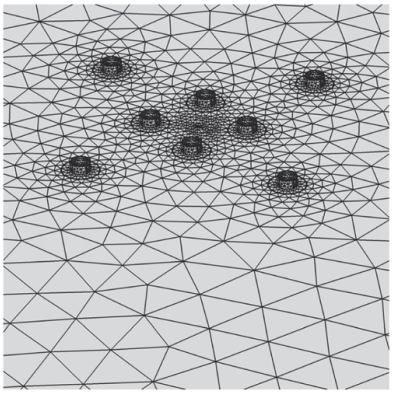

Figure 3. Surface mesh illustrating variable mesh structure.

The meshes were generated with settings that gave approximately 75 000 tetrahedral elements.

Figure 3 shows how the mesh is getting finer around the region of interest (the electrodes). For simplicity, only the surface meshes are shown.

The materials properties are shown in table 1.

The current flows from the electrode designated by the first letter through the model to the electrode designated by the second letter. Letters, where the first letter identifies the positive terminal and the second letter identifies the negative terminal, also identifies voltage pick-up electrodes.

For all set-ups, we are may say that we are making several measurements of the same quantity. In an ideal setting, each measurement would give the same value, and a summation of two measurement results would give the double of the real value, so to get the real value, we

Table 1. Material properties.

Material	Conductivity (sigma) (S m^{-1})	Description
Bulk	1	The bulk of the model
Electrode	100	Electrode material
Low conductivity	0.01	Inhomogeneity below electrode
High conductivity	100	Inhomogeneity below electrode

would have to calculate the average of the two values. Here, we follow the same logic; we do several transfer impedance measurements and take the average. In particular, what we do is to calculate the sensitivities for the different measurements and then average these. These calculations are all done within MPH. This method is in contrast to the work by Islam *et al* where results were added together (Islam *et al* 2010). Adding the results would enable comparison, but it would not let us use the result when calculating expected transfer impedance as we also do. The validity of our method has been verified by comparing FIM-simulations to phantom measurements (Abir *et al* 2013). Since all set-ups give different results, we may also argue that all measurements should be normalized, but we did not do this since we wanted to estimate final impedance.

2.1.1. FIM4. Four electrodes in a square. As described in Rabbani and Karal (2008). Electrode placement is as shown in figure 1(a).

The procedure:

(1) Measure transfer impedance using AC as CC, and BD as PU.
(2) Measure transfer impedance using AB as CC, and CD as PU.
(3) Calculate the average Z (transfer impedance).

2.1.2. FIM6. Six electrodes as described in (Rabbani *et al* 1999). Two independent current sources AB and AC. One PU, pq. Electrode placement is as shown in figure 1(b).

2.1.3. FIM8a. This is a set-up where two 4-electrode measurements are done, and the results averaged. For each of the two 4-electrode set-ups, the electrodes are placed in a row. The two set-ups are 90° on each other. Electrode placement is as shown in figure 1(c).

The procedure:

(1) Measure transfer impedance using AB as CC, and pq as PU.
(2) Measure transfer impedance using CD as CC, and rs as PU.
(3) Calculate the average Z (transfer impedance).

2.1.4. FIM8b. FIM 8b is an evolvement of FIM6 and FIM8a. Two sets of independent CC-electrodes 90° on each other. Two sets of PU-electrodes rotated 45°. Current is delivered simultaneously in the two CC-pairs, and PU is done in two rounds. Electrode placement is as shown in figure 1(d).

The procedure:

(1) Measure transfer impedance using AC and CD as CC simultaneously, and pq as PU.
(2) Measure transfer impedance using AC and DC as CC simultaneously, and rs as PU.
(3) Calculate the average Z (transfer impedance).

2.1.5. Simulation set-up. Simulations are done in COMSOL MPH version 4.3. A set of partially differential equations is needed to define how the FEM-tool are doing its calculations. In the cases where an appropriate pre-defined equation set is not defined, the generic equations (1) through (4) can be used. For the case of COMSOL MPH, there exist arrange of pre-defined equation sets that models several physical systems such as heat flow, electric currents, magnetic fields, acoustics, fluid flow, etc. For our models, we have used a predefined set called *Electric Currents* physics interface (COMSOL 2013) which contains the equations (1) through (4).

The interior of the materials are handled by

$$\nabla \cdot \mathbf{J} = Q_j \tag{1}$$

$$\mathbf{J} = (\sigma + \mathrm{j}\omega\varepsilon_0\varepsilon_r)\mathbf{E} + \mathbf{J_e} \tag{2}$$

$$\mathbf{E} = -\nabla \mathrm{V} \tag{3}$$

and the external boundaries by

$$\mathbf{n} \cdot \mathbf{J} = 0. \tag{4}$$

The simulations are done for DC only, which means that $\omega = 0$ in equation (2).

The symbols in equations (1) through (4) means:

$\nabla\cdot$ is the divergence of a vector field.

$\mathbf{J}$ is electric current density.

E is electric field intensity.

Q_j is electric charge.

σ is electric conductance.

j is the imaginary unit.

ω is frequency in radians per second.

ε_0 and ε_r are vacuum permittivity and relative permittivity, respectively.

$\mathbf{J}_e$ is external current density.

∇V is the gradient of the potential.

For a complete explanation please see the MPH reference manual (COMSOL 2013). For further information on FEM for electromagnetic problems, there are excellent text books available (Humphries 1997).

2.2. Extracted numbers

Several numbers are extracted from the model simulations.

2.2.1. Fractions. The negative fraction (NF) tells us how much volumes with negative sensitivity contribute to the measured transfer impedance. This is a number between 0 and 1, and should ideally be 0. The next number is called sphere fraction (SF) and tells us how much the sphere just below the model surface contributes to the measured impedance. SF is a number between 0 and 1 for a configuration with NF = 0 and should ideally be 1 if we want to focus our measurement on the sphere. If the NF is non-zero, the number might be higher than 1.

To calculate NF and SF, we first define volume impedance density (z) for each point in the model. This is simply sensitivity multiplied by the resistivity as shown in (6). Sensitivity is given in equation (5). If we integrate z for all points in the volume, we end up with the transfer impedance. If we integrate over a smaller volume, V_{SUB}, then the contribution from

Table 2. Sensitivity variables.

Variable definition	Description
$\mathrm{SR_{MAX}} = \frac{\max(\lvert S\rvert)}{S_{\mathrm{AVERAGE}}}$	Ratio between maximum $\lvert S\rvert$ for the whole model and average S for the whole model. Electrodes are not included.
$\mathrm{SR_{SPHERE}} = \frac{S_{\mathrm{AVERAGE-SPHERE}}}{S_{\mathrm{AVERAGE}}}$	Ratio between average S for the sphere and average S for the whole model. Electrodes are not included.

V_{SUB} to the total transfer impedance is the result. MPH has mechanisms to allow us to select such smaller volumes based on geometry or any available numerical property of a given point. This functionality allows us to investigate regions of special interest

$$S = \frac{\overrightarrow{J_{CC}}.\overrightarrow{J_{PU}}}{I_{CC}I_{PU}}\left[\frac{1}{m^4}\right] \tag{5}$$

$$z = \rho S\left[\frac{\Omega}{m^3}\right] \tag{6}$$

where

ρ is the resistivity of the material.

S is sensitivity.

$\overrightarrow{J_{CC}}$ is the current density originating from simulation where current is sent into the model through the CC electrodes.

$\overrightarrow{J_{PU}}$ is the current density originating from simulation where current is sent into the model through the PU electrodes, i.e. the reciprocal current.

I_{CC} is the measurement current used in the model.

I_{PU} is the reciprocal measurement current used in the model.

Both I_{CC} and I_{PU} is set to $1A$ to simplify calculations. Then the NF is calculated using

$$\mathrm{NF} = \frac{\left|\iiint z_{\mathrm{NEG}}\,\mathrm{d}V\right|}{\iiint z\,\mathrm{d}V} \tag{7}$$

where

$$z_{\mathrm{NEG}} = \begin{cases} \text{if} & \mathrm{z} \leqslant 0 : \mathrm{z} \\ \text{if} & \mathrm{z} > 0 : 0 \end{cases}. \tag{8}$$

And SF is calculated using

$$\mathrm{SF} = \frac{\iiint_{\mathrm{SPHERE}} z\,\mathrm{d}V}{\iiint z\,\mathrm{d}V} \tag{9}$$

2.2.2. Depth of negative sensitivity. To quantify how deep the region where S is negative is, the parameter negative sensitivity depth is defined as

$$\mathrm{NSD} = \frac{\text{Depth of negative } S}{\text{Distance between inner electrodes}} \tag{10}$$

and was found by probing an isosurface plot of $S = 0$.

2.2.3. Sensitivity ratios. Two ratios of sensitivities are defined in table 2. $\mathrm{SR_{MAX}}$ defines how large the sensitivity ratios are. A very high number indicates regions with high sensitivity that could potentially cause problems. The $\mathrm{SR_{SPHERE}}$ say how high the sensitivity is in the sphere where we want sensitivity to be high is. A high number means that the focus on the sphere is high.

Table 3. Impedance contribution definitions.

Variable definition	Description
$Z_{\mathrm{EL-ABCD}} = \iiint_{\mathrm{ELECTRODES\ ABCD}} z\,\mathrm{d}V\,[\Omega]$	Contribution from electrodes A, B, C and D to final measured impedance
$Z_{\mathrm{HSP-ABCD}} = \iiint_{\mathrm{HALFSPHERES\ ABCD}} z\,\mathrm{d}V\,[\Omega]$	Contribution from half-sphere below electrodes A, B, C and D to final measured impedance
$Z_{\mathrm{EL-pq}[rs]} = \iiint_{\mathrm{ELECTRODES\ ABCD}} z\,\mathrm{d}V\,[\Omega]$	Contribution from electrodes p, q, r and s to final measured impedance
$Z_{\mathrm{HSP-pq}[rs]} = \iiint_{\mathrm{HALFSPHERES\ ABCD}} z\,\mathrm{d}V\,[\Omega]$	Contribution from half-sphere below electrodes p, q, r and s to final measured impedance

2.2.4. Contribution from electrode regions. The fine simulation mesh in the electrode regions allowed us to have a closer look at the contribution to final impedance form these regions. Four electrode related contributions are defined in table 3.

2.2.5. Inhomogeneities. An extra set of simulations was done to the FIM8 a-model to investigate the effect of inhomogenities in the region below the electrodes. A base simulation was done with no inhomogeneities, and a number of combinations of low and high conductivities in the two regions were simulated. The percentage change in total averaged transfer impedance impedance was found.

3. Results

3.1. Sensitivity plots

Sensitivity plots from the simulations are given in figures 4–8.

3.1.1. Comparison of configurations. Figures 4 through 7 show plots of sensitivity for the different configurations. There are four plots for each configuration. Plot (a) shows the interface between the zone of negative and positive sensitivity. The plot is created by plotting a sensitivity isosurface with $S = 0$. For (b), (c) and (d) in all figures the plot range is from $-150\,000\,\left[\mathrm{m}^{-4}\right]$ (dark blue) to $150\,000\,\left[\mathrm{m}^{-4}\right]$ (dark red) via 0 (light grey), with the exception of the FIM4-plots (figure 4) where the range is $\pm 350\,000\,\left[\mathrm{m}^{-4}\right]$ due to lower and higher sensitivities. For plot (b), the inner rings in the electrodes are the electrode dimensions, while the outer ring is the half-sphere below the electrodes. The plots show the sensitivity in three different planes:

(1) One plane parallel to the electrode plane (figure *n* b)). This plane cuts the sphere in the middle, i.e. 1.33 cm below the surface.
(2) One vertical plane that is parallel with one of the sides of the model (figure *n* c)).
(3) One vertical plane that is rotated 45° (figure *n* d)).

To ease comparison, the viewpoint is the same for all models. The electrode radius is 4 mm for all plots.

3.1.2. Sensitivities in presence of inhomogeneities. The plots in figure 8 shows how the sensitivity changes in presence of inhomogeneities under an electrode.

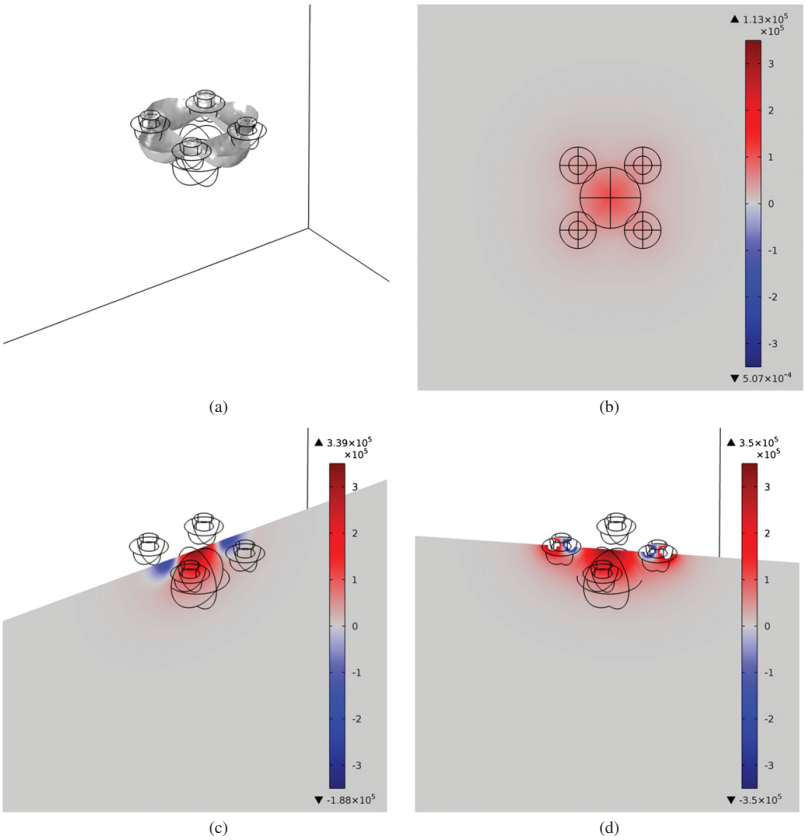

Figure 4. Shape of negative sensitivity region, and sensitivities for three different planes for FIM4.

3.2. Numbers

Tables 4 and 5 show the extracted number for all configurations.

The contributions to the average transfer impedances of the electrodes and the half-spheres under the electrodes are presented in table 5.

Percentage change of impedance due to inhomogeneities is presented in table 5 and figure 8.

4. Discussion

4.1. Model limitations and strengths.

By using a variable size mesh instead of the fixed-size mesh used by Brown *et al* and Islam *et al* we introduced a method to reduce the numerical problem, and thus made it easier to

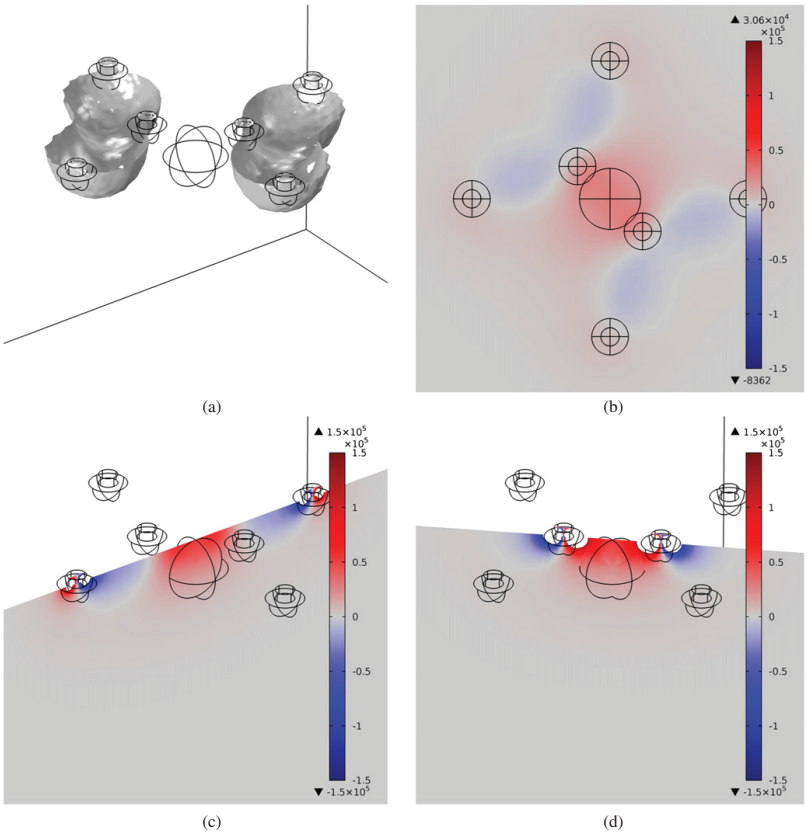

Figure 5. Shape of negative sensitivity region, and sensitivities for three different planes for FIM6.

keep the entire model in the computer memory. This may not be an issue for relatively small models, but by using variable-size grid, we may be able to analyse larger models than we were if we used fixed-grid models. Here, the term large model also means a model with high spatial resolution since it would require a large amount of grid points. It also means that it is possible to model geometries that are small compared to the complete model accurately. The Matlab method uses arguably less resources than a FEM-tool if the mesh was similarly sized and if we limit the model to only deal with a semi-infinite homogenous model.

For more complex models, and if we choose to extend the model to include frequency dependent properties, the variable mesh may make it difficult to find a numerical solution, and we may have to give up some of the dynamics in mesh size, and is by that falling back towards a mesh with points with fixed distance.

The model in the work presented here is for DC only since simulations in the frequency domain is identical but with numbers replaced with complex numbers. For models describing

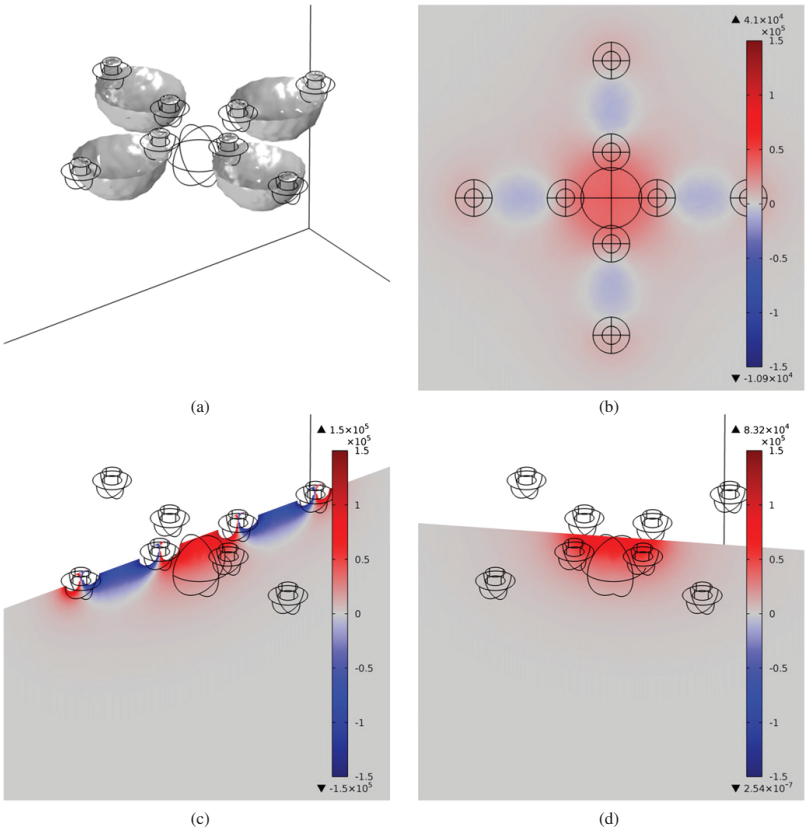

Figure 6. Shape of negative sensitivity region, and sensitivities for three different planes for FIM8a.

real-world geometries such as body organs with much more complex tissue properties like presented by Gabriel and Gabriel (1996) a frequency simulation would be appropriate. An example of such a model is given by Pettersen and Høgetveit (2011).

The number-crunching capabilities of Matlab are impressive. But Matlab has no infrastructure to let users create a simulation model. This effectively limits the complexity of Matlab models to very simple models similar to the ones presented by Brown *et al* (2000) and Islam *et al* (2010). MPH and other FEM-tools have an infrastructure that is geared towards complex models and powerful post-processing.

A half-sphere with the flat surface on the model surface would probably have given better SF for all models, but was not used since one goal of developing a FIM-method is to locate materials with different electrical impedance below the surface, and a submerged sphere is therefore more realistic. Examples may be a cancer tumour below the skin surface and measurement of the electric impedance of a specific organ.

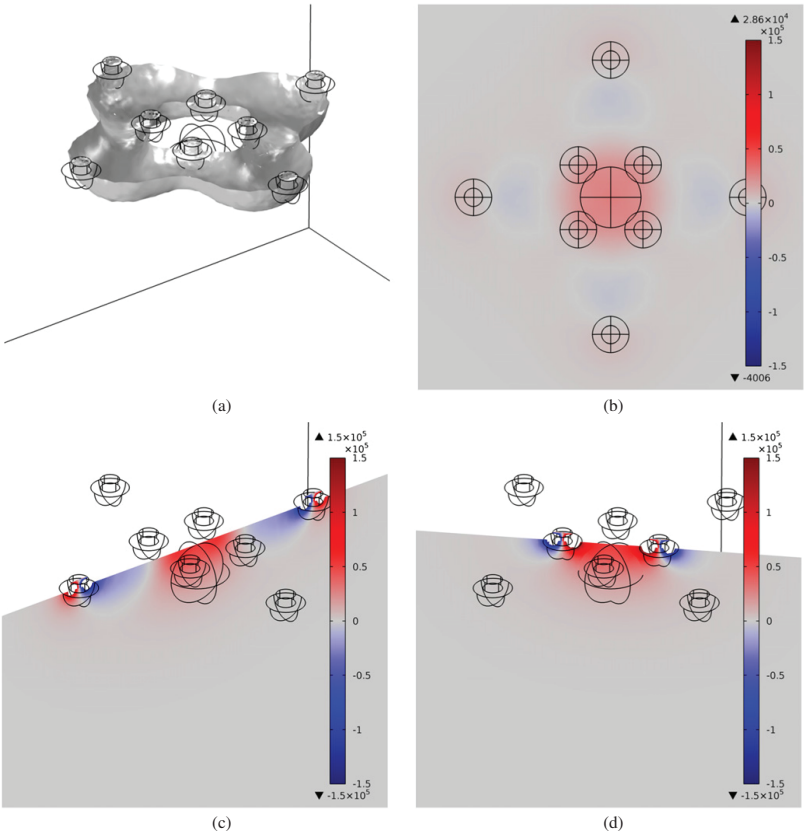

Figure 7. Shape of negative sensitivity region, and sensitivities for three different planes for FIM8b.

The configurations investigated here are only a small sub-set of all possible configurations. Which configuration to use depends on several factors like allowed complexity, focus requirements, and ability to detect a particular feature in the measurand.

The electrodes are modelled as cylinders that have a conductivity that is 100 times higher than the bulk material. The electrodes are set up to either carry no current or to carry a given current. In the case of no current, the electrodes are simply geometries with higher conductivity than the surroundings. In the other case, the top surfaces of the electrodes are defined to be a surface where a given current of 1 [A] is flowing. Since we are using an ideal dc current source, we do not have to consider interface effects such as polarization or contact impedance. We could do simulations with higher detail levels, and by that be able to see effects of interfaces. The given set of equations (1) through (4) will not be able to model all effects that are caused by the ionic nature of electrical bioimpedance and the interfaces between domains with electronic end ionic charge carriers. The simulations of inhomogeneities beneath one electrode will to

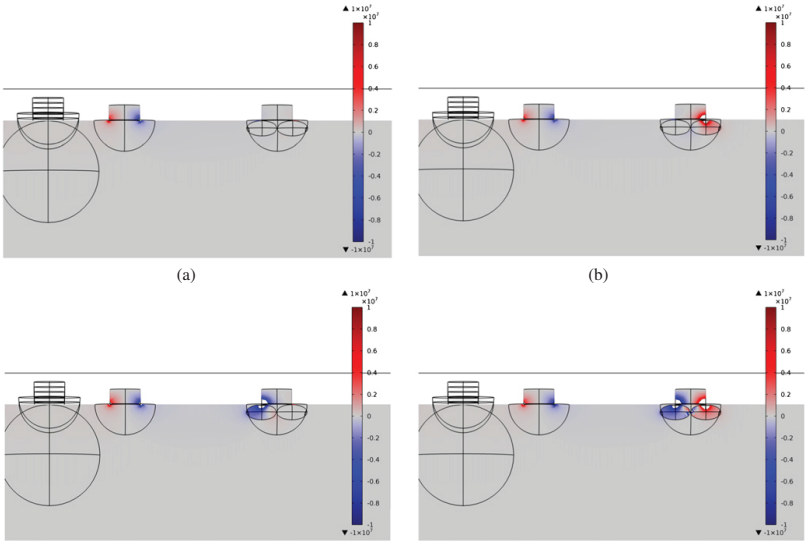

Figure 8. Effect of inhomogeneities illustrated by plotting sensitivity. The plots represent different configurations of conductivity in the regions of negative and positive sensitivity (a) low–low, (b) low–high, (c) high–low, (d) high–high.

Table 4. Numerical results from simulations. El. radius is electrode radius, and the variables NF, SF, SR_{MAX} and SR_{SPHERE} are defined previously.

Configuration	El. radius (mm)	NF	SF	SR_{MAX}	SR_{SPHERE}
FIM4	2	0.213	0.262	536 115	1651
	4	0.208	0.260	272 715	1641
	6	0.196	0.257	104 252	1617
	8	0.172	0.248	69 521	1565
FIM6	2	0.532	0.114	885 596	717
	4	0.532	0.114	448 783	719
	6	0.530	0.115	178 640	726
	8	0.527	0.118	126 373	746
FIM8a	2	0.491	0.100	725 337	627
	4	0.491	0.100	279 517	627
	6	0.491	0.100	124 070	632
	8	0.527	0.102	79 798	641
FIM8b	2	0.396	0.114	504 024	717
	4	0.396	0.113	235 780	715
	6	0.491	0.113	97 120	713
	8	0.527	0.113	65 690	713

a small degree illustrate some effects of what happens if the electrodes are not perfect or perfectly attached to the rest of the measurand. Since the models are simplified, and we use no 2- or 3-electrode configurations, we considered that the simplifications did not change the

Table 5. The contributions to the total average transfer impedance from electrodes and spheres below the electrodes are given as percentage of measured average transfer impedance.

Configuration	Variable	Min	Average	Max
FIM4	$Z_{\mathrm{EL-ABCD}}$	−0.029	0.144	0.815
	$Z_{\mathrm{HSP-ABCD}}$	0.053	0.816	2.049
FIM6	$Z_{\mathrm{EL-ABCD}}$	−0.085	−0.022	0.038
	$Z_{\mathrm{HSP-ABCD}}$	0.004	0.049	0.138
	Z_{EL-pq}	−0.077	0.087	0.425
	$Z_{\mathrm{HSP-pq}}$	0.033	0.335	0.793
FIM8a	$Z_{\mathrm{EL-ABCD}}$	−0.128	−0.039	0.022
	$Z_{\mathrm{HSP-ABCD}}$	0.006	0.049	0.159
	$Z_{\mathrm{EL-pqrs}}$	−0.035	0.326	1.302
	$Z_{\mathrm{HSP-pqrs}}$	0.012	0.510	1.205
FIM8b	$Z_{\mathrm{EL-ABCD}}$	−0.080	−0.022	0.021
	$Z_{\mathrm{HSP-ABCD}}$	0.004	0.048	0.144
	$Z_{\mathrm{EL-pqrs}}$	−0.001	0.465	1.796
	$Z_{\mathrm{HSP-pqrs}}$	0.015	0.622	1.449

Table 6. Results of inhomogeneities under electrode.

Conductivity–positive Region	Conductivity–negative region	Measured impedance change (%)
1	1	Reference
0.01	0.01	−0.30
0.01	100	−4.15
100	0.01	2.38
100	100	−1.14

results significantly. Details on error sources in tetrapolar impedance measurements can be found in Grimnes and Martinsen (2007), and should apply here with some modifications.

4.2. Sensitivity plots

There are clearly significant differences between the configurations. As expected the FIM4, FIM8a, and FIM8b have sensitivity fields that are symmetrical around the *x*- and *y*-axis, while FIM6 is clearly not symmetrical. It is interesting to see how high the sensitivities in and beneath the electrodes are. It may be naturally to assume that any inhomogeneity in these regions would affect measurements to a high degree, but the simulations with inhomogeneities (table 6) shows us that the effect is surprisingly small. This can be explained by seeing the electrode and the inhomogeneity as a different shaped electrode. Figure 8 shows how the sensitivity is changed if inhomogeneities are present. The plots show us that where the conductivity is low, the sensitivity is low too. This can be explained by seeing the electrode and the inhomogeneity as a different shaped electrode.

4.3. Numbers

The results in table 4 tells us that there are large differences in what the actual measured value consist of depending on which configuration we choose. If we consider only one electrode radius, 4 mm, looking at NF, we see that the negative fraction varies from 0.208 for FIM4 to

0.532 for FIM6. This means that the risk of errors caused by objects placed in a region with negative sensitivity is higher for FIM6 than for the other configurations.

The SF tells us that the contribution to the sphere is much highest for the FIM4 configuration. But even so, the SF is still only in the range 0.100–0.262. This means that even if we have relatively good focus in our focus region, 73.8%–90% of the contribution to the total transfer impedance is originating from outside the focus region. Which again indicate that the FIM configurations analysed here, and probably similar configurations too, may have a rather limited use.

The electrode size affects all numbers, but the sensitivity ratio numbers (SR_{MAX} and SR_{SPHERE}) are most affected. The smaller the electrodes are, the higher the sensitivity ratios are. This tells us that large electrodes might be better if not other factors dictates use of small electrodes. The SF and NF were relatively little affected by electrode size for all models except FIM4. FIM4 has best values for SF and NF, but if constant electrode size is important, then FIM4 might be a poor choice.

The results in table 5 tell us that the contributions from the electrodes and the regions just below the electrodes are small even if the local sensitivities are very high. Even if we put inhomogeneities in these regions, we see (table 6) that the effect is relatively small. The inhomogeneities were modelled as ellipsoids with conductivity that was either 100 times higher or lower than the conductivity of the surrounding material placed under the electrode as shown in figure 2. The small effects on overall result may be explained in several ways. We may say that where the resistivity of a region is increased, the current density will naturally decrease too as long as the current has an alternative way to flow (as it has here), and thus reduce sensitivity according to equation (5). Similarly, in the case where resistivity is decreased, the sensitivity will be increased due to higher current density. When looking at equation (6), we see that the regions contribution to measured impedance is not only given by sensitivity, but also by resistivity, and that is changing in the opposite direction, and thus trying to cancel out the effects of sensitivity change. Another way of seeing it is that the inhomogeneities are causing an effective change of electrode placement and shape in the 3D-volume. But since the changes were relatively small compared to the distances between the electrodes, the effects were small.

As mentioned above, inhomogeneities will alter sensitivity. To further illustrate this, we can consider the case where an object with reduced conductivity is placed within our desired sensitivity region. Two things will happen:

(a) A low conductivity object will cause currents to move around it and thus move the sensitivity region away. This will result in reduced transfer impedance according to equation (6).
(b) A low conductivity object has higher resistivity, and will therefore result in higher transfer impedance according to equation (6).

This means that we may see the problem form an entirely different angle. If conductivity in our focus region differ much from the surroundings, then we start measuring more or less of the surroundings.

5. Conclusion

The presented work has shown that MPH is a very useful FEM tool to investigate volume impedance measurement problems. This is especially true when we consider models where there are large rations between small and large objects and inhomogeneities. Simulations allow us to explore the electrode configuration space and visualize and quantize alternative configurations.

The simulations showed us that of the four configurations analysed here, the FIM4 configuration is superior in terms of SF and NF. The simulations also showed that the sensitivities in and beneath the electrodes were surprisingly high, but even so, the inhomogeneities beneath the electrodes did not affect the measurements as much as one might expect. Similarly, effects of objects within our focus region will not have as much influence as we might expect.

Acknowledgment

HF would like to express her gratitude to the Norwegian State Education Loan Fund for their financial support.

References

Abir R, Pettersen F J, Martinsen O G and Rabbani K S 2013 Effect of a spherical object in 4 electrode focused impedance method (FIM): measurement and simulation *J. Phys.: Conf. Ser.* **434** 012009

Brown B H, Wilson A J and Bertemes-Filho P 2000 Bipolar and tetrapolar transfer impedance measurements from volume conductor *Electron. Lett.* **36** 2060

COMSOL 2013 *COMSOL Multiphysics Reference Manual.* Part of software package: COMSOL

Ferdous H F, Baig T N and Rabbani K S-E 2013 Thorax mapping for localised lung impedance change using focused impedance measurement (FIM): a pilot study *J. Electr. Bioimpedance* **4** 57–61

Gabriel C and Gabriel S 1996 Compilation of the dielectric properties of body tissues at RF and microwave frequencies *Report No AL/OE-TR-1996–0037* (Armstrong Laboratory (AFMC), Brooks Air Force Base, TX, USA)

Geselowitz D B 1971 An application of electrocardiographic lead theory to impedance plethysmography *IEEE Trans. Biomed. Eng.* **18** 38–41

Grimnes S and Martinsen Ø G 2007 Sources of error in tetrapolar impedance measurements on biomaterials and other ionic conductors *J. Phys. D: Appl. Phys.* **40** 9

Humphries S J 1997 *Field Solution on Computers* (Boca Raton, FL: CRC Press)

Islam N, Rabbani K S-E and Wilson A 2010 The sensitivity of focused electrical impedance measurements *Physiol. Meas.* **31** S97–109

Kadir M A, Ferdous H, Baig T N and Siddique-e-Rabbani K 2010 Ventilation mapping of chest using Focused Impedance Method (FIM) *J. Phys.: Conf. Ser.* **224** 012031

Nopp P, Rapp E, Pfutzner H, Nakesch H and Rusham C 1993 Dielectric properties of lung tissue as a function of air content *Phys. Med. Biol.* **38** 699

Pettersen F-J and Høgetveit J O 2011 From 3D tissue data to impedance using Simpleware Scan FE+ IP and COMSOL Multiphysics—a tutorial *J. Electr. Bioimpedance* **2** 13–32

Rabbani K S and Karal M A 2008 A new four-electrode focused impedance measurement (FIM) system for physiological study *Ann. Biomed. Eng.* **36** 1072–7

Rabbani K S, Sarker M, Akond M H R and Akter T 1999 Focused impedance measurement (FIM): a new technique with improved zone localization *Ann. NY Acad. Sci.* **873** 408–20

Rabbani K S-E and Kadir M A 2011 Possible applications of focused impedance method (FIM) in biomedical and other areas of study *Bangladesh J. Med. Phys.* **4** 67–74

Russel W M S and Burch R L 1959 *The Principles of Humane Experimental Technique* (London: Methuen)

IV